Low Cost Bio-Robotic System Using Biometric Signals

A thesis presented in partial fulfilment of the

Requirements for the degree of

Master of Engineering

in

Mechatronics

at Massey University, Manawatu,

New Zealand.

Christopher Scott

2014

Contents

Table of Figures

List of abbreviations:

Targeted Muscular Reinnervation – TMR
Targeted Sensory Reinnervation – TSR
Electromyography – EMG
Proportional Integral – PI
Degrees of Freedom – DoF
Computer Numerical Control – CNC
Computer Aided Design – CAD
Computer Aided Manufacture – CAM
Computer Numerical Control – CNC
International Society of Electrophysiology and Kinesiology – ISEK
Common Mode Rejection Ratio – CMRR
Data Acquisition Card – DAQ
Fast Fourier Transform – FFT
Resistor Capacitor – RC
Mean Average Voltage – MAV
Integrated Circuit – IC
I/O – Input Output
Pulse Width Modulation – PWM
Integrated Development Environment – IDE

Abstract

The high cost of bio-controlled prosthetic devices is prohibitive to the general amputee population. This causes the majority of amputees to be forced to use mechanical or passive prosthetic devices which provide little to no extra functionality to the amputee's residual limb. The mechanical prostheses can actually cause damage to other parts of the amputee's body by the way they are mounted and actuated. By contrast, bio-controlled prostheses actually improve the functionality and quality of life to the amputee with little to no adverse side effects. The mounting device does not cause injury to other parts of the amputee's body and the amputee is able to lead a near-normal life. The barrier to these devices however is the price. In most cases, amputations involve a third party to pay for medical care and rehabilitation through either government funding or medical insurance. These organisations don't want to spend lots of money for every amputee and therefore have a maximum expenditure unless a special case is made. A passive or mechanical prosthesis is commonly able to be obtained for less than $3000, the price for a bio-controlled prostheses however is upwards of $5000. This maximum expenditure only qualifies most amputees for the mechanical type prostheses. This research funded by the Dick and Mary Earle Scholarship aims to break the cost barrier to the bio-controlled prosthesis by creating a bio-controlled device for a competitive price.

A proof of bio-controlled prosthesis design and a prototype testing platform was achieved using a series of low cost manufacturing and electronic techniques. The prototype was required to provide competitive functionality to the current bio-controlled prostheses on the market while retaining a similar cost of the mechanical prosthesis. To keep the cost of prototyping to a minimum a physical test platform was manufactured in-house at Massey University using the mechanical workshop and manufacturing technologies available. The mechanical prototype was first designed in a Computer Aided Design (CAD) package, and then transferred to a Computer Aided Manufacturing (CAM) software package. The resulting program was then loaded into the Computer Numerical Control (CNC) machining centre where the machine would follow the provided program and manufacture the required part out of aluminium. The CNC machine however was unable to create all of the mechanical parts used in the prototype prosthesis and some manual machining was required to bring the design to completion. The final mechanical system was functionally sound but lacked aesthetic appeal as it is a prototype testing platform and could be improved by changing manufacturing technologies. An alternative to the conventional manufacturing processes available to Massey was laser sintered 3D printing of titanium alloy. By changing from "material removing" technologies to "material adding" manufacturing the shapes of the prototype components would be able to be dramatically changed for both aesthetic qualities and for improved mechanical properties. Based on the prosthesis cost study, the titanium alloy would provide a lighter, stronger and more durable base for the prosthetic device for a similar price.

The prototype was to be controlled by Electromyography (EMG), a method of detecting electrical potential across a muscle when it is activated. When an amputation occurs the muscles controlling the lost limb are commonly left intact and the amputee is able to still control these muscles without any extra training. EMG produces a small differential voltage when the target muscle is activated. The ability to read the changes in potential provides the opportunity to use this signal as a control mechanism. The current market proprietary EMG sensors are part of the reason why bio-controlled prosthetic devices are

out of reach for so many amputees. These sensors cost above $500 each and include filtering and signal conditioning. This cost was dramatically reduced by creating an EMG sensor from scratch. The market EMG sensors output a signal that is suitable for pattern and feature recognition for high-level control. Eliminating the need for this high-level analysis in the control system means that the quality of signal and filtering was not required to be as stringent. Instead of outputting a high fidelity waveform, the conditioning circuit outputs a slow moving averaged waveform that is suitable for the input to a microcontroller. In such a way the overall sensor and conditioning circuit costs were reduced by almost half.

The control system was designed around an "accurate enough" mentality so the developed prosthesis would be able to provide a suitably accurate performance without spending excessive amounts of money. Because the majority of the processing was completed in hardware before the EMG signal reached the microcontroller, the specifications of the microcontroller were not onerous. This allowed the purchases of a relatively inexpensive microcontroller, a further cost reduction. The level of control required by the "accurate enough" control method was very limited, only requiring: two EMG inputs, five motors and five current sense modules. The two EMG inputs are used to activate the prosthesis in the forward and reverse directions. The action is undertaken by the five motors, one for each finger. To prevent the damage to the gripped objects and the motors, the current sensing modules are used to detect both the force and stalling of the motors. The only calculation that the microcontroller is required to perform is to compare the EMG signal and the current sensing inputs to the predefined threshold values.

The overall developed system was able to achieve the desired functionality for an overall price of $3,770. This price is not as expensive as other bio-controlled prostheses and is close to the price of the current hook prosthesis. At this price point a strong case could be made to the third party purchasing organisations to purchase a higher functionality prosthesis to greatly improve the quality of life for the amputee community. Taking into account that an initial prototype is inherently more expensive to produce than a commercial variant due to economy of scale, there is much promise for future revisions to become more competitive in the bio-controlled prostheses market.

The research reported in this thesis has published two articles in two international conference proceedings and also won a runner up best presentation award at one of these conferences.

Acknowledgements

Chapter 1 - Introduction

Amputations are a life changing event regardless of the area or severity of the amputation. After the traumatic event of losing a part of the body, amputees start out on the path of recovery, aiming to eventually return to a normal full life. This process of rehabilitation is long and difficult for every person who goes through it. During this process it is common for an amputee to be fitted with a prosthetic device to try and help them achieve a day to day functionality similar to what they experienced before the amputation. These devices range from passive devices which only serve the purpose to look good, all the way to smart robotic prosthetic devices which closely imitate the lost appendage. This wide range of devices also comes with a wide range of prices with the cheapest costing less than $2000 and the highest costing well over $50,000. Most amputees have their prosthetic device funded by an external source such as a government healthcare scheme or medical insurance; these organisations will commonly do a "needs assessment" to justify the expenditure on a prosthetic device. The result of these assessments is usually a prosthetic device between $3000 and $5000, cheaper if possible.

In most cases the amputee will then generally receive a prosthetic device that is either passive or a mechanical hook prosthesis so they are able to interact with the environment and go back to work. These prosthetic devices however are very limited in their functionality and are not always the best prosthetic device for the amputee's situation. There are some devices on the market that use biometric signals to control a prosthetic hand for a much higher price. These biometric devices are able to further increase the quality of the amputee's life and bring their life closer to achieving normality. The problem with these devices is the cost. Firstly the organisations that provide the healthcare favour economical solutions; secondly the purchasing interests are not willing to pay extra for what they see as a convenience; and finally, the maintenance service has to be accessible, easy and convenient especially for areas and countries that are far from the investors and manufacturing countries. This is where the topic of this study arises, aiming to develop a biometrically controlled prosthetic device at a competitive price point such that the purchasing interests would be more willing to invest and also increase the quality of life of a large portion of the amputee community.

1.1   The Research Topic

The research topic for this thesis is to investigate the viability of creating a low-cost prosthetic device controlled by biometric signals. The designed device would need to provide similar functionality to currently available devices on the market at a lower price point. The motivation behind this research is to bring bio-controlled prosthetic devices to the greater amputee community to increase their quality of life and day to day functionality. This can be achieved by making the device more affordable to the general amputee community and to the organisations responsible for assisting the amputees through rehabilitation. This device aims to replace the hook prosthetic commonly work by many amputees, increasing both their overall quality of life while also trying to reduce the stigma attached to amputation and prosthetic devices.

The prosthesis developed through this research is a product that consists of a series of design and manufacturing techniques and methodologies based around minimising costs, which include computer aided design, computer aided manufacturing, 3D printing as well as both manual and computer

controlled milling and manufacturing processes. To first prove that the prosthesis design would be able to provide the required mechanical functionality and be manufactured, a concept design was created in a 3D modelling system. By conceptualising the design in a digital environment it was able to be manipulated and tested in a virtual environment for no capital expenditure. When the initial design was deemed to be sufficiently functional, a set of finger designs were carried out. A group of finger prototypes were made by using different manufacturing processes such as CNC milling and rapid prototyping by printing them out of ABS plastic. A series of real world tests were performed on the prototype fingers in a relatively inexpensive fashion to make sure the design met the requirements of this research project.

Once the mechanical test platform had been created, the research was then focused on the control system. The control system consisted of EMG sensory input, signal filtering and conditioning circuits and a microcontroller. By using a philosophy of "accurate enough" control, the costs of this section were able to be much reduced as compared to the current market prosthetic control systems. Instead of opting for advanced pattern recognition techniques, a far more simple and reliable control paradigm was implemented by thresholding. By converting the EMG signals into a slow moving amplitude signal and comparing this to a known threshold, there were no onerous calculations to be done thereby enabling the use of a smaller and cheaper microcontroller. The microcontroller is used to detect EMG activation, control the motors which actuate the fingers and detect motor stalling. If the motors stall, they run the risk of damaging themselves. For this reason, there is a current sensing module for each motor. The control system uses the current sensing to detect when the associated finger has reached its limit and has exerted as much force as it is able to safely. The motor is then switched into an active braking mode to keep the fingers gripping the object. This control system allows for a basic tense and release grip which will provide an effective functionality to the amputee while still adhering to the accurate enough mentality.

An evaluation was also made on the prosthetic prototype system regarding cost, functionality and possible improvements. With the fast development in science and technologies and the continually decreasing cost for small sized smart controllers, more hand grasping functions can be realised using this prosthetic system.

1.2 The Scope of Research

The research in this thesis is limited to the development of a single workable prototype test platform for amputees with a wrist disarticulation. This test platform will be used as a proof of design concept for showing the capabilities of a device developed by using cost reducing design techniques. The cost distribution will be allocated as per current market distribution. Any items that are covered in a separate costing area such as batteries will be excluded from the device's overall cost. The developed device needs to be considered a complete system from physical functionality to electrical control and demonstrate an acceptable level of overall functionality. The specific biometric control signal that will be focused on in this research is EMG, using the muscles in the residual limb as an actuation method will attempt to make the control of the developed device more intuitive.

1.3   Research Objectives

Objectives of this research are to increase the quality of life experienced by the majority of the amputee community suffering from upper limb amputations by decreasing the exorbitant cost of bio-controlled prostheses. The solution will be in the form of a workable prototype proof-of-concept test platform which takes EMG signals as an input and produces a mechanised response in the fingers produced for cheaper than current market bio-controlled prostheses and closer to the mechanical prostheses price. The result of this outcome would prove that it is not necessary to charge high prices for the privilege of a bio-controlled prosthesis and provide an initial platform which could then be further developed into a saleable prosthesis.

1.4   Organisation of Thesis

This thesis is structured to provide a logical path through the research conducted. The thesis starts with background information in the form of a literature review to allow the reader to familiarise themselves with the current state of amputation, prosthetic devices currently used by the amputee community, available materials able to be used in development and finally the use of EMG as a control system in prosthetic devices. Chapter 3 provides insight into the current market numbers, causes of amputations and types of amputation. The mechanical system design process is described in Chapter 4. This process shows how and why each part was developed in the way that it was and the decisions that were made to reach the final prototype design. Chapter 5 are the available manufacturing methods and facilities for producing the prototype of the prosthesis. This is necessary as the manufacturing of the prototype is required to be performed in-house to reduce the costs and enable rapid revisions to the design. Chapter 6 and 7 will discusses the electrical, electronic system and circuit design and the realisation of each module required by the prototype. These modules include the EMG circuit, filtering, signal conditioning, control and motor driver circuits.

Chapter 8 is the cost analysis of development as well as the effectiveness of the design and manufacturing methodologies that comprise the final prototype. Chapter 9 and 10 of the thesis focuses on the outcomes and results found through this research, the discussions and possible further improvements. The findings are then reviewed with regards to the suitability of the first prototype and the sections of the design that are able to be improved for future revisions. Other research opportunities that were found during this research are also discussed. This thesis then finishes with the study conclusions and any additional reference material included in the appendices.

Chapter 2 - Literature Review

There are many types of amputation and a multitude of causes for receiving an amputation. Both the upper and lower extremity has multiple common amputation levels where the largest residual limb is retained for the higher functionality. The focus of this review is based around an upper limb amputation caused by trauma, disease or infection. There are four main types of prosthetic devices: passive, mechanical, myoelectric and robotic ones.

2.1 Types of Amputation

Many injuries and medical conditions lead to amputation, standardised set of terms are set to describe the different lengths and locations of an amputation. Amputation could be caused by trauma to a limb, cancerous tumours, congenital health problems, infection of an open wound and diabetes. The different levels of amputation in upper and lower extremities are shown in Figure 2.1 (Burns & M.D., 2011).
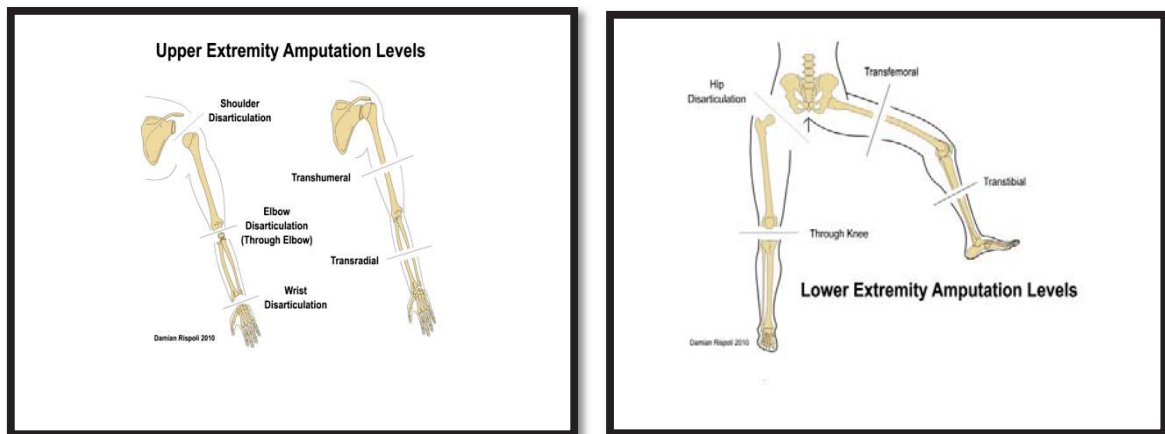
Fig. 2.1- Upper Extremity Amputation Levels (Left) and Lower Extremity Amputation Levels (Right)

2.1.1 Upper Extremity Amputation Levels

The following types of amputation shown in Figure 2.1 are common to the upper extremity of the body:

1. Shoulder Disarticulation
2. Transhumeral
3. Elbow Disarticulation (Through Elbow)
4. Transradial
5. Wrist Disarticulation

In addition to these common levels of amputation, fingers or partial hand (Transcarpal) is also commonly performed if the injury/condition allows. (Michigan, 2012)

2.1.1.1 Shoulder Disarticulation

A shoulder disarticulation is where the limb is separated at the ball (glenohumeral) joint and the whole limb below this point is excised. The common causes for a shoulder disarticulation are: tumour control and serious traumatic injury. This type of amputation is only performed if there is no option to salvage part of the limb, when this type of amputation is performed the impact on the patient's life is major. Due to the nature of this major change, prosthetic rejection rates are high because of many factors such as poor suspension, increased weight and inadequate function. (University of California, San Francisco, 2011)

2.1.1.2 Transhumeral

The Transhumeral amputation occurs between the elbow joint and the shoulder joint; within 6.5 cm of the elbow joint is preferred (Heikki Uustal & Edgardo Baerga, 2004), cutting across the humorous. The residual limb maintains maximum possible length to provide a long lever arm which assists in retaining the highest functionality possible. This method of amputation is preferable to the shoulder disarticulation due to the residual limb that remains. The residual limb is then able to be used for mounting prosthesis via a specially moulded socket. With the long lever arm, cable control difficulty is reduced and it is possible to gain some humeral rotation to assist with prosthetic movement. (University of California, San Francisco, 2011)

2.1.1.3 Elbow Disarticulation

An elbow disarticulation is defined as an amputation through the elbow joint, conserving the entire humorous and excising the remaining limb below the joint. This amputation is preferable to the Transhumeral amputation because it retains the ends (condyles) and it occurs through a joint, causing less disruption to tissue and bone around the amputation site. These condyles allow for a much better fit of a prosthetic device and allow much more of the humeral rotation to be transferred to the prosthetic. The major causes for an elbow disarticulation are trauma, cancer/ tumours and vascular complications caused by disease. Another advantage of this type of amputation is the enhanced prosthetic fit; the prosthetic can have a higher degree of self-suspension due to the socket fit around the condyles. (Heikki Uustal & Edgardo Baerga, 2004)

2.1.1.4 Transradial

A Transradial (also known as a Below Elbow) amputation has three levels: very short, short and long. These are defined as:

Very short: residual limb length of less than 35%

Short: residual limb length of 35% to 55%

Long: residual limb length of 55% to 90%

The Transradial amputation is the preferred amputation in most cases. Keeping with the pattern of the previous amputation types the longer the residual limb length, the more preferred the amputation type is. The long residual limb can retain from 60°-120° rotation while the shot below elbow residual limb retains less than 60° of rotation. For bodily operated prosthetics a long residual limb length is optimal to

18

allow the highest level of functionality and in most cases allows the patient to perform physically demanding work. However if the goal is an externally powered prosthetic device, a residual limb length of 60-70% is preferred as this allows for high functionality and cosmetic appearance. (Heikki Uustal & Edgardo Baerga, 2004)

2.1.1.5   Wrist Disarticulation

Wrist disarticulation spares the distal radial ulnar movement and allows a more complete control of the position of a prosthetic. This amputation however is not always preferred in place of higher amputation level as the extremely long residual limb may decrease functionality or cosmetics of a prosthetic device. However there are some advantages of this amputation level over the Transradial level, for instance the residual limb can be used effectively without a prosthetic, a bodily operated prosthetic device is easier to manipulate and the prosthetic device itself is able to weigh less and can be self-suspending. (Heikki Uustal & Edgardo Baerga, 2004)

2.1.1.6   Transcarpal

Transcarpal amputation occurs as a partial amputation of the hand or fingers. Special consideration needs to be taken when considering this amputation level to allow enough residual sensation and movement. As an alternative option, reconstructive surgery should be thoroughly considered as if the amputation is not done correctly, an aesthetically pleasing and functionally acceptable prosthetic device will become unlikely. There is little reason to salvage fingers if there are no metacarpals to provide a pinch action; at this point a wrist disarticulation is preferred.

2.1.2   Lower Limb Amputation Levels

Amputation of the lower limb or limbs is more common than the upper amputation levels; however the upper amputation levels produce more of an impact on the daily life of the patient. This is primarily due to the major reduction in the ability to perform manipulations of the outside world. In the period between 1989 and 1992 the most common cause of amputation was vascular disease (70) followed by trauma (22) at slightly under a third the number of vascular disease. As the age groups increased, the highest common cause of amputation changed along with it. In young children the most common cause is congenital disorders, as the age group increases to young teenagers the most common cause is cancerous tumours. Between 15 and 45 years old the most common cause changes to trauma and 45+ becomes vascular disease.

2.1.2.1   Hip Disarticulation

A hip disarticulation is similar to a shoulder disarticulation in definition with the key difference being the location on the body. Any amputation that retains less than five centimetres of a residual limb can be classified as a hip disarticulation.

The most common type of prosthesis associated with a hip disarticulation is Canadian hip disarticulation prosthesis. This is anchored around the pelvis hemisphere on the non-amputated side and encloses the amputated hemisphere, leaving an opening for the non-amputated leg to pass through the prosthesis.

2.1.2.2 *Transfemoral*

The Transfemoral amputation occurs partway between the knee joint and the hip. This amputation is preferred to the hip disarticulation if possible due to the length of the residual limb. The extra length allows for a much better power transmission to the prosthetic device as well as a higher level of control, this control is especially apparent in the walk gait shown by the patient. Prosthesis for this amputation level consists of a suspension socket to receive the residual limb's stump; it usually has an artificial knee and foot attached to aid in walking.

2.1.3 Knee Disarticulation (Through Knee)

Knee disarticulations are similar to elbow disarticulations where the surgery causes less disruption to the surrounding soft tissue and bones. In this case a prosthetic uses the condyle of the femur to bear weight and the socket is constructed such that rotation is unable to occur during normal operation. There are however, problems with fitting prosthetic devices to knee disarticulation due to the centre of rotation need to act through the knee joint. This is required to attain a symmetrical walking gait, aesthetic properties while sitting and a more stable knee platform. Most prosthetic solutions do not provide this, however one solution called the four-bar polycentric knee helps toward a solution.

2.1.3.1 *Transtibial (Below Knee Amputation)*

Transtibial amputation is far more preferable than the higher levels of amputation due to the retention of the knee. Having the knee salvaged means that the patient is able to maintain a controlled gait and a steady walking platform. The prosthetic devices that are fitted for this amputation level are not overly technical due to only having one rotating joint. Some prostheses have even gone so far to remove this rotating joint in favour of a springing material, providing a possible advantage for athletic competitors.

2.2 Types of Prostheses

There are multiple types of prostheses for most amputation levels ranging from prosthetic devices that are completely focused on providing an aesthetic normality to devices that are focused on high order functionality. Each patient has different expectations from a prosthetic, this has caused a need for multidiscipline prosthetic devices taking the advantages from two or three types and combining them into one device.

2.2.1 Passive

A passive prosthetic is purely focused on the aesthetic needs of the patient. With no added functionality at the end-affecter, this prosthesis can be used as a lever and a contact point when lifting and manipulating the environment but cannot grasp or hold any object by itself. This type of prosthesis is shaped as much like a real one as possible to reduce the awareness of the people around the patient. By reducing the awareness of the injury, some of the social stigma that can be attached to this type of affliction may be reduced.

Passive prosthesis can be made to differing lengths, skin tones, profiles and sizes to try and ensure a fit that is very close to looking like the remaining part of the limb. Another option for a passive prosthesis is using a standard hand shape without the colour pigmentation or specific materials that look like skin and then covering this prosthetic with a glove. The glove itself can either be a commercial glove such as the

fashionable female dress gloves or it can be a specialized glove made out of composite materials to imitate skin.

2.2.2 Body Powered

Body powered prosthesis use the residual limb in some form to actuate a mechanical system. The mechanical system activates the prosthetic end-affecter to help the patient manipulate the environment. The major advantage of this type of system is the ability to pinch or grasp an object with the end-affecter. Having the end-affecter under control allows the patient to complete certain tasks like carrying in the groceries, picking up a briefcase and grasping handles.

Having the ability to manipulate the environment affords the patient a new sense of independence. Not all tasks will be able to be done individually. There are still tasks that require fine motor skills to complete like eating with knife and fork. This type of prosthesis is the choice for most working class patients who are still active members of the workforce. The reason is the level of functionality provided by the prosthesis is sufficient in most cases to continue fulfilling the same role.

The disadvantage of this type of prosthetic is that for upper extremity devices a pulley system is needed to activate the claw end-affecter. After wearing the pulley system for extended periods of time numbness or pain will be developed even without sleeping on the shoulder where the harness has been mounted.

2.2.3 Electrically powered (Externally Powered)

The prosthesis in this category do not use the body in any way to exert power through the prosthetic device. This does not imply that the body does not play a part in the use of this type of prosthesis; This type of prostheses may use some bodily signals to activate the prosthetic response.

The advantages of this type of prosthesis when compared to the mechanical ones are: Electrical power can provide high grip strength, eliminate the need for harness and cable, and increased functionality. However there are some disadvantages that have to be mentioned. The amputee must consider the battery life in daily use and the entire device becomes heavier due to the need for batteries.

Depending on the patient there are different types of electrically powered prostheses to suit each individual person's needs. The common types of electrically powered prosthesis are: electric switch prosthesis, myoelectric and robotic prostheses.

2.2.3.1 Electric Switch Prosthesis

The electric switch type prosthesis is actuated by the amputee, using the residual limb to press against an electrical switch. This could be a pressure switch, potentiometer or other convenient switching device that the amputee can activate. Each switch can have one or multiple functions depending on the combination of switches activated. This allows the amputee to manipulate the prosthetic device using the limb in a specific set of ways as well as providing a stable control platform. There is comparatively little training required to operate this type of prostheses because all of the switches have a set function.

2.2.3.2 *Myoelectric Prosthesis*

The difference between the electric switch and the myoelectric prosthesis is the way they are actuated. Whilst the electric switch type is actuated by the physical press of a switch, the myoelectric prosthesis is actuated using the process of electromyography. Electromyography is used to detect muscular impulses from the surface of the skin, these impulse are then classified and used to control different actions performed by the prosthesis. Myoelectric prosthesis is popular because the sensors are non-invasive and making the amputee continue using the muscles helps reduce the atrophy effect in the residual limb.

An advantage of this type of prosthetic is the ability to program a large range of different manipulations in relation to the myoelectric signals received. This degree of customisation enables amputees who have specialist tasks required by either their work or hobbies to request unusual grip types.

2.2.3.3 *Robotic Prosthesis*

Robotic prosthetic devices are similar to myoelectric prosthetics with three differences: being able to "feel", using a controller to control the device and price points. Normally robotic prostheses contain many sensors such as accelerometers, pressure sensors and absolute encoders so the controller is aware of movement, position, grip pressure, temperature etc.

A bio-signal driving robotic prosthesis is usually coupled with targeted muscular reinnervation (TMR). TMR is a process where the motor nerves affected by the amputation process are surgically moved to another large muscular group. This process enables a small region of the large muscular group to be activated when the amputee thinks about moving what the nerve was previously attached to (The index finger for example). This now enables a sensor to be placed accurately on the location of reinnervation to detect any attempted movement of the lost extremity. Being so precise enables a much finer control of the prosthetic device.

A new procedure called targeted sensory reinnervation (TSR) is emerging as an additional procedure which is trying to enable sensory feedback from the prosthetic device to the user. The process involves rerouting sensory nerves to the skin instead of the muscle. This development will enable the amputee to feel sensory inputs such as temperature and pressure which occur on this portion of the skin as if they were occurring from the prosthesis. With further development this technique may enable the amputee to gain a relatively normal feel and use of the prosthetic device.

The bio-controller acts as the brain of the device, it does the processing of the input signals from the sensory equipment such as the electromyography sensors and any physical sensors. It then translates these input signals, calculates the desired response and then sends out the signals to the physical actuators.

2.2.4 **Hybrid Powered**

Hybrid powered prosthetic devices use a combination of body and electric power to achieve actuation. This system takes the strong grip strength of the myoelectric prosthesis, reduced weight of the basic electrical powered device and reduces the harness system of the mechanical system. This combination provides a large functional range with advantages of all prosthetic types without many of the disadvantages of a specialized type. The hybrid device does still have some disadvantages like the

reduced specialization in programmability and is still required to use the harness system to actuate some of the functions.

2.3 Prosthesis Design Process and the Related Cost

The costs associated with amputation are not only the one off cost of a prosthetic device. There is a process that needs to be followed by the prosthesitist to ensure that the amputee gets the best treatment and receives the best prosthetic device to suit their lifestyle and residual limb. Every hour that the patient spends with the clinic is an expense and the amputee is required to see the prosthesitist from time to time for the maintenance and creation of new prosthesis. The process normally consists of five stages: assessment, design, fabrication, trial and final fitting.

2.3.1.1 Assessment

Every new patient to a prosthetics clinic needs to be assessed to try and find the best prosthetic solution to suit their needs. In upper extremity amputations the prosthetic is designed with multi functionality in mind as the hand bends and twists to complete tasks while lower extremity amputations are designed mainly only to step. Every patient is different in their needs, personality and lifestyle, and therefore they all need to have different prosthetic designs. For example different professions will require different performance from a replacement limb; a typist will require less durability and grip strength than a builder. By conducting an interview with the patient the clinic can ascertain their history, range of movement, strength and their overall goals.

2.3.1.2 Design

This is where the information gained in the interview is put to use, allowing the prosthesitist to decide on the required durability of the prosthetic parts. There are many different parts made to differing strengths and durability by many manufacturers to provide a wide range of options. The options can range from plastic for light users to aluminium or alloys to increase strength. The aim is to provide a long-lasting prosthesis that enables the patient to continue their daily routine with minimal disruption.

2.3.1.3 Fabrication

In the first visit to the clinic, an imprint of the residual limb is taken by either using a traditional plaster cast or by using a plotting device called the Tracer. From this imprint of the residual limb, a socket can be created using plastics (e.g. Duraplex) and resin from the clinic. If a digital imprint was created using a Tracer for example, a central fabrication facility will send a check socket to the clinic to test with the patient. The socket can have different lamination types and this is where some differential costs can occur, for instance you can laminate with Dacron, cotton, nylon, Kevlar and carbon fibre. The lamination is chosen to best suit the patient's needs, carbon fibre for strength or fabrics for weight and comfort.

Once the socket is complete, components are then able to be fitted to the end, the set of components are the principal difference between patients. Each set of components are prescribed to meet the functional requirements of the patient (valves, clamps, pumps etc.).

2.3.1.4 Trial

The prosthesis gets fitted with a temporary set of components to enable the clinic and the patient able to evaluate the "fit" of the component set. At this point the prosthesis should have all of the functions

desired by the patient and the clinic with some adjustment and alignment components built in. These adjustment components allow the clinic to optimise the prosthesis and account for changes such as changes in the volume of the residual limb, range of motion and strength. This can be considered as a reassessment point as the patient may change between the initial assessment and the final fitting.

2.3.1.5 *Definitive Fitting (Final)*

This is the point where the patient is fitted for a more permanent prosthesis where the clinic has finished their adjustments. The socket has a final lamination which is the same as the fabrication stage but it adds another layer to the socket for strength and stability. The trial components are taken off the device at this point and the final components are fitted to the device, the final components are similar but simpler in the fact that there is less adjustment needed. The final stage of this step is to order the final end-affecter for the patient.

2.4   Materials Commonly Used for Prosthetic Devices

Each prosthetic device is different to cater for the special needs of the patient. For this reason different materials need to be used for the components that make up the prosthetic device. Below is a list of materials that are commonly used in making a prosthetic device and the reasoning behind using them.

2.4.1   Electroactive Polymers

Electroactive polymers are not currently used in the production of prosthetic devices; however they do show some promising characteristics that may allow them to become useful. Electroactive fibres can change their mechanical properties when an electrical signal is passed over them, for example the length can change or the fibre may become rigid when it was flexible initially. These fibres could potentially be used to emulate tendons in the fingers, removing the need for moving motors to pull the fingers into a gripping pattern.

2.4.2   Carbon Fibre

Carbon fibre can be used in the terminal device as well as in the socket for the residual limb. Carbon fibre is predominantly used in a composite form to provide strength to plastics without adding excess weight. As mentioned above, when carbon fibre is used in the socket the main motivation is to add strength to the existing socket material without adding excessive weight. The reason carbon fibre is used in place of metal alloys is the ability to mould and form it to any shape easily where metals need to be cast or machined. The motivation behind using carbon fibres in the terminal device is for durability and weight reduction of surface components such as fingers and the palms.

2.4.3   Aluminium

Aluminium is used in the majority of prosthetic devices due to the low weight vs strength ratio. The components that aluminium is commonly used in are the structural based components; these include finger "bones" and the palm structure. Plastic components can be interchanged with aluminium components depending on the requirements of the patient.

2.4.4   Plastics

Plastic is used in many prosthetic devices because it is very lightweight and easily formed, mainly the myoelectric, passive and the robotic end-affecters. Plastics excel at providing aesthetically pleasing

terminal devices but can lack the strength or environmental resistance required by the patient. The components where plastic is typically found are coverings for the palm and fingers, due to these being the environmental interaction surfaces some specialist patients are unable to use plastic coverings.

2.5   Electromyography as a Control Method

Electromyography (EMG) is able to gain electrical signals from the skin and be used in the control of a prosthetic device. The application of EMG, however, is far out of the reach of most prosthetic users due to the expensive setup procedure and the required intensive training. The signal processing and data acquisition phase of the EMG is done on proprietary hardware, using many sensors along with powerful computational equipment thus driving up the price of the solution. To avoid this increase in price, there is a need to develop a more economical solution that is attainable for the day-to-day use of the general amputee community.

2.5.1   Application of Electromyography for prosthetic devices

2.5.1.1   Non-invasive control method

EMG is a method of using a series of electrodes on the surface of the skin to gain the electrical potential released by the muscle fibres contracting beneath when motion is performed. This system can be used on able-bodied people as well as amputees as the amputee is still able to perform an isometric contraction of the muscles of the residual limb. EMG is called a non-invasive method because it does not require any entry into the body to gather information. Comparatively a neuromotor sensory array requires a sensor to be implanted directly onto a person's cortex via invasive surgery to be able to gather the neural information needed and is known as an invasive method. (Hochberg, et al., 2006)

2.5.1.2   Effective control

There are many different ways of using EMG signals to control a prosthesis and many different uses once this control is achieved. The most popular method of control is called pattern recognition. This type of control is achieved by using multiple channels of electrode signals, sending this data to a computation program via filtering and then looking for patterns in the waveform. This data acquisition hardware, filtering hardware and computation software are all expensive proprietary equipment which is the main cause of the price of this type of control being so high. The computation program needs to be trained to recognize the signal patterns and then assign each pattern to a known movement, the data is compared to these predefined patterns and a decision is made. This is then sent to the prosthetic device to perform the action that was programmed in response to that specific decision. It has been shown that up to 10 movements can be accurately classified using pattern recognition method in able-bodied patients and up to 6 in amputees (Daley, Englehart, Hargrove, & Kuruganti, 2012).

2.5.1.3   Integration into prosthetic devices

For EMG to be a viable form of control, the entire system must be able to be integrated into a prosthetic device without making it cumbersome and restricting. As outlined above the pattern recognition system relies on a computer to process the data and make the decision on what movement to perform. This would imply that the prosthetic device would need to be attached to a computer at all times, however with the advancement of microcontrollers this processing can be brought on-board the prosthesis and the wiring becomes self-contained (Lock, Simon, Stubblefield, & Hargrove, 2011). One possible way to attach the EMG electrodes to the skin is via a gel liner with the electrodes implanted within its structure. The wires all run through the gel lining to the edge where they are able to be connected to a microcontroller. This presents an easy donning and doffing method for the amputee without much of the hassle of traditional EMG controlled Prosthetics. This however creates a challenge in placing the electrodes in the optimum position on the muscle every time and can cause the strength of the EMG signal to fluctuate. These fluctuations can cause problems in the pattern recognition process and make control a more difficult task. (Lipschutz & Lock, 2011)

2.5.2   Hardware Requirements for EMG

2.5.2.1   Sensory Equipment

To gain the signals needed for electromyography, special sensors need to be used in conjunction with instrumentation amplifiers. The expected signal strength of the myoelectric signals is in the range of micro/nano volts. The electrode pads need to be made of a highly sensitive material such that they produce negligible resistance; an example is silver chloride. Before a pad is applied, the skin needs to be prepared using a conductive gel to reduce the resistance of the skin and help the signals pass through to the electrode. Three electrodes for each channel are required: two for differential signals and one electrode for a driven grounding circuit for the body (Texas Instruments, 2007). Each of the electrodes needs to be connected to the processing equipment via a low impedance cable and connected to the input of an amplifying circuit. Some post amplification filtering may be needed to clean up the output of the amplifier before passing the signal to the computational hardware.

2.5.2.2   Computational Equipment

The computational side of electromyography can vary widely with some processing being completed on high powered computers and others being completed on microprocessors. Desktop computers are much more powerful than microprocessors but lack the advantage of being highly portable. Because microprocessors are portable and consume much less power they are the choice used in prosthetic designs. Microprocessors are capable of performing the necessary calculations per second to analyse the stream of data coming from the sensory equipment.

2.5.3 Control paradigms associated with EMG

There are different methods of obtaining control over a system using the data from EMG sensors. Some of these methods are outlined below along with the pros and cons of each method.

2.5.3.1 *Shannon Entropy - (Potluri, et al., 2011)*

Methods of recognition – This is a method of using threshold control however instead of using an absolute scale the entropy is used as it is independent of the absolute scales of time and frequency.

Number and location of electrodes- Between 3 and 16 electrodes can be placed on the motor points for index, middle and ring fingers

Signal processing and statistical analysis of raw data - ADC Converted with a 10 bit resolution, Compare to threshold. Feed into PI loop trying to reduce error to zero, Via UART to Matlab

Strength of signal – -5mV to +5mV

Price - $10,000-$15,000NZD

Pros – Small microcontroller based prosthesis for implementation, very simple proportional control which eliminates the need for absolute scales as it uses entropy instead.

Cons – This being a type of threshold control there is very little in the way of speed of actuation control. The equipment for this approach is very expensive.

2.5.3.2 *Support Machine Vector – (Leon, Gutierrez, Leija, & Munoz, 2011)*

Methods of recognition – Uses a single or set of hyperplanes in high-dimensional space to classify patterns within a set of data.

Number and location of electrodes – 4 bipolar electrodes placed on: Extensor digiturm, Extensor carpi radialis lungus, Flexor carpi radialas, Flexor Carpi ulnaris

Signal processing and statistical analysis of raw data – 50% overlapping 250ms windows, feature extraction (Autoregressive, Root Mean Square and Discreet Fourier transform)

Strength of signal - 50μV-5mV

Price – 2,500 NZD

Pros – The Support Vector Machine produces a more effective classification technique, this along with feature analysis retain a higher accuracy and offer a relatively simpler structure.

Cons – Support Vector Machines are harder to train and implement compared to the Linear Discriminant Analysis. This research only looked into the movement of the hand as a whole, so the control of a single finger might not fit within its effective use.

2.5.3.3 *Linear Discriminant Analysis – (Lock, Simon, Stubblefield, & Hargrove, 2011)*

Methods of recognition – This is a simple to train and simple to implement classifier

Number and location of electrodes – 4 bipolar placed on the wrist flexor/extensor and equidistant from the elbow and wrist on the forearm.

Signal processing and statistical analysis of raw data - Sampled at 1000Hz using a 16 bit ADC converter, Pre-filtered between 10 and 500Hz, Windowed at 256ms and then pattern recognition is performed. Window slides for continuous decision making.

Pros – This is a high accuracy, low response time and intuitive control interface with relatively simple signal processing demands.

Cons – This method had not been tested on a physical prosthesis stated in the research article.

2.5.3.4   Feature Recognition - (Leon, Gutierrez, Leija, & Munoz, 2011)

Methods of recognition – This is a broad covering control system. This can be made up of pattern classifiers such as LDA and SFV but also made up for statistical patterns such as zero crossings and change of sign of slope.

Number and location of electrodes Recognition – 4 bipolar placed on the wrist flexor/extensor and equidistant from the elbow and wrist on the forearm.

Signal processing and statistical analysis of raw data – Feature recognition works with the majority of the signal processing methods outlined in this section.

Pros – Feature recognition provides the ability to recognize different movements within the same muscle rather than just one movement to trigger all response.

Cons – This method requires a large deal of signal conditioning along with a computationally heavy classifier.

2.5.3.5   High density EMG – (Daley, Englehart, Hargrove, & Kuruganti, 2012)

Methods of recognition – In this method many electrodes are used to map all of the actuation that occurs in the muscles of the arm. From this data it is much easier to pinpoint the optimum points for electrodes to be placed along with the ability to discern many different movements.

Number and location of electrodes – Electrodes are placed in a grid formation across the patients forearm

Signal processing and statistical analysis of raw data - Sixth order Band pass Butterworth filter between 10 and 500Hz, 60Hz notch filter to remove power line noise, sampled at 2000Hz

Price – Very high due to the use of many electrodes and a data acquisition system that can take many channels of data simultaneously.

Pros – This method can accurately define the optimal electrode placement sites on the forearm and then accurately classify the type of movement that has been produced in both able-bodied subjects and amputees.

Cons – This requires a large number of electrodes and high computation to effectively use this method. This would make the cost of implementing this method very high.

2.5.3.6   Threshold – (Matrone, Cipriani, Carrozza, & Magenes, 2011)

Methods of recognition – This method is used when there is a threshold set as a lower value for the EMG signal to put it at "rest" once the EMG signal rises above this point, the prosthesis is activated.

Number and location of electrodes – 2 or 4 bipolar electrodes placed on: Flexor carpi radialis, extensor carpi radialis, Flexor carpi ulnaris and extensor carpi ulnaris

Signal processing and statistical analysis of raw data - Sampled at 250Hz and integrated over 20ms windows

Price - $3500 NZD

Pros – This is a viable approach for non-precise power grips to be performed by prosthesis and provided a successful mapping of voluntary muscle movements to motor controls on the test prosthesis.

Cons – Precision grasps were more difficult than power grasps in this method. It was also tested on able-bodied patients only. This could introduce problems in the future if an amputee were to follow this method

2.5.3.7 *Proportional – (Fukuda, Bu, & Ueno, 2010)*

Methods of recognition – This method uses a proportional controller so the higher the amplitude of the EMG signals taken from the sensors is the faster that the prosthesis actuates.

Number and location of electrodes – 2 single differential surface electrodes placed on the Flexor carpi radialis and extensor carpi ulnaris

Signal processing and statistical analysis of raw data - Sampled at 1 KHz, Rectified, Low pass filtered, resample at 20Hz.

Price - $3000+ NZD

Pros – the EMG signals are as representative of a person's intent as a force measure. This method provides an intuitive way for the user to define a rate of movement so that they have control over how tight the grip is and fast the grip is formed. It also has relatively simple signal processing and retains control of the movement speed.

Cons – The proportional control of the signal is a much slower process than the threshold counterpart and this only controls the grip strength of virtual prosthetic, not an individual finger in its own right.

2.5.4 Other Methods of control

Passive control was the first type of prosthetic, for its control it had to be positioned using the other hand and was used primarily for cosmetics. Physical control is where the amputee wears a harness and manipulates the control cable of the device with their body to realize activation of a claw or similar mechanism. EMG control started as early as 1948 for control of upper body prosthesis. Proportional Integral (PI) control is based primarily on the EMG control method however it takes the signals and puts them into a PI controller for the applications such as regulation of force in prosthesis. Fuzzy logic control is also usually based on the EMG signals but instead of using a set of fully defined actions resulting from different patterns, fuzzy logic can be implemented to give a more flexible control system (Zecca, Micera, Carrozza, & Dario, 2002). Inter corticullar control is a very new type of control as the ability to make sensors small enough to be surgically placed on the brain has only recently been achieved. Intercorticullar control system reads the signals directly off the person's brain rather than trying to detect them at the skin. This method is an invasive technique and is only used in extreme situations such as with people with the likes of tetraplegia and locked-in syndrome (Hochberg, et al., 2006). Displacement motor drive control is used for positioning prosthesis relative to the residual limb of an amputee. This is still in the experimental stage and involves implanting a magnet in the residual limb of an amputee, then surrounding it with hall-effect sensors to determine the displacement from the origin. This displacement is then used as an input to a motor which is driven until the displacement of the prosthesis from the residual limb is zero (Rouse, Nahlik, Peshkin, & Kuiken, 2011).

2.5.5 Effectiveness of control

Passive control is not a very effective control method because it requires the use of the person's other hand to position the prosthesis, restricting the use of the able-bodied hand for other possibly more important tasks.

Physical control is the most commonly used method due to its relatively cheap implementation, the strength of grip, its ease of use and the easy donning and doffing methods. This type of control however only provides the gripping capability for one "finger".

EMG has proved effective in many different implementations and settings. The use of EMG has been shown to be able to not only classify different types of movements that an arm performs, but also to provide an analogue to the physical performance of a grip's strength. Different signal processing and interpreting methods continue to expand the capabilities of EMG control and make it one of the most versatile control methods in this review.

Inter corticullar control is a very expensive but very powerful control method. The signals obtained from the electrodes placed on the brain are a much more direct indication of what the intended motion was to be performed. With our ever-expanding knowledge of how the brain works, this control method could prove to be the most powerful method of control for prosthesis. The major drawbacks such as invasive surgery however will likely limit the use of this method to extreme cases (Hochberg, et al., 2006).

Displacement motor drive is still in the development stage; however its use is limited because it depends on a physical implant on a residual limb. This implies that the control would only be able to be used to control the overall orientation of the prosthesis on a person. There is no way to adapt this method of control to be able to include the actuation of individual fingers or complex prosthetic tasks.

2.5.5.1 Comparison to EMG

Passive control is the most basic control in that it must be pre-positioned before use. This method is cheaper than EMG by a long way, but almost no control over the limb is achieved.

Physical control is still much cheaper than EMG as it is a fully mechanical system consisting of the prosthetic device with a pulley harness system. The physical system is limited to at most 2 degrees of freedom (DoF) while EMG has been shown to achieve 16+ DoF's.

Inter corticullar control is by far more expensive than EMG and involves invasive surgery, however this method may prove to be much more powerful than the EMG however more studies have been performed as there are many more signals to be obtained and processed from the brain compared to the skin.

Displacement motor drive control is not able to provide prosthesis with any more than 1DOF as it relies on a rotation displacement to actuate its control. This could be used in conjunction with EMG or inter corticullar control, but not by itself very effectively.

2.5.5.2   Price

Passive – Very low cost as there is little to no control associated with this method

Physical – low cost as the entire system is mechanical

Inter corticullar – Extremely high as the sensory array to be used is very small and used to send signals through the skull to a set of signal processing equipment. Since the signal from the brain is so complex and small, the processing equipment must be highly sensitive.

Displacement motor drive – Low cost as this system is comprised of a magnet, a set of hall-effect sensors and a microcontroller to do the processing.

2.5.6   Testing of control methods with an amputee

2.5.6.1   Control method testing

Only a few methods of testing were actually performed on amputees and this raises questions on the feasibility of some of the testing methods and whether they will transfer from an able-bodied subject to an amputee.

Chapter 3 - Preliminary Amputation and Prosthesis Cost Investigation

3.1 Nature of Amputee Environment

This research is based around providing a low-cost prosthetic device to the hand amputee community. To investigate the environment associated with amputation some patient data was received from a rehabilitation clinic and as to their gender, injury and the cause of the injury as shown in Fig. 3.1. This would shed light on the distribution of injuries and the most common cause for amputation as well as the gender differences.

Gender	
Female	19
Male	107
Injury Cause	**Number of Injuries**
Work	31
Diabetes	21
Pvasc	34
Farm Injuries	7
Gunshot	3
Cancer	5
Accident	9
Type of Amputation	**Number of Amputations**
Left Above Knee	11
Right Above Knee	4
Left Below Knee	38
Right Below Knee	32
Right Above Elbow	3
Right Below Elbow	7
Left Above Elbow	1
Left Below Elbow	10
Hand	2
Foot	1
Knee	3

Fig. 3.1 - Amputee Survey Numbers

The above results show that the ratio of genders is heavily biased in favour of the males. This is generally attributed to two things: females usually maintain a better quality of health and are less prevalent in high risk industry jobs. Females generally look after themselves better than males. They see their physician more often and therefore get any problems seen at earlier stages before the problem gets to

the point of requiring an amputation. Due to the lower number of females in heavy industry there are less amputations resulting from accidents and severe trauma. With this balance of genders it is able to be deduced that the majority of prosthetics are harder wearing and functionality focused.

The portion of injury causes of the survey shows that the distribution between accidental injury and medical causes such as diabetes is slightly in the favour of the medical causes. The total ratio is 60 medical causes and 50 accidental/ traumatic causes for amputation. This ratio lends itself to a conclusion that there is no significant bias to either medical or traumatic causes of amputation.

Finally, the types of amputation that occur most often are below the knee amputations on both the left and right legs. Generally these are attributed to the medical causes such as diabetes or vascular problems, whereas the accidental amputations are not caused by the same situation and therefore are not limited to specific bodily areas. This explains that high focus on lower limb prosthetic devices in the market and there is a higher demand as well as a guaranteed need for these prosthetic devices.

3.2   Current Market Prices

At the beginning of this research, the target had to be set to judge the success of the research outcome and the finally developed prototype. To determine a target figure, a combination of current market prices of myoelectric devices and government funding for amputees were used. These government numbers are not readily accessible to the general public. Therefore the numbers given are taken from the only source able to be found, the government of Alberta, Canada. The price of the current devices on the market was used as a deciding factor in the target price because they are the benchmark for any future devices entering the market. The government funding was also included because they are the funding body for most accidental injuries resulting in amputation which is the focus point of this research as the medical causes are usually limited to lower limb prosthetic devices. For this device to succeed as a low-cost option to amputees it would need to cost less than the government contribution limit while still increasing the quality of life and functionality of the amputee.

Current market prosthesis	Price
System Electric Hand Digital Twin®	$4,094.00
5 Finger Prosthesis	$5,520.80
Transcarpal Hand Digital Twin®	$5,544.00
Otto Bock Electrohand 2000	$5,711.00
Transcarpal Hand DMC plus®	$6,768.00
System Electric Hand DMC plus®	$7,948.00
MyoHand VariPlus Speed	$8,547.00
SensorHand Speed	$9,277.00
Michelangelo Hand System	$30,257.00

Fig. 3.2 - Currently Available Prosthetic Devices (USD$)

The current prosthetic devices on the market are shown in Fig. 3.2. These devices range from $4094 – $30,257 USD. The entry level prosthetic device in this range is the Otto Bock Hand Digital Twin®. This device allows for single-site EMG control with a basic grip to manipulate the external environment. This is the device that will be a benchmark for the prototype developed in this research. As a note, the price indicated above is only for the device, not inclusive of mounting or accessories such as wrist actuators and connection cables. This research can be considered a success if the initial prototype is the same or slightly cheaper than the Digital Twin® because the price per device would be reduced when the device is taken to mass production. The next point of concern is the amount the government is willing to fund for an amputee to receive a higher quality of life and increased functionality in day to day life.

Many countries have healthcare for their citizens in case of accident or emergency. These healthcare schemes usually cover the victim up to a certain amount for the injury and then have a secondary cover amount for on-going rehabilitation. The price of a prosthetic device in perspective with the overall cost of the injury can cost far more. Fig. 3.3 shows three common procedure costs.

Transhumeral (TH)	$2,622.79
Transradial (TR)	$2,072.63
Wrist disarticulation (WD)	$2,339.57

Fig. 3.3 - Common Amputation Procedure Prices

This research focuses on the wrist disarticulation. The cost of the procedure is around $2,340. This shows that the overall cost of the prosthetic device is nearly double that of the initial procedure.

The government in Alberta, Canada is willing to pay for 75% of the cost to upgrade an amputee from a passive prosthetic device to a myoelectric controlled one assuming that the amputee shows an aptitude for muscle control in rehabilitation. The costs in Fig. 3.4 show the maximum contributions by the government towards different aspects of an amputee's prosthetic device.

Part	Total Cost	Government Maximum Contribution (75%)	Patient Maximmmum contributiuon (25%)	Quantity	Per # of years
Socket costs above conventional socket - WD finishing included	$2,124.00	$1,624.00	$500.00	1	3
Custom upper extremity liner for use with myoelectric electrodes.	$1,658.34	$1,243.75	$414.59	1	1
2 Batteries	$693.99	$520.49	$173.50	2	2
Battery Chargers	$1,106.84	$830.13	$276.71	1	4
Battery Mounting Set	$244.87	$183.65	$61.22	1	3
Connection Cables	$271.22	$203.41	$67.81	3	3
Electric Hands & Hooks	$8,523.48	$8,023.48	$500.00	1	3
Electrodes	$1,158.81	$869.11	$289.70	2	3
Switch Control	$1,425.92	$1,069.44	$356.48	1	2
All Up Costs	$17,207.47	$14,567.46	$2,640.01		

Fig. 3.4 - Government Contribution toward Prosthetic Related Items

Fig. 3.4 shows that the government is willing to pay up to $8,000 for a prosthetic device for an amputee. Another point of interest in this figure is the breakdown of the funding for different parts of the prosthetic device. The allocated funds are for specific uses and not used in one lump sum. The overall sum is broken down into: socket, electrode compatible socket liner, batteries, battery chargers, battery mounting set, connection cables, electrodes and switch control. With this breakdown of costs, the cost analysis of the prototype designed in this research can exclude all parts other than the hand prosthetic itself such as the cost of the batteries. This cost breakdown also provides a target for the circuit development in the prototype to replace the expensive components and interface with EMG sensors as some of the current EMG sensing components in the device can make the cost up to $1000.

Chapter 4 – Prosthesis Mechanical Design

4.1 Finger Design

The finger is arguably the most important part of a hand. It is the interaction device that enables fine manipulation of the physical environment around the user, this made requirement to find an effective finger design imperative. It was decided that the prototype's finger should retain similar physical dimensions, functionality and appearance as a natural finger. The reasoning behind the restriction to a natural form factor was to take a step towards reducing the stigma that is associated with being different. Ultimately the hopes were to be able to fit the fingers into a glove to make the difference as inconspicuous as possible.

4.1.1 Actuation Methods

There are three types of actuation for robotic end-affecters, under-actuated, over-actuated and fully actuated. The differences between these actuation methods are related to the number of actuators compared to the degrees of freedom of the actuator. A system is considered under-actuated if the DoF exceed the number of actuators for the system. If the system has additional actuators compared to DoF the system is considered over-actuated while if the number of actuators and DoF are equal they are considered fully actuated systems. The most common type of actuation system found in the lower cost prosthesis is an under-actuated system due to the reduced need for expensive actuators. In an under-actuated system the finger usually deforms to accommodate complex shapes due to the lack of ability to follow an arbitrary path through space. Fully actuated systems are able to grip an item while remaining in place with no deformation. However fully actuated systems are liable to singularities while over-actuated systems are less likely to due to the redundant actuator (Fukuda, Bu, & Ueno, 2010). The decision was made to use an under-actuated system in the prototype design due to the reduced cost on both actuators and in control system.

There are multiple under-actuation methods that have been proven to allow for a useful bending arc in a prosthetic finger: Three-phalanx, Multiple motor, Electroactive polymers and Cable actuation. When three-phalanx is used in a prosthetic finger it uses the theory of a three bar linkage to drive the finger from above and behind the contact surfaces. This three bar linkage enables the smooth bending of the contact surfaces and allows for the curvature of the surfaces to accommodate for complex shapes. The force imparted on the object in the finger's grasp is made to be equal such that the complex object is able to be held firmly. A disadvantage of the lever linkage is the amount of space required to implement the control from behind.
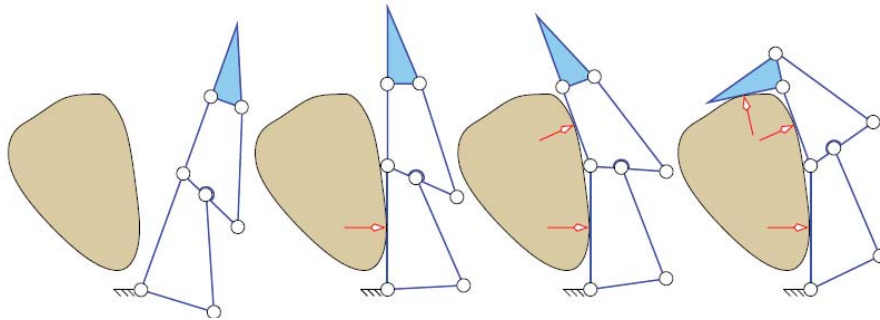
Fig. 4.1 - Grasping sequence of the three-phalanx under-actuated finger (Lionel Birglen, 2006)

The additional room needed for the three-phalanx actuation method is shown in Fig 4.1. This additional room needed for the linkages would exclude the possibility of the fingers being encased in a glove.

Multiple motor actuation has been used to good effect when designing prototypes in the past. This actuation method requires the use of a motor at each joint to allow the system to move, for this to be an accurate control method extra encoders need to be fitted to the motors to allow the control system knowledge of the exact positioning of the physical system. The ability to move each joint individually allows for a greater accuracy in control, however it also requires a much more advanced control system. The other drawback of this actuation method is the cost of equipment. With low-cost being the focus for this study the decision was made not to use multiple motor actuation on the design.

Electroactive polymers are a recently developed media which has promising attributes when considered for prosthetic device applications. The term Electroactive refers to the ability of the polymer to change its physical attributes when subjected to an electric source. The principal behind the Electroactive polymer actuation method is inspired by nature, the polymer string could be used to replace muscle strands in a human hand analogue. The specific attribute that has been considered for use in prosthetic hands is the ability for the polymer to either shorten or bend when exposed to the electric source. This change in the physical structure could eliminate the need for motors entirely when considering the actuation of a finger system. The price however, is prohibitive for use in a low-cost prosthetic design and as such was rejected for this study.

Cable actuation is the final actuation method and the one that was ultimately chosen. This actuation method is similar to the three-phalanx method in terms of actuation arc and number of actuators that are needed to drive the system. The Cable actuation method uses a loop of Cable and a set of pulleys to move the system about a series of joints. This system relies on current sensing through DC motors to gauge the force being applied through the contact surfaces to the object. This is done by mounting two pulleys onto one motor and winding the cable in such a way that it is always in tension. The cable will be wound in a clockwise direction on one pulley and anti-clockwise on the other to ensure whichever way the motor turns the cable will remain tight while providing both a forward and reverse actuation. This type of system needs to have hard stops in place to allow the tension to build up enough to overcome the current sensing threshold to deactivate the motors. The current sensing acts both as a safety device for the prosthetic device itself, but it also protects the object that the prosthetic device is holding.

4.1.2 Form Factor

The geometry and form factor of the finger needs to be specially designed with the requirements of the cable actuation system in mind. The protection of the actuation cable and the joint preference as created by the cable must be taken into account. Because the cable needs to be protected from the object that is being held, the form factor of the finger must internalise the cable and also provide the actuation surface for the cable to act upon.

This internal actuation surface must then be designed to get the preferable joint priority order. The joint priority order is the order which the joints are preferred to move when the system is actuated. In the case of the finger, the joint closest to the palm would have top priority followed by the joints in order to the tip which has lowest priority. This priority order gives a natural grip curve and allows the digit to form around a complex object easier.
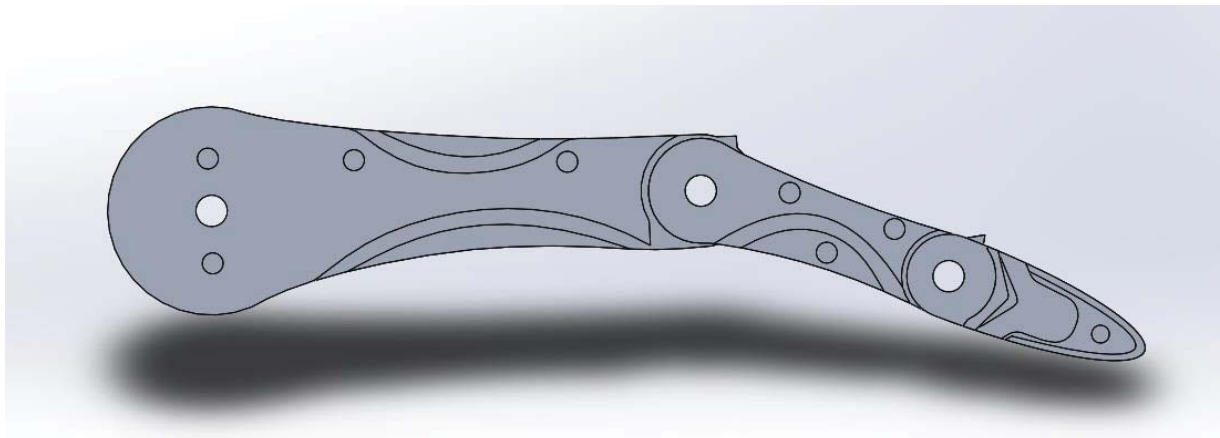
Fig. 4.2 - Internal Design of the Index Finger Including the Cable Actuation Channels

The cable channels and actuation surfaces of the index finger are shown in Fig 4.2. The joint priority order is implemented by changing the curvature of these internal channels thereby increasing or decreasing the friction between the cable and the actuation surface. The joint with the lowest friction is the first joint to move and then this is followed by the next joint with the lowest friction. This naturally lends itself to forming around a complex object. When the first joint is stopped by an external force, its effective friction goes up sharply while the second joint is still free to move thus making the effective friction lower than that of the first joint. This continues until the second joint contacts the object and is in turn stopped, producing an increased effective friction. The tip rotates as the final joint around and touches the held object and completing the grip. When all joints have a high effective friction, the surface the cable is acting upon provides an inward force upon the held object. When this force reaches the threshold set by the current limiting circuitry the motors turn off and hold the item until the motors are actuated again and driven in the opposite direction.

When the joints are moving in the reverse or "Flex" motion, a series of physical stops were incorporated to stop the finger from bending too far in the reverse direction. Due to the under-actuated nature of the finger design, the cable would not produce this result on its own. The movement arc of the finger needed to be physically constrained for the cable to effectively produce a useful actuation path.

4.1.3 Dimensions

The physical dimensions of the fingers were taken from measurements of a sample human hand and then translated into a design that was easy to manufacture. Hinge dimensions were decided to be 3mm to allow sufficient aluminium around the joint to prevent tear-out.

	Index	Middle	Ring	Pinky
Joint 1	46.7	52.2	47.5	36.7
Joint 2	24.96	28.8	27.4	22.7
Tip	21.06	24	22.6	20
Total	92.72	105	97.5	79.4

Fig. 4.3 - Finger Dimension Table (mm)

The dimensions that are shown in Fig. 4.3 are taken from the sample hand and were worked into the design of the finger. The dimensions given are the distance between the knuckles at each end of the designated joint of the sample hand. This was then translated to the distance between the centres of the hinges at either end of the specified joint.

4.1.3.1 Prototype Revisions

The finger design of this research began with a concept of the finger being produced as a 3D model in Solidworks; the design however provided no impact on how the finger would translate into the physical world. At this point a 3D printed model was created and assembled to assess how the finger would move in a physical environment. The first prototype model did not include any cutaways for the finger; this did not allow the finger joints to have a free range of motion. The second revision of the finger included a set of cuts to allow the finger to move more freely and gain the full range of motion. This revision however did not include a set of physical stops, this allowed the finger to have a full range of motion in both directions. Having such a large range of motion was detrimental for the under-actuated control method which the finger was to be controlled by.

Fig. 4.4 - 3D Printed Finger Revision 1 (Left), 3D Printed Finger Revision 2 (Right)

The third revision of the finger introduced hard stops for the fingers so they would be unable to travel past the point of a normal finger extension. This third revision also introduced a return cable channel so that the prototype was able to be controlled in both directions. For the prototype to be analysed in sufficient detail and for the actuation to occur, a mounting block was designed. The mounting block consisted of: a slot for the finger, a hard stop at the top of its return travel, a shaft mounting hole and a spring mounting. The most insightful use for this mounting block was to observe the contraction via a manually pulled cable and the automatic return via a spring. This allowed the confirmation of the bend order for the joints and the ability to form a grip around more complex objects.
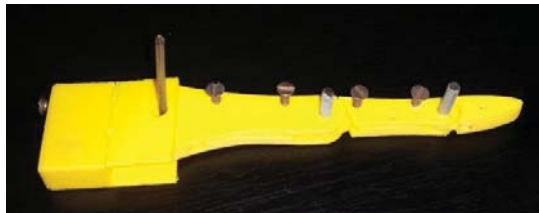

Fig. 4.5 - 3D Printed Finger Revision 3

This final revision of the finger prototype was then manufactured via a CNC mill to ensure ease of manufacture. This aluminium prototype was then used in the mechanical analysis testing for motor torque requirement calculations and grip suitability of objects.
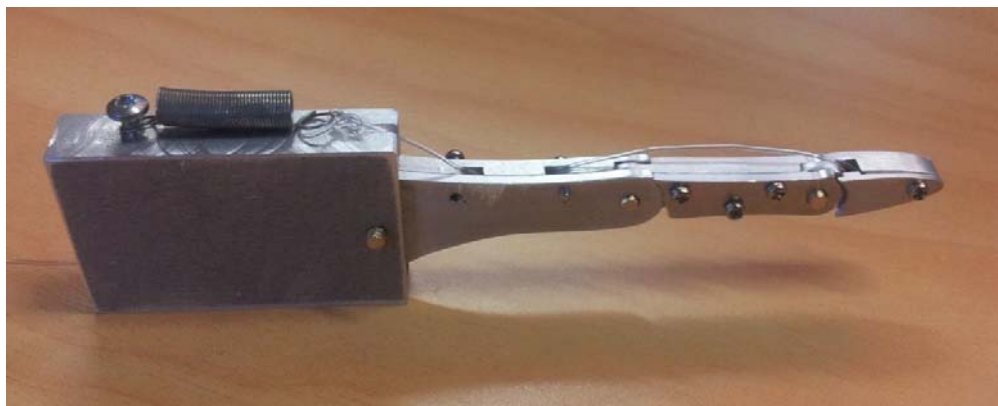
Fig. 4.6 - Final CNC Prototype of Index Finger

Fig. 4.7 - CNC Prototype Testing Grip Pattern

The problem with directly mimicking the contours of a human hand is it is very costly to manufacture and requires expensive equipment to produce which Massey University does not own. The alternative design was created to minimise the number of directions that the stock material needed to be machined from to enable it to be produced on-site. This consideration limited the design to curves in a maximum of two planes. A conventional hand bone is effectively cylindrical with two spheres on each end and this type of shape is very expensive to manufacture. Due to the requirements of the actuation system, the curves were limited to following the length of the finger and as such have flat sides. These flat sides however provide an opportunity for the fixtures and hinges to be easily inserted.

4.2   Torque Calculation for Finger Mechanical Advantage

For the actuation of the prototype device to be effective, the torque required by the finger had to be found. To do this a series of mechanical lift tests were conducted with known weights at the tip of the finger to emulate the maximum force required to lift a certain weight in the worst case scenario. As previous discussions with the amputee about his current prosthetic mounting system revealed the limb socket would be detached if he tried to lift more than 10Kg with his current prosthetic system. Since the limb socket will still be the mounting point for this prototype the same weight limit would apply.

The mechanical tests were conducted using the prototype aluminium finger and the finger mounting block. The mounting block was placed in a vice such that the finger would bend in an upwards direction and a Kevlar string loop was placed on top of the third hinge joint. Weights were then added to the Kevlar string loop in increasing mass from 0.5 Kg through to 2.0Kg. The actuation string was then tied to a strain gauge in preparation for measuring the required pull strength to lift each weight.

Fig. 4.8 - Weight Lift tests of Prototype Finger Worst Case Scenario

Tip Weight	Required Pull Force
0.5Kg	3Kg
1.0Kg	6Kg
1.5Kg	10Kg
2.0Kg	13Kg

Table 1 Required Pull Force to Lift Varying Weights

Table 1 shows the force required to lift each set of weights when located at the tip of the finger. From these values a worst case mechanical advantage could be calculated by using equation 4.1.

$$F_{Pull} = m_{Tip} \times 6 \qquad\qquad [4.1]$$

From the above data we can extrapolate the maximum lift weight of this device to be 2Kg x 4 = 8Kg. This is slightly under but still in line with the maximum weight of the limb socket and is therefore acceptable. This lifting data also allowed a suitable motor to be selected by providing a maximum required force and using a minimum pulley radius.

4.3 Mechanical Analysis

This section focuses on the mechanical analysis of the finger design, proving that the finger is sufficiently strong to hold the maximum design load of 2Kg at the tip.

4.3.1 Finger Strength

Strength analysis for the tip of the finger:
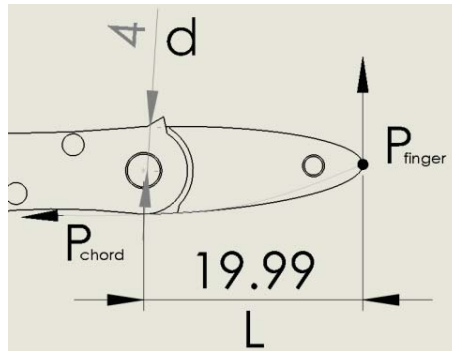
Fig. 4.9 - Finger Tip Dimensions for Strength Analysis

Taking moments about the tip joint to determine the chord load

$$P_{Finger} \times L - P_{Chord} \times d = 0$$

$$P_{Finger} \times L = P_{Chord} \times d \qquad [4.2]$$

$$P_{chord} = \frac{P_{finger} \times L}{d} \qquad [4.3]$$

$$P_{chord} = \frac{2kg \times 9.81 \times 20mm}{4mm} = 98.1N$$

For the Entire Finger:
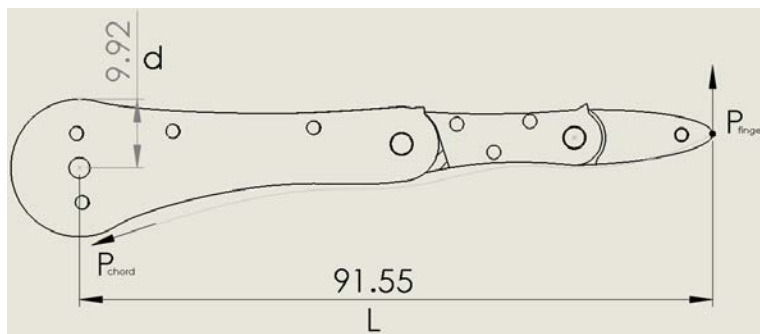
Fig. 4.10 - Dimensions for Full Length Strength Analysis

Taking moments about the base pivot to determine the chord load

$$P_{Finger} \times L - P_{Chord} \times d = 0$$

$$P_{chord} = \frac{2kg \times 9.81 \times 91.55mm}{10mm} = 180N$$

4.3.2 Bending in the Finger

Bending analysis for the main finger joint through point C-C as an indication of total finger bending strength
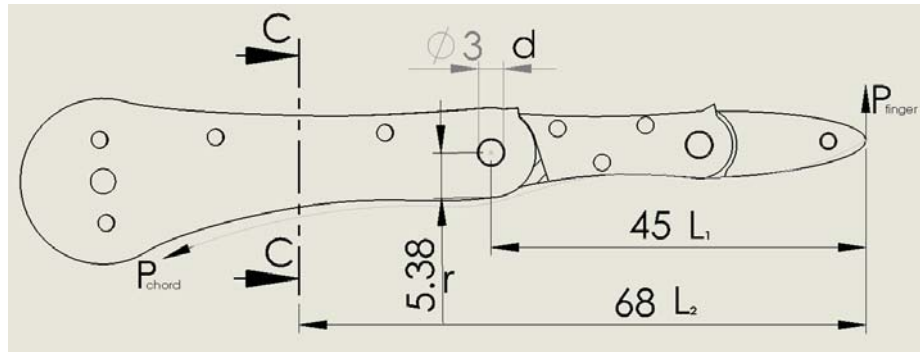
Fig. 4.11 - Finger Dimensions for Bending Analysis
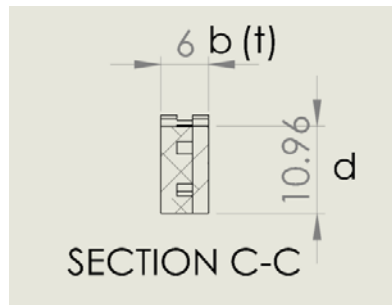
Fig. 4.12 - Finger Dimensions for Second Moment of Area Calculation

$$\sigma = \frac{My}{I} \tag{4.4}$$

$$I = \frac{bd^3}{12} \tag{4.5}$$

$$M_{C-C} = P_{finger} \times L_2 \tag{4.6}$$

$$M_{C-C} = 2 \times 9.81 \times 68 = 1334 \ N.mm$$

$$\sigma = \frac{My}{I} = M_{C-C} \times \frac{12}{bd^3} \times \frac{d}{2} = 1334 \times \frac{6}{6*11^2} = 11MPa$$

Yield Strength of finger material (3003 H12 Aluminium) = 124MPa

$$F.S \gg 10 \ and \ is \ acceptable$$

4.3.3 Joint Pivot Pin Bearing

The load at the joint is the vector sum of the P_{chord} and P_{Finger}.
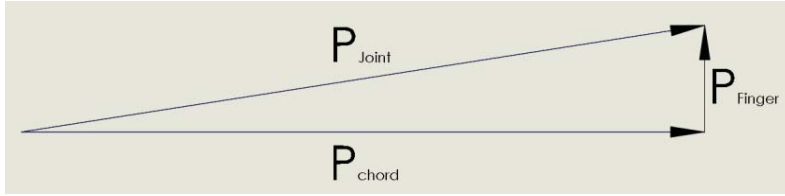
Fig. 4.13 - Vector Sum of Finger Forces

$$\sqrt{P_{chord}^2 + P_{Finger}^2} = 181N$$

$$\sigma = P/A \qquad\qquad [4.7]$$

$$\sigma = \frac{181N}{d \times t} \quad = \quad \overline{3 \times 2} \quad = \quad 30\ MPa$$

Shear Strength of finger material (3003 H12 Aluminium) = 82.7MPa

$$F.S > 2\ and\ is\ acceptable$$

4.3.4 Joint Pivot Pin Shear Out
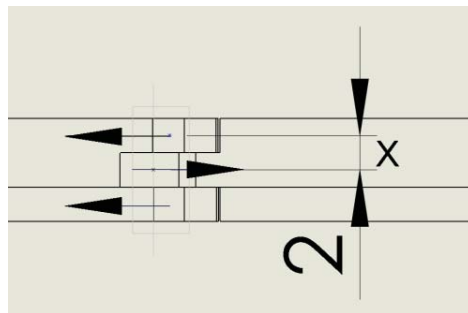
Fig. 4.14 - Pin Joint used for Shear Out and Bending Calculations

$$\tau = \frac{P_{Pivot}}{A} = \frac{P_{Pivot}}{2 \times t \times D}$$

Shear Strength of Finger material (3003 H12 Aluminium) = 82.7MPa

$$F.S \gg 10\ and\ is\ acceptable$$

4.3.5 Joint Pivot Pin Shear

Shear strength analysis for the pivot pins using double shear.

$$\tau = \frac{P}{A}$$

$$\tau = \frac{P_{Joint}}{2} \times \frac{1}{\frac{\pi}{4}d^2} = 181N \times \frac{1}{\frac{\pi}{4}3^2} = 12.8\ MPa$$

Shear Strength of pin material (mild steel) = 240MPa

$$F.S \gg 10\ and\ is\ acceptable$$

$$Stress \approx F_{TU}\ max$$

4.3.6 Pin Bending

To check that the pivot pin will not bend at the maximum design load:

Assuming a simply supported beam with the pivot loads acting at the midpoint of the bearing surfaces
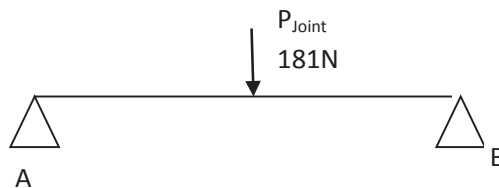
Taking moments about the centre

$$M = \frac{P_{Joint}}{2} \times x \qquad\qquad [4.8]$$

$$Bending\ Moment = \frac{181\ N}{2} \times 2 = 181Nmm$$

$$\sigma = \frac{My}{I} = M \times \frac{64}{\pi D^4} \times \frac{D}{2} = 181 \times \frac{64}{\pi D^4} \times \frac{D}{2} = 12MPa$$

Tensile Strength of pin material (mild steel) = 300MPa

$$F.S = 25 > 1\ and\ is\ acceptable$$

4.4 Pulley Requirements to Drive Finger

The mechanical testing performed on the final aluminium finger designs allowed the required pulley diameter to be calculated due to the length of the cable channels. The overall travel of the string was measured at full extension and at full retraction, and then it was converted into a suitable pulley diameter by the formula below.

$$D_{Pulley} = \frac{l_{String}}{\pi} \times 1.5 \qquad [4.9]$$

With this known required diameter the motor could be chosen such that the applied torque from the motor would be able to lift as close to the required 2Kg as possible. Once the motor was chosen the pulleys were able to be reduced in size as needed. The diameter of each pulley was calculated based on the travel of each finger's unique channel length. Each sting was measured at both full extension and full contraction, these measurements were then multiplied by 1.5x to increase the radius of the minimum value to make it over 8mm. This 8mm was the minimum amount of material for a grub screw to be effective to hold the pulley in place on the shaft.

Pull Distances								
	Flex	Tense		Flex Ø	Tense Ø		Flex Ø	Tense Ø
Index	22mm	37mm		7mm	12mm		10.5mm	18mm
Middle	32mm	38mm		10.2mm	11.8mm	X1.5	15.3mm	17.7mm
Ring	25mm	37mm		8mm	11.8mm		12mm	17.7mm
Little	26mm	32mm		8.3mm	10.2mm		12.45mm	15.3mm

Table 2 - Pulley Dimensions and Cable Measurements

4.5 Palm Design

The palm plays a vital role in the human hand. It provides a surface for the fingers to apply pressure against and it also provides a structure to hold the fingers together at the same time. The design of the palm provided a challenge. It needed to be light, strong, provide a reaction surface and be large enough to house all actuation methods. The design must incorporate all of these features while also retaining the ability to be manufactured.

4.5.1 Form Factor

The form factor of the palm was taken from the same sample hand as the fingers to ensure a consistent dimension throughout the prototype. This was done by outlining the sample palm on a 2D plane and then taking measurements from this 2D palm profile.
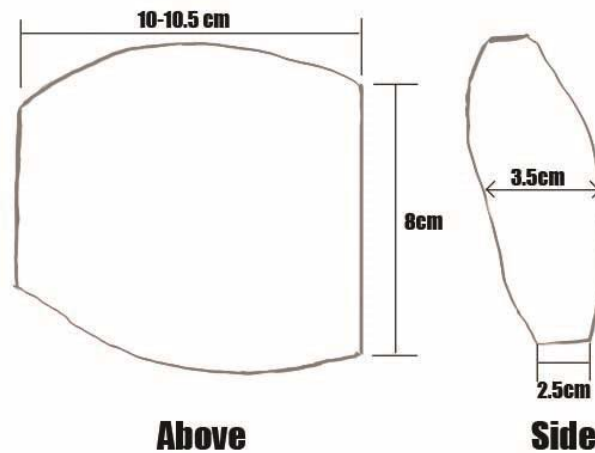
Fig. 4.15- Palm Sketch with Dimensions

The digitised version of this profile is shown in Fig. 4.15, the sketch of the palm area and the related measurements that were taken to design the prototype's palm surface.

Due to the available manufacturing processes on site, the same considerations were made as in the finger design in regards to the number of sides that part was to be machined from. This caused the palm to be manufactured in three separate parts with a maximum of two sides requiring machining. When designing the palm's form factor, the decision was made to keep a minimum wall thickness of 3mm around the outside of the parts to ensure the part retained structural strength when impacted from the side. An additional factor that influenced the 3mm wall thickness decision was the motor choice, allowing the maximum free area in the middle of the palm for motor mounting and positioning means that a larger calibre motor could be chosen. This minimum side-wall allowed sufficient space for fixtures to be hidden in the wall to increase aesthetic qualities of the prototype. As the right hand sketch in Fig. 4.15 shows there is a plain curvature in the side of the palm where the fingers would apply pressure. This however would be extremely costly to manufacture and would provide limited benefit to the prototype at this stage in development. This surface was instead used as a known flat base for the rest of the prototype to be built from.

For the fingers to be able to be mounted in a straight line, a set of inserts was designed and included in the palm. On either side of the slot for each finger an additional cavity was cut in the shape of a square to allow for a bushing insert to be added in assembly. Along with the cavity for the bushings another cavity was made for a cable guide insert which was to be manufactured out of plastic to reduce the friction on the cables as they pass from the motor housing area to the finger actuation.

The motor housing area required the maximum amount of space possible to allow for the optimum motor choice and pulley size for this application. Once the palm and the motor dimensions were decided, the holes for mounting the motors were able to be finalised. The positioning was done in such a way that the centre of the motor shaft was in line with the centre of the finger slots.
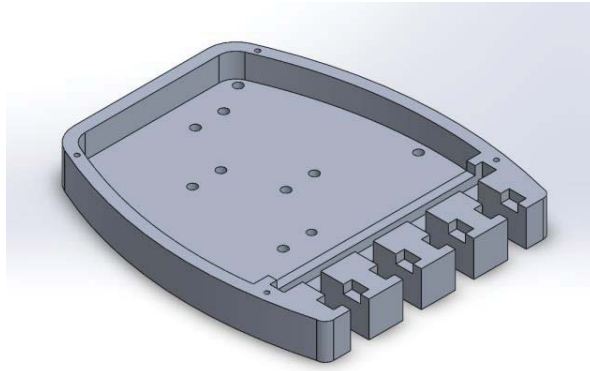
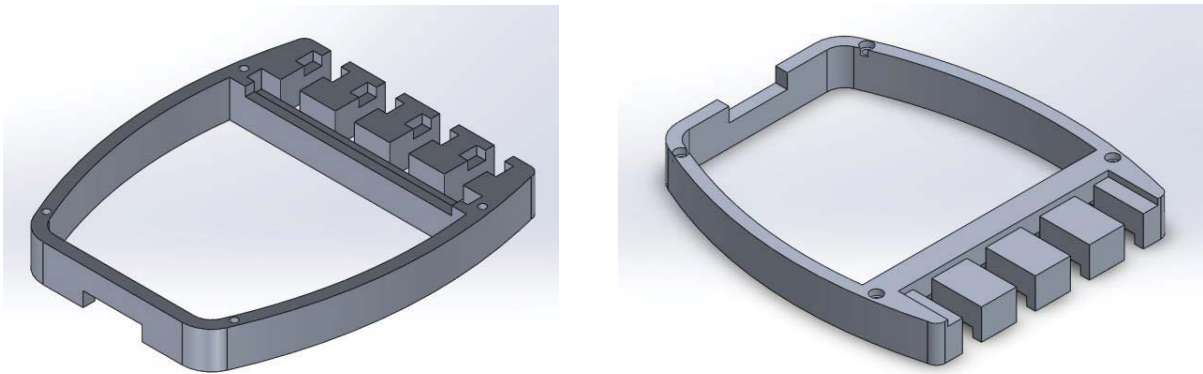**Fig. 4.16 - Palm, Bottom Section**

Fig. 4.17 - Palm, Middle Section. From Below (Left) and from Above (Right)
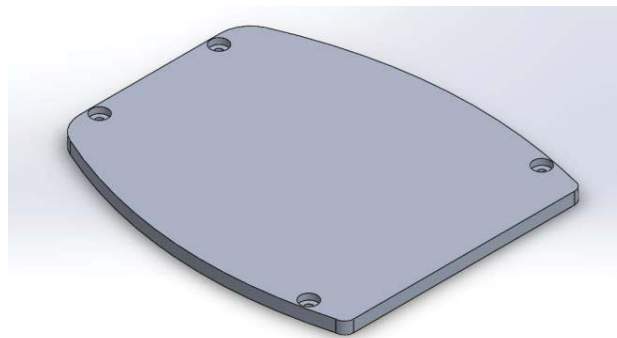

Fig. 4.18 - Palm, Top section

The middle section of the palm had a pocket machined from the top to make room for a rubber insert backstop for the finger's return path. This rubber insert is held in place by the top cover for the palm section.

4.6   Thumb Design

The thumb is the part of the hand which allows humans to effectively manipulate the outside environment and hold objects such as tools effectively. The opposable thumb has been the key point of physiology for a human hand and as such needed to be given careful thought regarding design and implementation. It is a complex digit which offers movement along two axes to accommodate gripping a large variety of sizes and shapes.

4.6.1   Form Factor

For this part to be manufactured the number of axes that it can move along had to be restricted to one, any more and the design would have become costly and unnecessarily complex. To accommodate for the loss of one axis of movement the thumb was to be mounted at an angle offset from the normal 90 degrees. The shape of this part was the most complex piece of the prototype to manufacture. For this part to function correctly in a grip, it needed to follow similar shapes as a natural thumb. This included a curve up from the surface of the palm to the digit mounting point to allow for a tighter grip on an object.
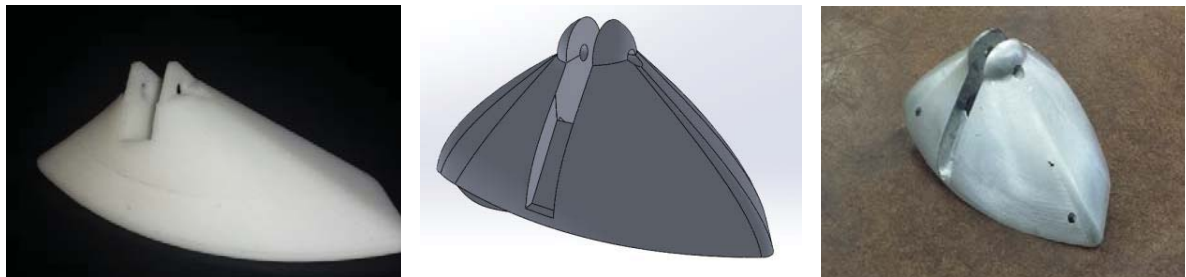
Fig. 4.19 - Thumb, First Attempt (Left), Final 3D model (Middle), Final Form (Right)

The first iteration of the thumb mounting part is shown on the left of Fig 4.19. This design was 3D printed as a prototype and was fitted to the palm assembly. This part was aesthetically unpleasant but did provide both an effective mounting point and an ability to assess the grip angle of the thumb before manufacture. The 3D CAD model after the required editing is shown in the middle of Fig. 4.19, showing the changes to the thumb mounting angle and the added grip channel. The final prototype form is shown on the right of Fig. 4.19 which includes improvements to the aesthetics by including a slope receding from the mounting point to sit flush with the side of the palm assembly.

The curvature of this final prototype caused issues when it came to manufacture, due to the overhang required to sit flush with the side of the palm, this required the part to be milled both from above and below. Not only did this part require multiple setting up for the milling, but the overhang made it impossible for the part to be clamped flat on the machining bed. To counter this, a set of mounting holes were purposely drilled in the part to serve as a datum when the part was turned over. The first side to be machined was the underside allowing the beginnings of the motor cavity, the shape of the overhang and returning curvature to be machined. The last step on this side was to cut away the outlying material so the shape was defined. After the material was cut away a new piece of stock was placed in the mill and a negative cut was done around the shape of the flat which was to sit against the palm. Three holes were then drilled into this piece of stock in the same pattern as the thumb bust underside. This effectively made a mounting block for the thumb bust where the overhang would sit snug against the mounting and

the bust could be held down by the three mounting screws screwed in from the underside. Once the thumb bust was mounted on this bracket, the top side was able to be milled. The majority of the top side was able to be milled from this setup, however the thumb mounting point and the thumb movement channel were unable to be milled from this direction. This forced the use of a conventional mill and an angle vice.

4.7 Wrist Fixture Design Consideration

The amputee currently possesses hook type prosthesis and has been fitted with a limb socket to which the hook mounts. This limb socket can be used to mount the new prototype provided that an adapter is manufactured.

4.7.1 Amputee's Current Mounting System

The amputee's hook prosthetic is attached to a limb socket which is made from carbon fibre. This carbon fibre limb socket is used as a support for the hook so when something is lifted with the hook, the load is transferred through the stiff limb socket and into the remaining bones of the forearm. The actuation method for the amputee's current prosthesis is a pulley system with a harness over the opposite shoulder. When the shoulder is moved forward it places tension on the harness and opens the hook, allowing the hook to be able to grip and lift objects. This harness however provides a strain on the user's body and often causes pain after a full day of use.

Fig. 4.20 - Current Carbon Socket (Left), Socket with Hook Attached (Right)

Fig. 4.21 - Hook Prosthetic Actuation Harness (Left), Hook being Closed by Harness (Right)

4.7.2   Required Functionality and Critical Dimensions

The new mounting is required to provide a minimum of the same level of functionality as the previous mounting system. This was measured by the ability to hold similar weights, provide acceptable support when lifting objects. Additional to this requirement, the mounting system aims to eliminate the need for a harness and thus the discomfort the amputee would feel while using the prosthesis.

The critical dimensions for the adaptor for the amputee's current mounting system are based around the silicone sock and the end of the carbon fibre socket. The silicone sock prevents the prosthetic device from separating from the amputee's residual limb. This is done by using the friction between the skin and the silicone to create a suction to act in opposition to the pull of the prosthetic device. The prosthetic device is attached to the silicone sock by means of an embedded steel threaded rod shown in Fig. 4.22.

Fig. 4.22 - Silicone Sock for Mounting Hook Prosthesis

When the amputee inserts their residual limb into the carbon fibre socket, the threaded rod remains exposed through a hole in the socket end as shown in Fig. 4.23. The hook type prosthetic screws onto the external thread of the threaded rod from the silicone sock as well as the internal thread of the carbon fibre socket's end hole.

Fig. 4.23 - Mounting Arrangement of Current Prosthesis

Analysing this design, an adaptor is able to be manufactured. The critical dimensions for this design are the thread size of the threaded rod, the carbon fibre socket's end hole diameter and the size of the metallic pressure plate at the end of the socket. Taking measurements the external thread of the rod is an M8 thread size, the internal hole diameter is 14mm and the pressure plate's diameter is 45mm.

Chapter 5 – Prosthesis Manufacturing

5.1 Available Manufacturing Technologies

The prototype needed to be manufactured in-house to reduce the cost of development. It was then pertinent to assess the available technologies as well as what costs they would incur on the project. These technologies included: CNC milling, 3D plastic printing, injection moulding, conventional hand milling, lathing and welding.

Each manufacturing technology enabled differing possibilities for the prototype's form, strength and material composition. The decision was made to eliminate injection moulding as a possible manufacturing option for the initial prototype due to the costly one off manufacture, inability to make changes quickly and limiting nature of material selection. However this technology may be of use if the prototype were to become mass-produced.

5.1.1 3D printer

The Up Plus 3D printer is a rapid prototyping machine which uses melted ABS plastic to print layers on a heated baseplate. The ABS plastic cable is heated to 260®C as it is passed through the print head, when this melted material contacts the baseplate it sticks like ink would to paper. ABS plastic will also stick to itself when heated, making this printing process possible. The movement of the base and print head are controlled by timing belts connected to simultaneously moving stepper motors. This rapid prototyping machine takes 3D models of objects created in CAD software such as Solidworks and converts it into a series of triangles. These triangles represent the surface dimensions of the original part and allow the printer's control software to break the shape down into layers of approximately 0.2mm. Once the printer has converted the shape into a series of 0.2mm thick layers, the print head begins to print the layers one at a time on the heated base board. When a layer is finished the base plate moves down 0.2mm and the next layer is printed directly on top of the previous. If a shape requires an extrusion with no other structure underneath, the printer creates a scaffold like structure to support the overhanging layers. Once the shape has been completed the scaffold support structure breaks away easily, leaving behind the target shape.
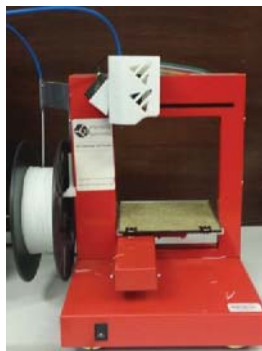

Fig. 5.1 - UP Plus 3D Printer

5.1.2 CNC Machining Centre

The Acumen 500 CNC (Computer Numerical Control) Machining Centre is a milling machine that is controlled by an on-board computer rather than directly by the operator. The Acumen is a 4 axes mill with X-translation, Y-translation, Z-translation and Z-rotation axes. This machining centre has a maximum operational size of 400mmx400mm in the X and Y planes with an effective Z axis travel of 350mm. Several features have been included with this machine to improve ease of use and to protect the operator. The first feature of note is the door safety mechanism, if the door is opened mid operation the process will stop and the cutter will stop spinning. This is primarily to protect the operator from harming themselves on the spinning tool. Another feature is the access panels on the sides of the machine for easy access to the auxiliary systems, removing the need for the technician to enter the machine with their whole body. The last two ease of use features are to do with machinability and visibility. In the Acumen 500 there is a pre-installed light, air blower and coolant hose all of which are directed at the spindle. The coolant allows the machine to process the materials being machined much faster while the air blower acts to blow the excess coolant away from the stock material so that the operator can see the cut much easier with the light.

Fig. 5.2 Acumen 500 CNC Machining Centre

The Acumen 500 is controlled by an on-board computer with a custom machining operating system. This operating system is used to interface between the machine and the design computers. The on-board computer is able to access the university network, this allows programs to be transferred from the university computers directly into the machine's system. The machine accepts only programs in a machine language called G-code. Massey uses a 3D modelling CAD (Computer Aided Design) software called "Solidworks" to produce a virtual prototype of a desired part. When this part is ready to be machined the file is transferred to another piece of software called SolidCAM, Computer Aided Manufacturing software. In SolidCAM the virtual part is converted into a square piece of stock material, from this point, a datum is set and then a series of machining operations can be programmed to make

56

the correct profiles to create the part as it was designed in Solidworks. The depth of specification available in the machining operations enable the technician to change variables such as feed rates, spindle speeds, maximum step down values and much more. SolidCAM uses these variables to allow the user to create simulations of the machining operations to check the profile after the operation is complete, enabling easy fault checking and time estimation. Once the technician is happy with the program and is ready to start manufacture, the operations are then converted to G-code. Once the G-code file is saved it can be transferred to the machine and then manufacture is able to start.

Fig. 5.3 - Control Panel for Acumen 500 CNC Machining Centre

The Reason that this is referred to as a "machining centre" rather than a conventional machine is the automatic tool changer. The ability to change between milling tools, drills and bull nose cutters means that this machine is able to provide a complete manufacturing solution when milling from one direction. When this is not enough, smart use of datum and fixtures enable the machining from more than one direction. With the ability to machine from both sides of a part means that most designs without complex internal structures are able to be milled via this method. The machining centre changes tools by rotating the tool holder shown in Fig. 5.4 until the required tool is in the bottom position. The spindle is

then stopped, the bottom tool is rotated in the tool holder by 90 degrees then an arm grips the current tool and the replacement simultaneously then exchanges them. This means that there is no need for an operator to intervene when a tool change is required. If the required tool is not currently in the tool changer, the technician is able to exchange an unused tool in the holder or add a tool into an unused slot, further expanding the abilities of this machining centre.

Fig. 5.4 - Automatic tool changer for the Acumen 500 CNC Machining Centre

5.1.3 Mill

The Kondia Powermill is a conventional milling machine, this mill comprises of 5 axes similar to the CNC machining centre. These axes are translation in the X,Y and Z axes as well as rotational in the Z direction. The conventional mill is used to complete profile and plunge cuts on stock material. Like the drill press the conventional mill has varying speeds to process different materials from wood and plastic through to steel. This mill also has a power feed feature to allow a smooth cut and a good aesthetically pleasing finish.

Fig. 5.5 - Kondia Powermill

5.1.4 Lathe

The Couchester Student 1800 Lathe is a turning machine used to create cylindrical objects by removing material while the stock is spinning. This is the opposite of the milling and drilling operations because the tooling on the lathe is stationary and the stock material is spinning. This lathe provides variable speeds, automatic feeding, thread cutting, coolant pump and digital readout. The variable speeds along with the coolant pump allow for a multitude of materials to be cut on this machine, a quick reference guide is also readily available at this workstation for the speed to cut each material. The auto feed and the thread cutting feature work together to create a thread at a specified diameter, pitch and depth. This makes cutting threads such as a standard M4 into a piece of stock material much easier. The auto feed also allows for a consistent cutting finish on the object when the shape has been machined. To allow for high accuracy cuts on this machine, the digital readout can be used to measure the cut to the specified diameter within 10 microns. This allows bearing fit shafts to be manufactured using this machine.

Fig. 5.6 - Couchester Student 1800 Lathe

5.1.5 Drill Press

Fig. 5.7 - The Hafco MetalMaster Drill Press

The Drill press is a rotary plunging tool and is used to create precise holes and other plunge cuts. This drill press features: an interchangeable chuck, directional coolant hose, variable spindle speeds and an adjustable height table. The adjustable spindle speed function is highly useful as it allows this machine to process multiple materials. Unlike the milling machine, this rotary cutting machine lacks two of the axes that allow the part to move beneath the spindle. The only two axes that this machine possesses are the rotational axis for the spindle and the Z axis for cut depth. The tools that were used in conjunction with this machine were: Spot drill, drill bits, countersinking bit, end mill, reamer and the metal vice also showed in Fig. 5.7.

5.2 Material Selection

There were many possible materials can be used to prototype the prosthesis design. The main constraints for this project pertaining to the material selection were: cost, strength, durability, and ease of manufacture, availability and the availability of the manufacturing facilities.

The reasoning behind the given constraints will be explained in this section. Cost is a major factor for the prototype due to the nature of this study. In the interests of reducing costs, the materials must all be carefully weighed up in a cost-benefit analysis to ensure the most effective use of funds to reduce the overall cost of the project. Due to the nature of the prosthetic device, strength properties of the selected material needed to also be considered. The finger and palm material needs to be able to lift adequate weights without failure to be a useful device in the day-to-day life of an amputee. Along with the material's strength, it must be hard wearing so the repetitive use every day for up to 5 years will not be cause for failure in the device. This would include such factors as temperature resistance, hardness, natural wearing rates and repetitive wearing rates.

To further the evaluation of the material cost, the difficulty of manufacture must be taken into account. This is because the more difficult a material is to manufacture, the more machine and technician time will be required. The easiest material to manufacture will also likely become the cheapest material for the prototype to be manufactured from. Each material considered is also subject to availability; in the costing analysis the availability of each material has to be researched. Any materials that are difficult to obtain or in short supply are eliminated from consideration. The last selection criterion is the requirement of the manufacturing processes that are available to be used for making the prototype. The processes dictated that metals softer than steel were to be used to make the milling and turning operations simpler while still retaining the required durability and strength. The available 3D printing at Massey used ABS plastic which was not deigned to possess the required strength or durability for the final prototype.

Material	Price	Availability	Machinability	Durability	Strength	Process Requirement
Aluminium	Low	High	Easy	Moderate	Moderate	None
Steel	Moderate	High	Moderate	High	High	None
Titanium	High	Low	Difficult	Very High	Very High	None
Nylon	Moderate	High	Easy	Low	Low	None
Teflon	Moderate	High	Easy	Low	Low	None
ABS	Moderate	High	Easy	Low	Low	3D Prining

Fig. 5.8 - Material Selection Criteria

The final Materials that were used in the prototype were Aluminium, rubber, silver steel and Kevlar fibre. Aluminium was used due to the ease of machining as well as its high availability and low cost compared to other hard metals. However, aluminium is a soft metal and therefore a higher degree of care is needed when considering the ways in which it interacted with other parts of the prototype. Because both the palm and the fingers were made from aluminium, care was taken where the fingers would impact on the palm to reduce possible damage to one or both parts. This is where the need for a rubber stop was introduced such that there was a buffer between the two aluminium parts.

The rubber which was selected is a commonly available firm rubber from a local business. The rubber is weather treated so it will last in harsh environments and therefore should not break down during the useful life of the prototype.

The fingers required a hinge to act as a knuckle joint and to provide the axis to bend around to achieve a natural grip curve. The fingers were manufactured from aluminium, therefore the hinge needed to be manufactured from a harder metal such as steel. Due to the nature of a press fit, the steel would need to be of an exact diameter to achieve the required fit tolerance. The hinge diameter was designed to be 3mm, instead of turning down a larger piece of mild steel to the tight tolerance required; the decision was made to purchase silver steel. Silver steel is ground to a diameter with a very tight tolerance before it leaves the factory; using silver steel vastly reduced the machining time by only requiring a parting operation.

Kevlar string was used due to its cheap nature and strength characteristics. The Kevlar sting has a breaking strength of 12kg per strand therefore the string needed to be braided to provide the required breaking strength to produce the results required by the prototype. Kevlar was chosen over a steel alternative due to price, flexibility and minimum bend radius. If steel was used inside the finger design it would cause two problems: it would wear through the cable channels because it is harder than the aluminium it is encased in as well as be problematic in the pulley design due to having a minimum bend radius larger than the diameter of the pulley.

5.3   Design Changes Due to Manufacture

5.3.1   Palm

5.3.1.1   Manufacturing Concerns
There were multiple manufacturing concerns to do with the manufacturing of the palm sections. These included the number of sides that a part was machined from, making corners pointed and material thickness. The main manufacturing concern for the palm section was the number of directions the part was to be machined from. The reason behind this being a large concern is because every time a part is moved in the machining process, the datum is lost. Setting this datum again is very important so all of the following machining operations are done in correct relation to the initial ones. As such the maximum number of directions the part can be machined from was decided to be two. This would require only one movement of the part and extreme care was used when resetting the datum for the next set of milling operations.

Making the corners pointed provides a problem when milling a part if these corners occur on the inside of a profile. This is because when the milling tool is rotating all of the cuts are in a circular path. No matter how small the cutter is, the corner will always have rounded off corners and a square insert will not fit. Instead of trying to round off the corners of all the inserts, a small hole is drilled at the point of each corner before the profile is milled. This creates a cavity where the corner would usually be rounded, making the effective corner pointed and the insert able to fit with no extra operations.
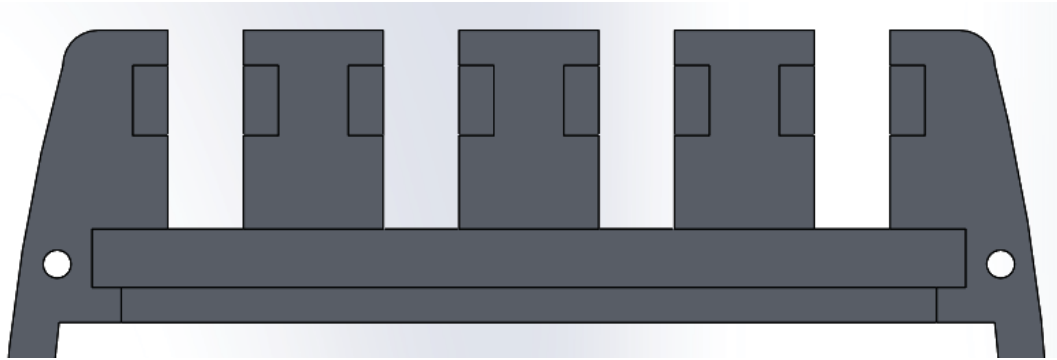
Fig. 5.9 - Designed Corners (Above) Vs Machined Corners (Below)

Material thickness is a large concern when making a prototype in both terms of cost and machinability. The overall measured thickness of the sample hand was 35mm. To reduce the wastage of the material, two lots of 12.5mm thick aluminium were used instead of one piece of 25mm for the base of the palm. By splitting the design in half, more features were able to be added to the design and the number of machining directions was reduced. This also allowed more accessibility to the internal assembly locations such as motor mounting screws and motor shafts for pulleys.

5.3.1.2   Assembly Concerns

The assembly of the palm area of the prototype needed to be designed in such a way that all fixtures and additional parts were able to be accessed by the required tool. Along with the requirement of access, the highest degrees of aesthetic qualities were retained. Balancing the functionality and the aesthetics required thoughtful placement of fixtures as well as paying attention to the order of operations to assemble the prototype. This was most important when considering the method which was to be used to mount the motors. The other major concern when the prototype came to being assembled were the fingers, the fingers were required to be both assembled and have their cable threaded through the cable guide before the palm could be assembled. This was due to the lack of access to the required areas of the palm when it was assembled.

The palm itself is assembled using a set of tapped M2 holes and M2 machine screws to fix the middle section to the bottom. These are used in conjunction with a set of M3 tapped holes and machine screws to fix the top plate to the middle section and to hold the rubber stop in place.

5.3.1.3 *Dimensional Restriction*

The palm size was constricted by the physical dimensions of the sample hand, this created a premium for space. Some of the side wall had to be machined to allow room for one of the pulleys to be mounted correctly on the motor shaft. The radius required by the pulley to effectively use a grub screw to lock itself in place was larger than first expected and as such the dimensions exceeded the initial allowance given in the design. The first design intended to include the electronic sections in the same area as the motors mounts. After revising the design and selecting components for crucial parts of the functionality the decision was made to separate the electrical side from the mechanical for the first prototype revision.

5.3.1.4 *Finger Mounting*

As mentioned above in the palm design section, the fingers were mounted using a series of bushing inserts supporting silver steel hinge rods. The bushing inserts were made out of polycarbonate plastics, this reduces the friction and are easily replaced.

5.3.1.5 *Motor Mounting*

The hand required one motor for each finger that was required to move and each of these motors needed to be fixed in space to allow maximum torque to be applied. A bracket was manufactured such that it was able to be mounted to the palm initially by two M3 screws, then the motor was able to slide into the bracket and fixed in place by two M1.6 screws.

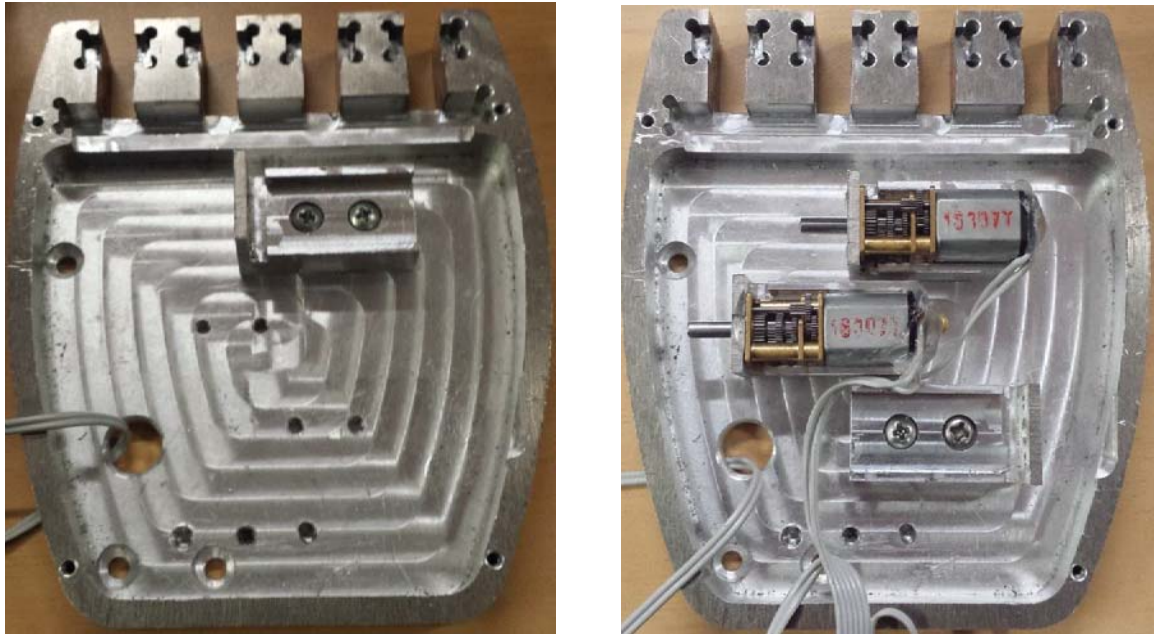**Fig. 5.10 - Motor Mounting Bracket**

Fig. 5.11 - Bracket mounted in the palm (Left), Motor mounted in the bracket (Right)

The last section of the motor mount assembly is to add the pulley onto the motor shaft and lock it in place with a M3 grub screw. However, in the case of the motor bracket closest to the wrist potion, there was another set of fixtures required to be fitted before fixing the motor bracket in place. In this case the screws for the thumb needed to be fitted beforehand. This was because the mounting screws for the thumb were countersunk below the motor mounting to reduce impact upon the aesthetic design that screw heads would have created if mounted from the other side.

5.3.1.6 Actuation Considerations

The palm design and motor mounting system provided some actuation concerns, primarily the string pathways and motor interference. Due to the size restriction of the palm and the motor mounting pattern, the rear most motor was mounted in an interference position such that the actuation cables did not have a direct line to the actuation channel. To overcome this, the strings are run over the top of the motor in front. To reduce any damage caused to the motor or cables a protective cover was created to be placed over the motor. This allowed the cables to move freely over the obstructing motor while reducing the risks of cables being caught in the gears of the motor.

5.3.2 Thumb

5.3.2.1 Motor Mounting

Milling this part from both sides however was not enough, for the motor to be able to be mounted inside this thumb bust a slot needed to be milled at an angle to the flat face above it. This presented a problem for the CNC machine as it only has X, Y and Z axes while this slot would have needed an additional rotation axis. To achieve the desired angle and setup an angle vice needed to be used. A problem became apparent while attempting to mill the motor mounting slot while in the mounting bracket; the slot would require the bracket to have a hole for the cutter to pass through. After modifying the

mounting bracket so the motor mounting slot was accessible to the cutter the milling was able to begin. A long shanked end mill was required to achieve the required depth of cut to allow the motor to be fully inserted. As per the design, the corners of the motor mounting slot needed to be sharpened to allow the motor to fit correctly. For this job a 3mm end mill was used in conjunction with a handheld Dremel rotary tool.
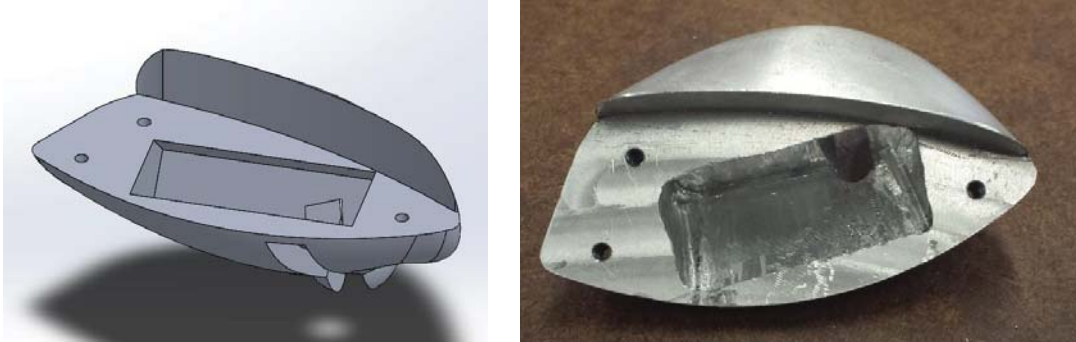

Fig. 5.12 - 3D Model of Motor Mounting Cavity (Left), Final Machined Cavity (Right)

Fig. 5.13 - Long Shank End mill and Angle vice Setup

This motor mounting produced a concern for actuation of the motor. Due to the metallic nature of the prosthetic and the nature of the DC motors used, extra care needed to be taken to eliminate any shorts between the motor terminals. The motor's terminals are exposed at the rear of the device, the fit of the motor in the cavity would cause the terminals to contact the metal of the thumb profile and therefore create a short on the motor. To prevent this short from occurring, a plastic insert cover was placed on the rear of the motor between it and the thumb bust.

5.3.2.2   Thumb Mounting Angle

As mentioned previously, the decision was made to reduce the number of axes from 2 to 1. This has been compensated for by changing the angle of the 1 axis to allow for the most effective grip pattern. The 3D printed prototype mount showed that the angle used was too shallow and would not provide enough force toward the fingers and palm to provide an effective grip. The angle was then changed to a deeper angle that was deemed to provide the correct angle to allow the thumb to reach the fingers and close around a smaller object.

Machining this angle caused issues for the CNC machine because of the complex angles required to give the thumb complete clearance to be able to touch the palm. The preliminary channel was able to be machined into the curved face of the thumb bust by the CNC machine. However, the angle vice was once again used to complete this channel.

Fig. 5.14 - Guide Channel Manufacture

5.3.3 Pulley

5.3.3.1 Changes to design due to Manufacture Limitation

The pulley designs were modified due to the method of fixing. For the pulley to be able to mount the cables effectively there was a need to fix the cables rigidly onto the outside of the pulley. The initial fixing design idea was to use a grub screw on the flat of the pulley to pinch the cable to allow the correct tension to be applied. The issue with this design idea was the width of the pulleys, to allow for the amount of material needed for an effective grub screw mounting made this idea prohibitively large. An alternate idea was formed which was not as precise, however it is far easier to manufacture and implement. This final fixing method required extra holes to be drilled into the circumference as well as the flats. The hole orientations are shown in Fig. 5.15.
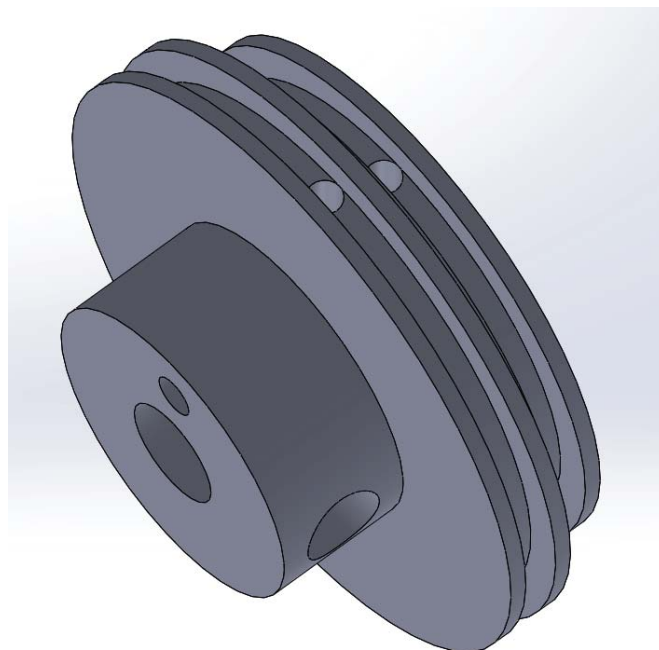

Fig. 5.15 - Pulley String Hole Locations

These holes are located in such a way that they are 90 degrees rotated from the grub screw fixing hole. This allowed the cables to be fed down into the stock shank and then outwards to the non-mounting side of the pulley. The cables are then wound into the channels, tightened and a knot is tied at the exit point of the pulley shank.

Chapter 6 - Electrical and Electronic Systems Design

This chapter focuses on the electrical and electronic components as well as the systems of the prosthesis design such as sensing, conditioning, control and safety. In most commercial biometric controlled prosthetic devices the electronics used to drive and control the prosthesis contribute a large portion of the overall cost. This is usually because of the use of proprietary EMG sensing electrodes with on-board filtering used in conjunction with a high powered processor to identify the patterns in the data. In this application all electronics used are commercially available and open source, this is a major factor on keeping costs to a minimum.

6.1   Electromyography Sensing Design and Investigation

Electromyography has been chosen for use in this prototype because of the previous success it has provided in allowing biometric controlled prosthesis. These devices are referred to as "myoelectric prosthesis" and use EMG with varying post processing to achieve the control. The post processing of the higher end devices does not only increase the features but also increases the manufacturing cost dramatically. For this reason the amount of post processing for a low cost prototype would need to be kept to a minimum whilst still retaining an acceptable level of accuracy and functionality.

6.1.1   Appropriate sensing method

Due to the low cost nature of this prototype a pre-existing EMG sensing solution was unacceptable. The available solutions for EMG sensing are usually around $500USD comprising of both sensors and on-board signal processing. One of the reasons that these solutions are so expensive is because of the need for medical applications using EMG related signals and components, which require higher tolerances and stricter specifications. Creating a sensing solution for this project from basic components and doing the signal processing in-house would reduce the costs dramatically.

After researching existing EMG sensing methods and materials a set of passive, disposable, skin adhesive, silver chloride electrode pads were chosen for their hypoallergenic and sensing qualities. These electrode pads were made to be paired with a medical grade EMG cable, the cable possess very low impedance and active shielding which made it perfect for this application.

6.2   Ethical Concerns

Due to the need for human testing for the EMG circuit an ethical concern was raised. The Massey University code of ethics dictated that the ethics board would need to be notified. To assess the level of risk this testing would pose a meeting was held with the project supervisor and a risk survey was carried out. The survey indicated that the level of risk this study posed was low and thus a low risk notification needed to be submitted to the ethic board. The identified risks for this study were limited to possible electrocution and allergic reactions.

The allergic reaction risk was reduced by using hypoallergenic adhesive pads, as this is the only part in contact with the skin so no other hypoallergenic parts were needed. If there was an allergic reaction, skin cleaning pads were kept close to the experimental setup to remove any reactive material from the skin. The possible electrocution risk was minimised by conducting the tests in a laboratory environment with equipment that was current and voltage limited. This reduced the possible shock transferred to the

testing subject to safe levels and a maximum of slight discomfort. The low risk notification was accepted on the 8th of July and the testing was cleared to begin.

6.2.1   Preparation

In the testing of EMG on patients the skin needs to be prepared for the best signal to be obtained. This includes cleaning the skin with rubbing alcohol to ensure a good connection (Daley, Englehart, Hargrove, & Kuruganti, 2012) and should be treated in accordance with the International Society of Electrophysiology and Kinesiology (ISEK) protocols (Potluri, et al., 2011).

6.3   First Design

The first design for the EMG sensing circuit was a single channel design inspired by an ECG design. The first step in designing the EMG sensing circuit was to locate a relatively cheap set of effective sensors. The sensors that were chosen are a set of hypoallergenic silver chloride sensors, each pad had a set of 3 sensors mounted. The three sensors are used to not only sense the changes in the voltage of the muscle underneath, but also to drive a signal back to the body. To enable the interface between the sensing pad and the rest of the sensing input circuit, a suitable cable had to be chosen. The cable that was chosen is a Snap-on cable that was designed to be used with medical sensing pads. The cable itself is also medical grade with three sensor interfaces as well as an active shielding running along the length. This active shielding reduces the interference caused by the long cables acting as antennas.

The three sensing pads are used to gain two differential input signals from the muscle to use as inputs and then the third pad is used to drive a reference signal to the skin of the body. This reference signal acts a grounding signal for the body, without this signal the EMG input would move arbitrarily based on the noise of the rest of the body. The two differential inputs are fed from the cable directly into the inputs of an instrumentation amplifier, the INA2128 (Datasheet included in Appendix 1). This instrumentation amplifier has a large gain factor and it has very high common mode rejection ratio (CMRR). Having a high CMRR means that the instrumentation amplifier rejects the common signals on the inputs, only amplifying the difference between the two signals.

The difference between the signals is then amplified 1000 times to a level that is detectable by oscilloscope or Data Acquisition Card (DAQ). The gain of the instrumentation is set by the gain equation in the INA2128's Datasheet; the natural difference in the signal is measured in microvolts and for this the gain has to be set to 1000x to raise the difference signal to the millivolt range. To achieve a gain of 1000 a 44Ω resistor is required. The active shield and the body reference signals are generated out of the back of the gain resistor. This signal is then buffered and sent directly to the active shield output of the Snap-on cable. The same buffered signal is then amplified and fed back to the body through the body reference pad. This application and schematic are included in the application information in the INA2128 datasheet (Appendix 1 pg. 10).

6.3.1 Initial Design Schematic and PCB

The schematic and the PCB Design of the first sensing circuit were designed using Altium which are shown in Fig 6.1 and 6.2 respectively, taken from (Scott, Tang, & Gupta, 2012). The part list is presented in Fig. 6.3.
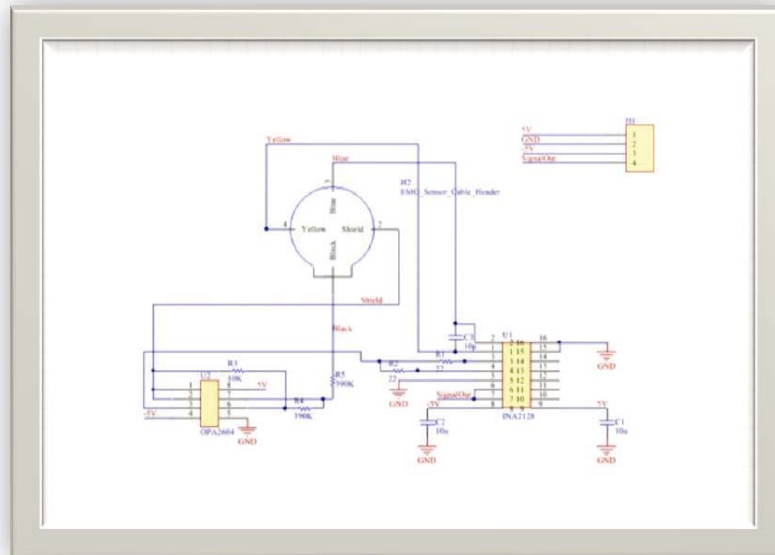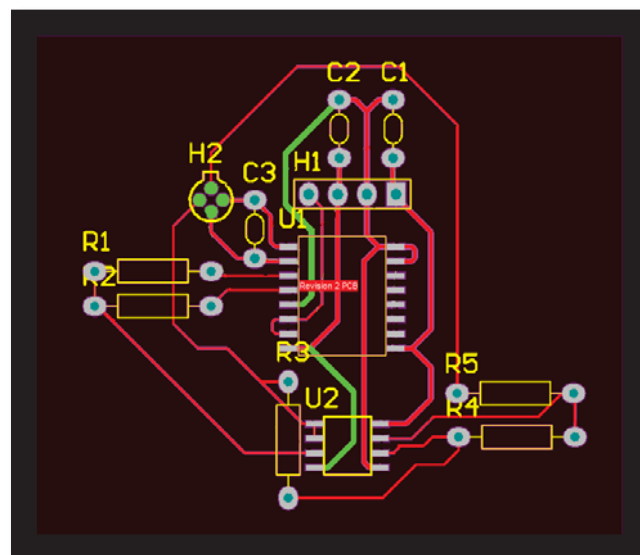

Fig. 6.1 - First Design Schematic

Fig. 6.2 - PCB Layout of First Design

Part	Quantity
INA2128	1
OPA2604	1
22Ω resistor	2
390KΩ resistor	2
10KΩ resistor	1
100nF Capacitor	2
10pF capacitor	1
4 pin header	1

Fig. 6.3 - Parts List for First Design

6.3.2 Initial Design Output

The output of the first attempt was acquired using a National Instruments DAQ in conjunction with National Instruments programming tool "LabView". Because the DAQ was manufactured by National Instruments, it worked flawlessly with LabView's inbuilt data acquisition interface. A program was created to test the circuit and the strength of the signals it produced. This program was used to indicate to the test patient when to activate and deactivate the muscle, what the output looked like and recording the output to a file for later analysis. The program used a flashing green light to indicate when the patient was to activate the target muscle, this allowed the output to be easily read if the circuit was working or not. Shown below is the LabView program interface front page, block diagram and circuit output. The sample rate chosen for the data acquisition card was set at 1000Hz due to research showing the frequency range of interest to be between 60Hz and 180Hz (Jamal, 2012), 1000Hz would both provide a simple period between samples (1ms) and satisfy the Nyquist criterion.
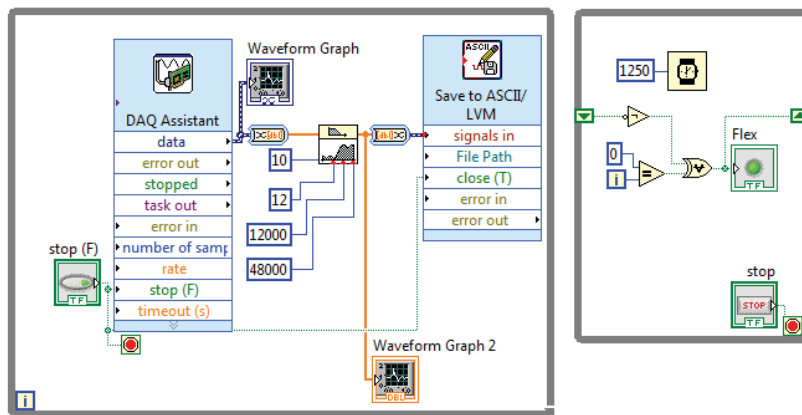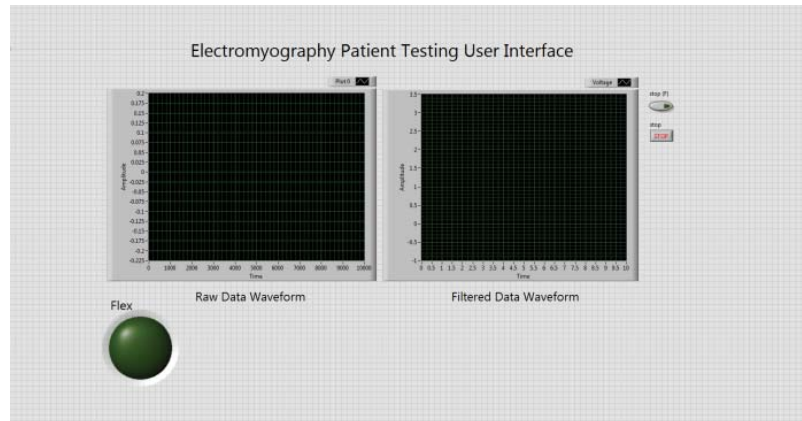
Fig. 6.4 - EMG Capture Program Interface (Top) and Block diagram (Bottom)

The output of the circuit was measured for both an able-bodied person and for an amputee to ensure that the control method is able to be used with the end user. The output of the circuit was then compared between the amputee and the able bodied person to gauge the potential difference affect an amputation has. Fig. 6.5 shows the comparison between similar aged males and the amputee's amputated arm when asking them to grip a ball. The processing of the raw signal to achieve the waveforms shown in Fig 6.5 was to take an absolute moving average with a 30 point window.
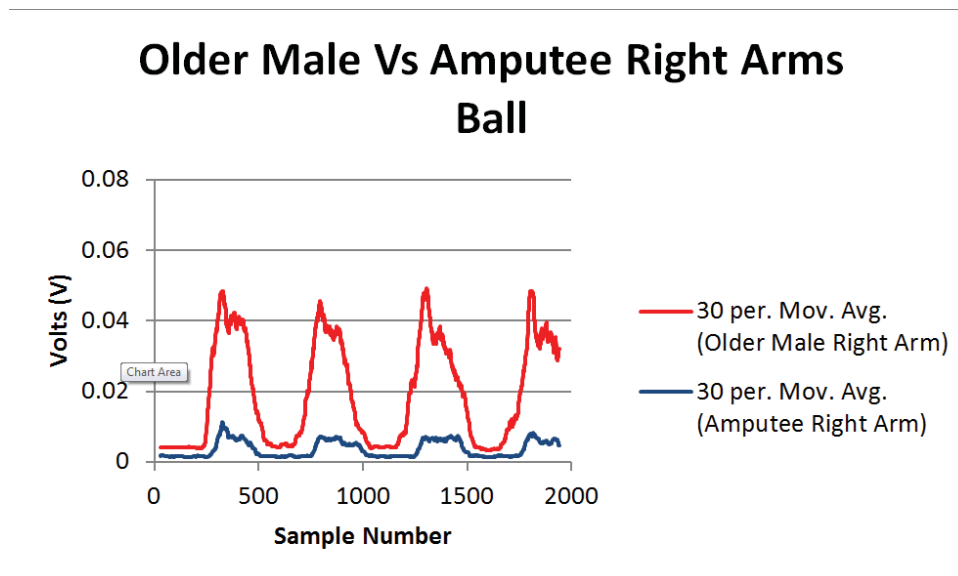
Fig. 6.5 - Comparison between Similar Aged males and the Amputee's Amputated Arm

6.3.3 Initial Design Output with Amputee

The sensing circuit when tested on the amputee provided unexpected results. The first test session with the amputee provided largely reduced amplitude when compared to an able bodied person. This was expected due to the lack of use of the target muscle. The unexpected result was the degree of reduction of the amplitude, an observation was then made that the sensor pad was not lying directly on top of the muscle. This observation caused a series of measurements to be taken on the able-bodied patient to find the maximum potential for EMG. This was then converted into % length of limb, % limb muscle and distance from elbow. Each of the sensor positions were then tested on an able bodied person and the overall output was averaged into a voltage using Matlab. These averages were used to assess the relative strength of each position. The %limb length means that the sensor pad could be accurately applied to the amputee in the correct location.
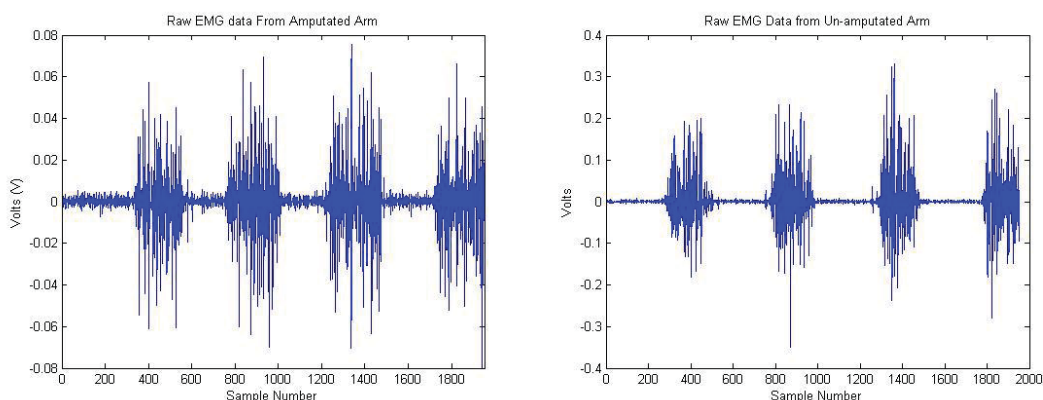

Fig. 6.6 - Amputee Data Amputated Arm (Left) Vs. Uninjured (Right)

74

The output data above shows the effect that the amputation has taken upon the strength and response of the muscle. The left shows the signal captured from the arm which suffered the amputation while the right shows the signal from uninjured arm. The points of note are the shape of the waveform and the amplitude of the response. The shape of the waveform is notable because it retains the pattern shown by the uninjured arm. This proves that the amputation has not affected the ability of the muscle to produce the expected signal and has not distorted the output significantly. The amplitude of the amputated response is significantly reduced. This can be seen by the amplitude of the waveform between the two graphs. The maximum output of the uninjured arm was approximately 0.3V as compared to the reduced amputated arm amplitude of 0.06V maximum. This has an amplitude of only 20%.

6.3.3.1 Sensor Positioning

To ensure the best possible signals that were able to be obtained off the arm used in analysis, sensors were placed along the target muscle group and conducted the base case test on myself. After logging the data from each sensor a MATLAB 'm' file was created to read in the data to turn each test into its absolute equivalent and then average them together with the other tests performed at that sensor location (4 tests from each position). Fig. 6.7 illustrates the sensor locations. This gave the absolute average data stream for each position. The next operation that was performed through the 'm' file was to scan the waveform and perform a threshold evaluation to find the 4 pulses. At the end of the scanning, the average of the recorded points was taken to find the overall average response.

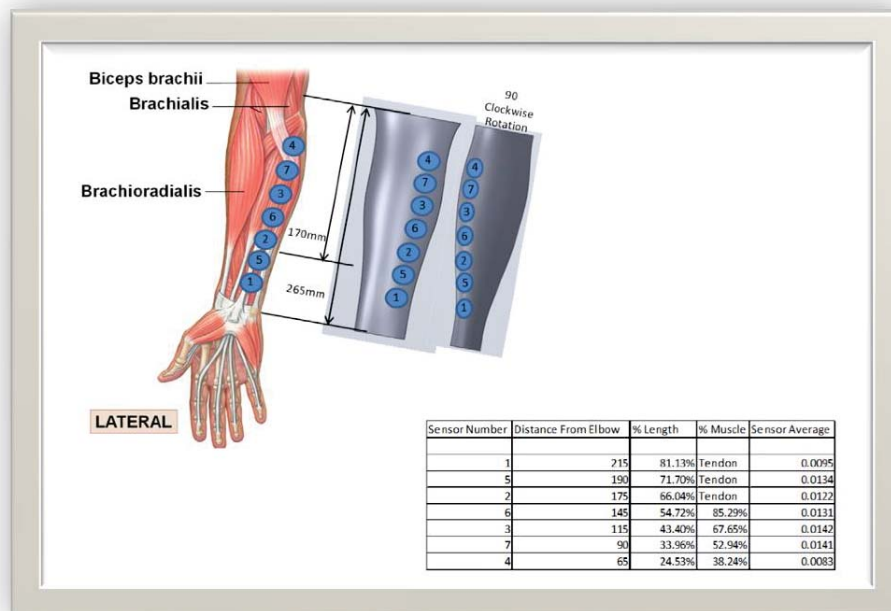| Sensor Number	Distance From Elbow	% Length	% Muscle	Sensor Average
1	215	81.13%	Tendon	0.0095
5	190	71.70%	Tendon	0.0134
2	175	66.04%	Tendon	0.0122
6	145	54.72%	85.29%	0.0131
3	115	43.40%	67.65%	0.0142
7	90	33.96%	52.94%	0.0141
4	65	24.53%	38.24%	0.0083

Fig. 6.7 - Sensor Positioning Test

Sensors 1, 5 and 2 are all positioned at the hand end of the arm over the smaller groupings of muscle fibres and tendons, causing a lower response than the other sensors placed on the larger portion of the muscle. Sensors 6, 3, 7 and 4 all showed a significantly higher response, the two that stood out however were sensors number 3 and number 7 with a response of 0.0142. Position 3 was chosen to conduct tests as it showed a marginally higher response but position 7 would have also suited the testing procedure.

6.4   Dual Channel Design

After the successful output of the first EMG sensing circuit, a revision was made to include a second EMG input channel. This allows the use of both the agonist and antagonist muscles for an activation and deactivation of the device. The INA2128 instrumentation amplifier suits the conversion to a dual channel design as it contains two instrumentation amplifiers in one device. This means the conversion to a dual channel design only requires one extra op-amp, a capacitor and 5 extra resistors. These extra components are cheap compared to the INA2128 and therefore the extra channel will not impact the cost of the project significantly.

6.4.1   Part Choices

The part choices for this circuit were driven from the first circuit design experience. The tri-pad electrodes were augmented with a set of single pad electrodes to allow for a more dynamic placement on the muscle. The single pad electrodes are also hypoallergenic with a conductive gel underneath the electrode to reduce the resistance of the skin on top of the muscle. A longer EMG snap on cable was also purchased to allow some flexibility for testing by removing the physical restriction in testing created by the initially short snap on cable.

6.4.2   Design Schematic and PCB

The circuit schematic and the PCB design to realise the dual channel operation are shown in Fig. 6.8 and Fig. 6.9. The design shows an exact mirror of the original circuit using the second channel of the INA 2128 instrumentation amplifier.
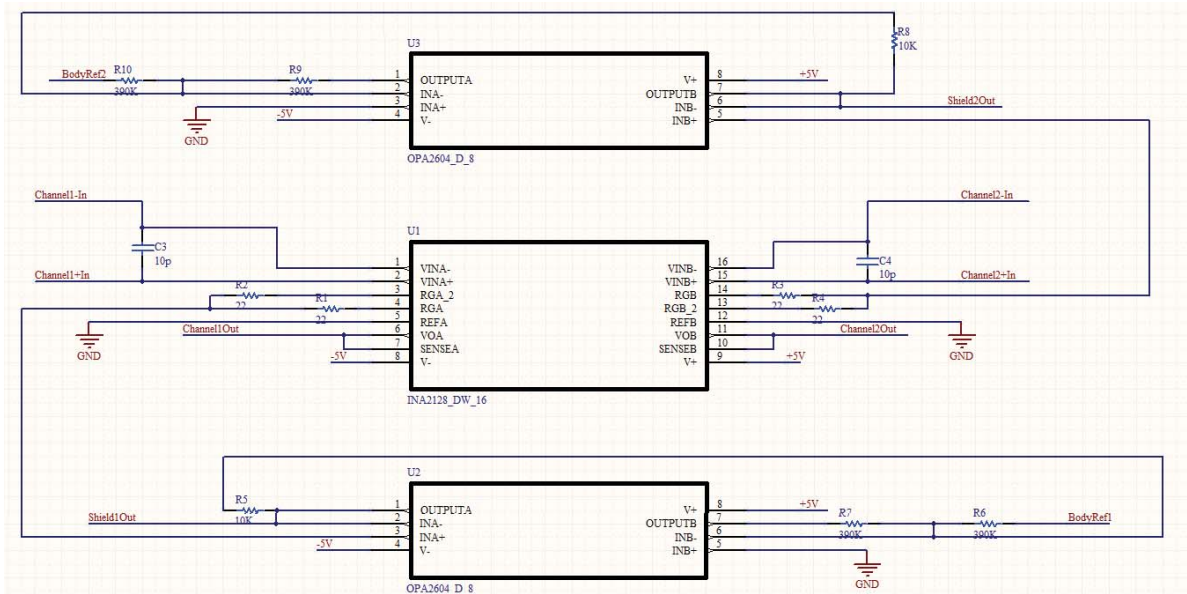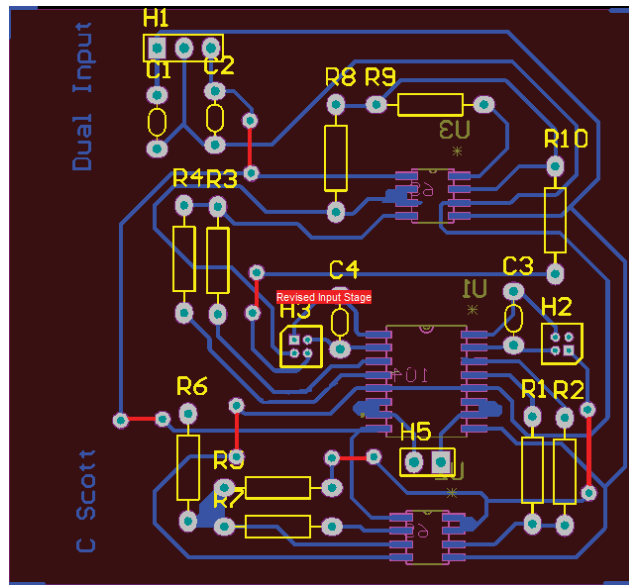
76

Fig. 6.8 - Dual Channel EMG Schematic

Fig. 6.9 - Dual Channel EMG PCB Design

6.4.3   Design Output

The output of the dual channel circuit is as expected. The output for each channel is the same as the single channel. This allows for the required dual channel output to control the prosthetic device in both the forward and reverse direction, therefore proving that this is a viable solution to be implemented for the prosthesis prototype design.

6.5   Filtering

EMG input signals are a highly varying signal with many frequency components. The body is an inherently noisy environment caused by muscular crosstalk and other bodily functions. In addition to the internal noise generated, the body and sensor cables act as antennas picking up external noise. The additional signals that are picked up by these antennas are power line noise and induced noise mostly at 60Hz. This additional signal needs to be removed from the input signal before any control methods are able to be applied. The waveform that was captured from the EMG sensing circuitry was analysed by using a Fast Fourier transform (FFT) to produce the frequency components of the input. Signals are able to be represented in both time and frequency domains, by analysing the input in the frequency domain the main frequency components of the waveform are able to be deduced. The Fourier response is shown below.
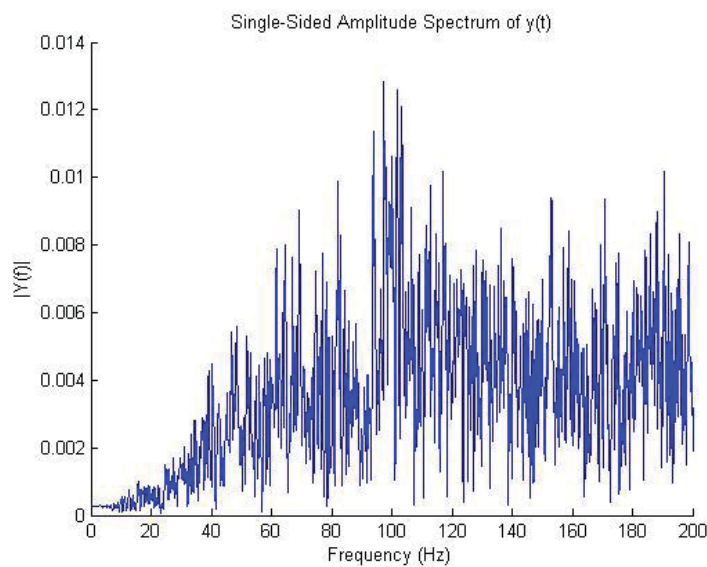

Fig. 6.10 - Fast Fourier Transform of Captured EMG Data

Studies show that the primary frequency components that EMG is comprised of are between 60 and 180Hz (Jamal, 2012). The input signal captured by the prototype circuitry shown in Fig. 6.10 contains far more frequency components than the ones lying in the range shown in the studies. To remove unwanted signal components on the input waveform, a filter was required. The filter designs are to be implemented in hardware to keep the computational cost down for the microcontroller, allowing a cheaper microcontroller to be used for control.

There are three possible filter designs that are able to provide the desired frequency response. These filters are: a low pass filter, a high pass filter and a band pass filter. The next section covers the function of the filters and the specific application to this prosthesis prototype.

78

6.5.1　High Pass Filter

The high pass filter is a filter that is used to remove the low frequency components of a signal. The basic high pass filter is a Resistor and Capacitor (RC) circuit placed in-line with the signal. Shown below is the configuration of the RC circuit.
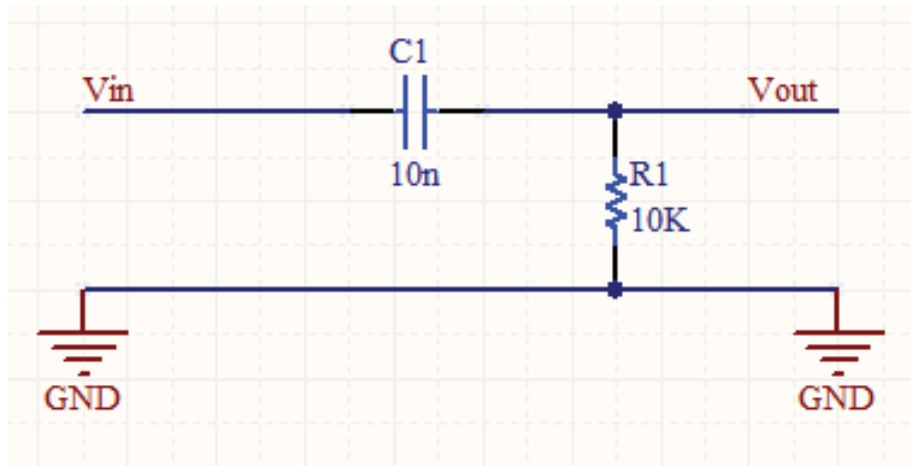

Fig.　6.11 - Basic Highpass Filter

The capacitor in series with the signal allows a highly varying signal pass through easily as if in short circuit across the capacitor while a slowly varying signal would charge the capacitor slowly and this charge is then dissipated through the resistor to ground. This filter is considered to be a single pole filter and has an attenuation effect of -20dB per decade, for a higher attenuation rate a filter with additional poles would be needed. The reactance of the basic high pass filter is shown in equation 6.1.

$$Cutoff\ Frequency \qquad f_c = \frac{1}{2\pi RC} \qquad\qquad [6.1]$$

To allow for a higher attenuation rate and a larger degree of accuracy an op-amp is able to be employed in filter applications. These op-amp filters are capable of higher numbers of poles and therefore a steeper rate of attenuation, however they are much harder to design. For this reason a filter design tool was used to attain the required filter parameters and response. This filter tool is called "FilterPro" by Texas Instruments and is available from their website for free. The design process for filters is covered in section 6.5.4.

The requirements for the high pass filter design in this application were to filter out all frequency components below 60Hz because the range below this point only consists of noise and unwanted frequencies. To reduce the components sufficiently to make them negligible, an attenuation rate of at least -90dB per decade was preferred to ensure a clean signal therefore at least 2 stages were required. The filter design generated by FilterPro is shown below along with the frequency response of the pictured filter.
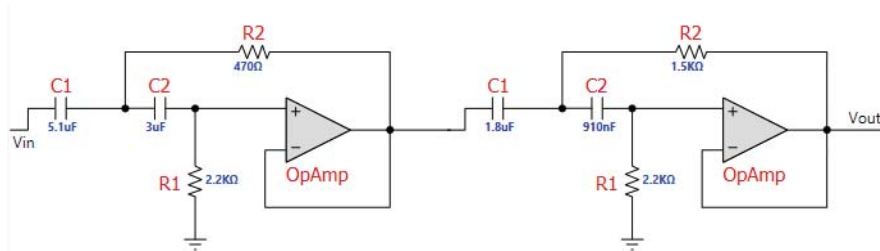
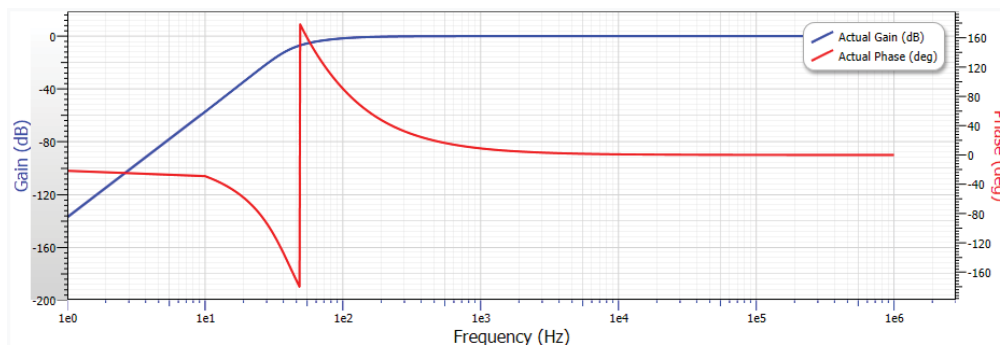**Fig. 6.12 - Highpass Filter Design 65Hz Schematic**

Fig. 6.13 - Highpass Filter Design 65Hz Response

6.5.2 Low Pass Filter

A low pass filter is intuitive in such a way that it does the opposite of the high pass filter. This type of filter is designed to only allow the low frequency components of a signal pass through while attenuating the high frequency components. The basic design of a low pass filter is another RC circuit with the difference being the orientation of the resistor and capacitor. In a low pass filter the resistor is the component placed in-line with the signal and the capacitor bridges the signal and ground lines. Having the capacitor placed between the signal line and the ground line make it act like a short circuit to ground for high frequency components of the input while the low frequency components bias the capacitor slowly enough for the low frequency components to pass through the resistor and continue into the input. The cut-off frequency of this filter is governed by the same transfer equation as the Highpass.
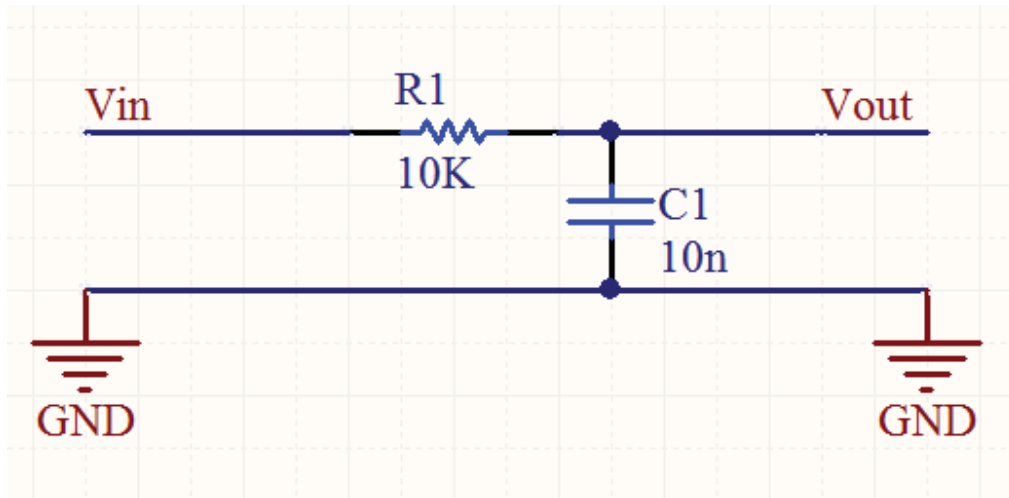
80

Fig. 6.14 - Basic Lowpass Filter

The requirement of this low pass filter is to remove any high frequency noise that is received from the surrounding environment such as radio frequency. With EMG only requiring the range between 60 – 180Hz the low pass filter needed to be set to attenuate all frequencies above 180Hz. 180Hz is still relatively low in relation to the radio frequency noise, the attenuation does not need to be as high as the high pass filter. Shown below is the generated low pass filter from FilterPro.
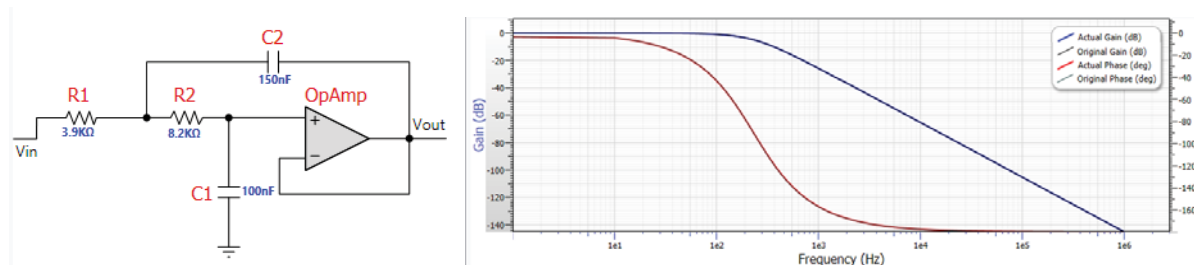

Fig. 6.15 - Lowpass Filter Design 180Hz Cut-off - Schematic (Left) , Response (Right)

6.5.3   Band Pass Filter

The band pass filter is a filter that only allows through a "band" of frequencies. These are generally comprised of a low pass and a high pass filter and will be able to achieve the same level of accuracy and attenuation as separate filters, however they may have additional stages. The band pass filter was designed to remove the need for two separate filters and to reduce the overall complexity of the circuit. The FilterPro design is shown below.
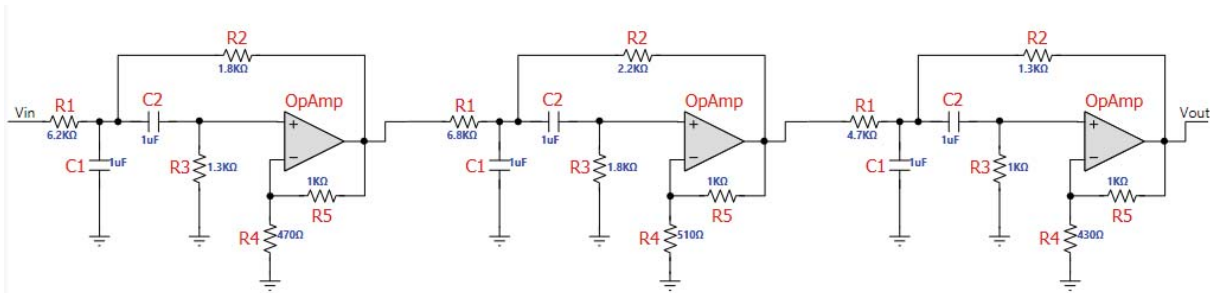
Fig. 6.16 - Bandpass filter 65-180Hz Passband

6.5.4 Filter Design Using FilterPro Software

FilterPro is a filter design tool which is capable of designing five different types of filters: Lowpass, Highpass, Bandpass, Bandstop/Notch and Allpass (time delay). This tool is used predominantly by following the design wizard shown below. The first step in the wizard is to select the desired filter.
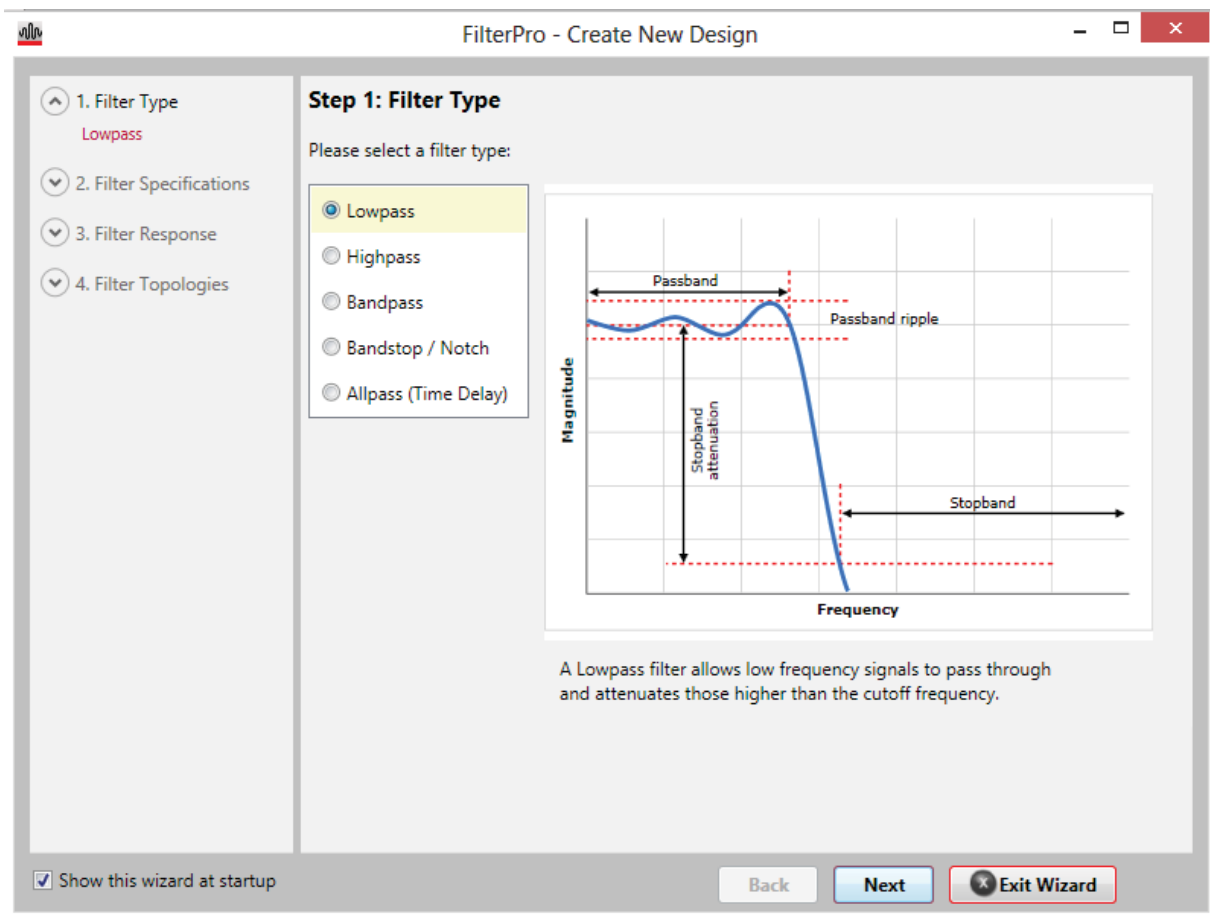

Fig. 6.17 - FilterPro Wizard Step 1 (Filter Choice)

Once the desired filter is chosen an appropriate set of dialogue boxes and explanation text is shown for the user to enter the required parameters of the filter. These parameters include: the gain, passband frequency, passband ripple, stopband frequency and stopband attenuation. For this application the

82

highest frequency required by the EMG input was 180Hz, this frequency is the final non-attenuated frequency in the low pass filter and therefore is the value at which the passband ends. Radio frequency noise is higher than 5KHz so the default value for the stopband is allowable. Finally the attenuation needs to be set, -45dB is a standard attenuation rate for a filter.
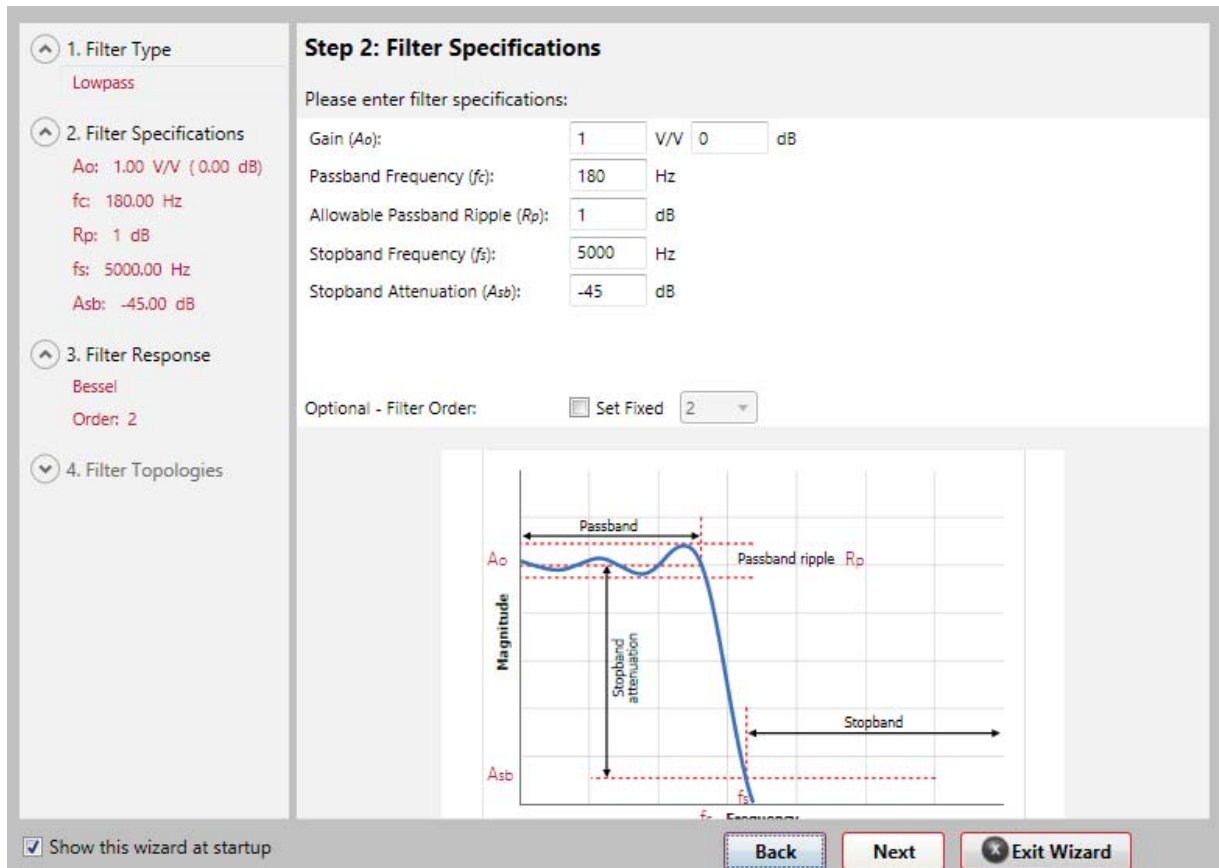

Fig. 6.18 - FilterPro Wizard Step 2 (Entering Filter Values)

The third step to designing a filter in FilterPro is to choose the filter characteristic. There are multiple characteristic filtering methods that produce slightly differing frequency responses, FilterPro will usually default to the simplest and most accurate method for the user. Each method's frequency response is shown at the bottom of the wizard so the user is able to make an informed decision before proceeding to the final step. Additionally each method has a complexity shown alongside its name in the selection area, the complexity is comprised of poles and stages. A higher number of poles allows for a sharper attenuation however they will usually require additional stages. Additional stages require extra op-amps and components making the filter more expensive to manufacture so the simplest design is usually preferred. The Bessel filter was chosen because of the low number of stages and the acceptable response shown in the graph.
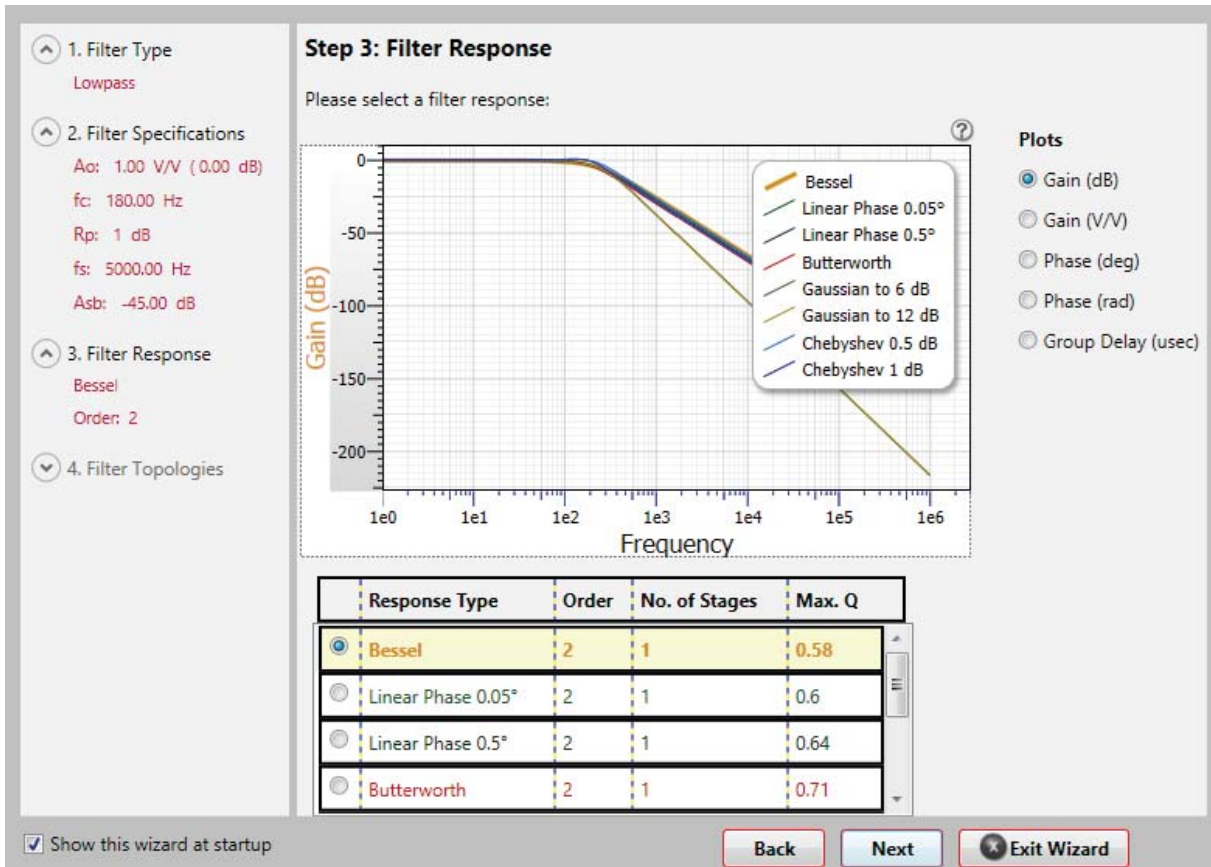
Fig. 6.19 - FilterPro Wizard Step 3 (Selecting Filtering Method)

The final stage of the FilterPro design wizard is to select the topology of the filter. FilterPro offers three different options for the design topology of the filters: Multiple Feedback (Single Ended), Sallen-Key and Multiple Feedback (Fully Differential). The Multiple feedback topologies are used when low component count is desired while the Sallen-Key design is designed to be user-friendly. Sallen-Key topologies were chosen for the applications required by this prototype due to the user-friendliness and easy implementation.
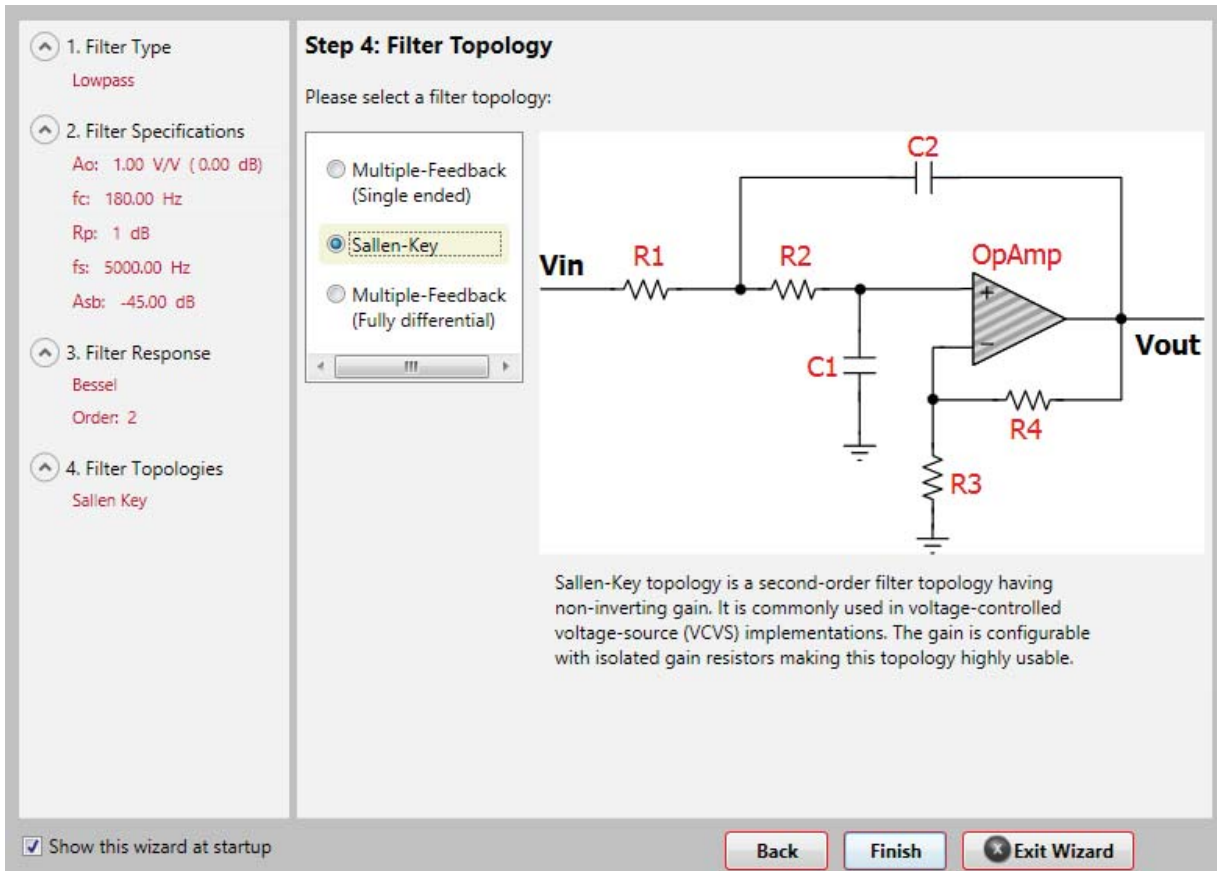
Fig. 6.20 - FilterPro Wizard Step 4 (Choosing Topology)

After the wizard has been completed, the desired filter is generated and displayed in the main window of the software. From this point it is important to note that all of the shown resistor and capacitor values are exact. Using exact values commonly requires costly and rare components to realise the filter, to mitigate this cost an option is available to change the tolerances of the components in the filter. This allows the components used in the filter to be matched closely to a common component value while still retaining the majority of the specifications set in the wizard. The filter frequency and phase response is shown in a panel at the bottom of the main screen and updates with every change that is made to the design such as component tolerances.

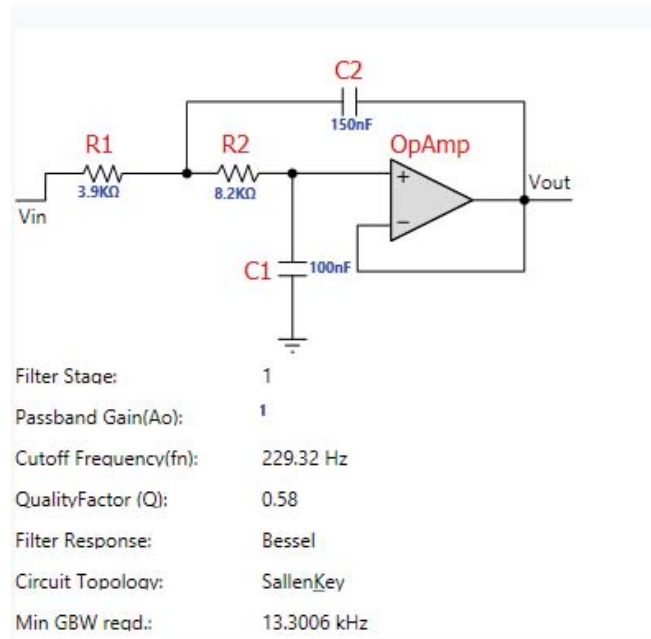**Fig. 6.21 - FilterPro Component Tolerance Bar**

Fig. 6.22 - FilterPro Filter Schematic Output

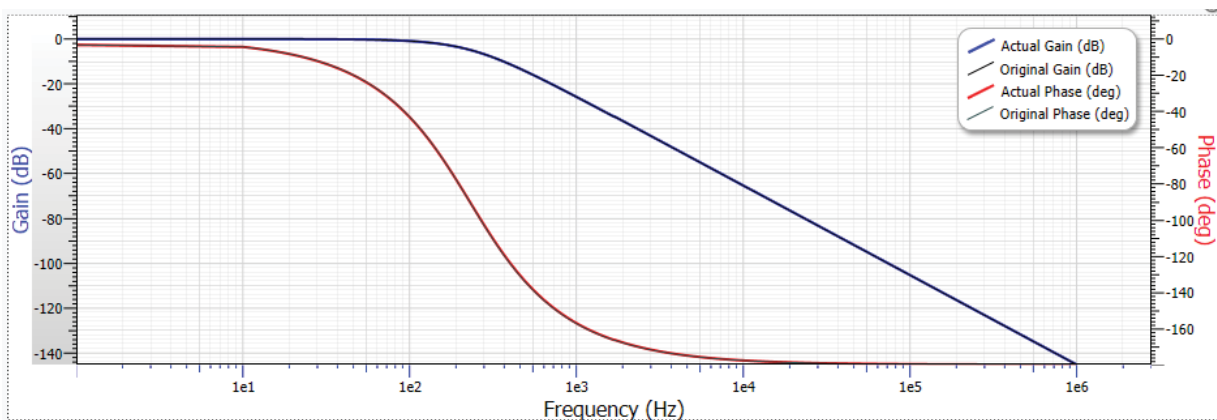| Filter Stage:	1
Passband Gain(Ao):	1
Cutoff Frequency(fn):	229.32 Hz
QualityFactor (Q):	0.58
Filter Response:	Bessel
Circuit Topology:	SallenKey
Min GBW read.:	13.3006 kHz

Fig. 6.23 - FilterPro Schematic Frequency and Phase Response

6.5.5   Simulated Filter

Due to the limited time to develop the filtering and the ease of buying off the shelf filters, it was deemed unnecessary to create the filters from scratch for the initial prototype. However in future revisions a specific filter such as those designed above should be used. Instead of procuring hardware to do the filtering, a software filter was created in LabView to produce an analogous result. This software filter was then built into the data acquisition VI. The difference in signal is shown in Fig. 6.24.
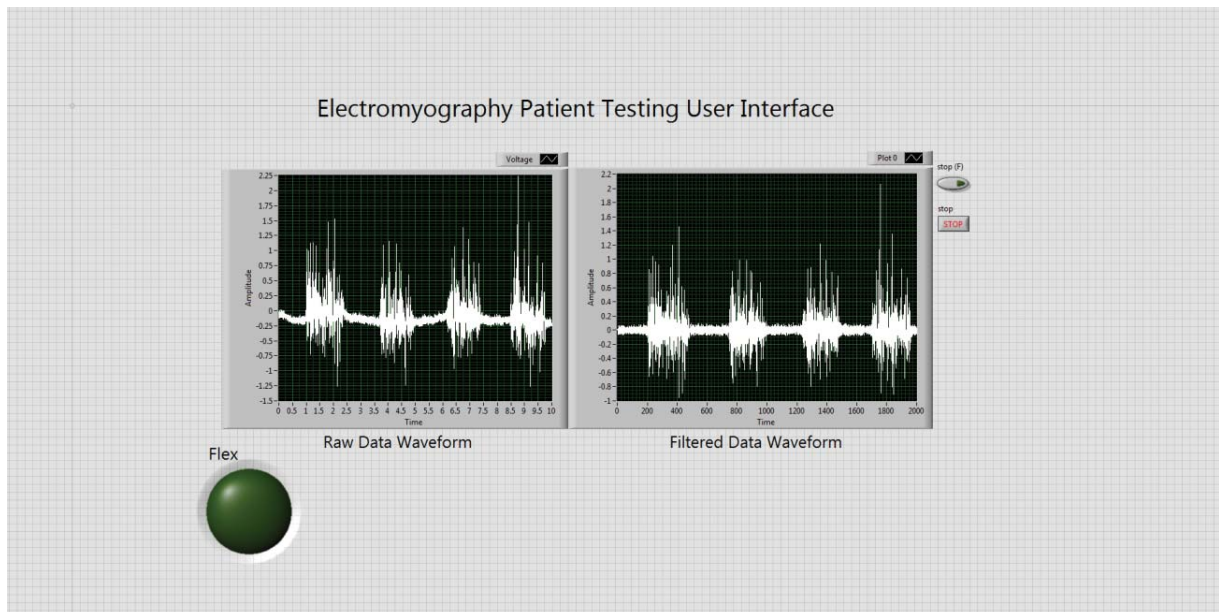
Fig. 6.24 - Signal Comparison after Filtering

6.6 EMG Conditioning

Once the EMG input signal has been filtered to remove the unwanted frequency components it is still not ready to be used as a control input to the mechanical prototype. The waveform is still a highly varying signal and is not suitable for the requirements of a microcontroller's input pin. The signal must occur between 0V and 3.3V and provide a solid activation window when the muscle has been contracted. The EMG signal needed to be converted from its natural +/- < 1V highly oscillating signal to a slower moving signal between 0 - +3.3V while retaining the activation information. This conversion can be done in software on a personal computer, however this is not suitable due to the lack of portability. The conversion could be completed on-board a high powered expensive microcontroller but that works against the low-cost option of this project. The final decision was made to do the signal conditioning in hardware to reduce microcontroller processing and memory overheads. This enabled a cheaper low-powered microcontroller to be considered for control. This section discusses two different signal conditioning methods to prepare the signal for input into the control system.

6.6.1 Mean Average Voltage Circuit

The Mean Average Voltage Circuit (MAV) is a series of circuits designed to take the input signal and transform it from a fast moving small amplitude signal into a slower moving higher amplitude signal suitable to input into a microcontroller. As the name suggests, the final output is an averaged voltage of the input over a short window, essentially a moving average of the input signal. There is more than one possible implementation of this MAV circuit. In the following section, some selected implementations are discussed followed by details of the individual circuits.
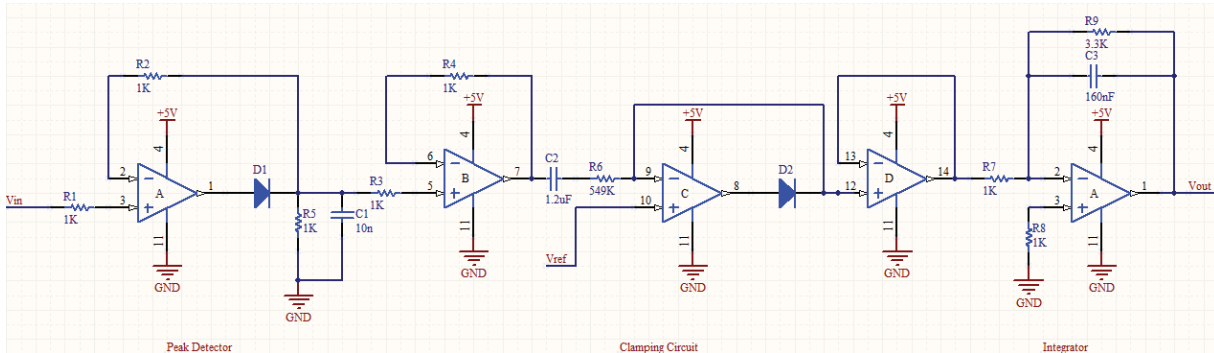
6.6.1.1 *Implementation 1*

Fig. 6.25 - MAV Implementation #1 Schematic

Implementation 1 process block diagram is shown in Fig. 6.25. As the filtered input waveform is fed into the conditioning circuit it is passed into a peak detecting circuit. The purpose of this circuit is to accentuate the peaks of the input waveform so they are more easily observed and the added amplitude is an important feature for the rest of the MAV circuit. The waveform is then clamped to a safe and useable voltage before it proceeds into an op-amp integration circuit. The purpose of the integration circuit is to smooth the detected peaks and to provide the averaging function across the window to allow a more reliable control signal for the microcontroller.
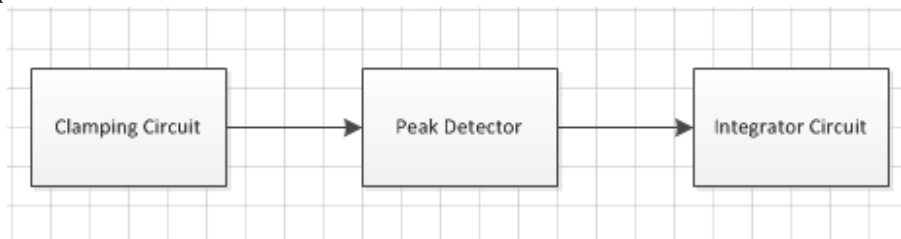
6.6.1.2 *Implementation 2*

Fig. 6.26 - MAV Implementation 2 Block Diagram

The second possible implementation method is to rearrange the order of operations to clamp the signal before the peak detection phase. By moving the clamping circuit to the beginning of the conditioning series, the input waveform is shifted in amplitude such that the peaks of the waveform are higher in amplitude and therefore more of them are likely to be detected by the peak detector. This clamping shift would however pose a problem after the integration stage because when the entire waveform was amplified instead of just the peaks, the overall waveform would have higher amplitude and therefore be too large for suitable input into the microcontroller. In this case an additional level shifter would be required to make the input suitable.

6.6.1.3 Implementation 3

Fig. 6.27 - MAV Implementation 3 Block Diagram

The third Implementation is to use a clipping circuit in place of the clamping circuit in the first implantation. Using a clipping circuit instead of a clamping circuit would clip the waveform at 3.3V rather than allow it to move within the full 5V range. This would restrict the integration circuit from ever exceeding the 3.3V limit of the microcontroller.
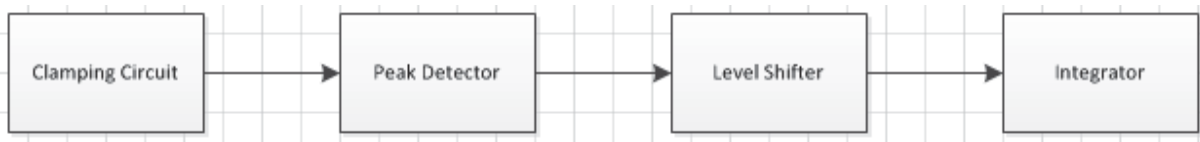
6.6.1.4 Implementation 4

Fig. 6.28 - MAV Implementation 4 Block Diagram

The final implementation discussed in this section is similar to implementation number 2 except the level shifter is placed in front of the integration circuit. In this implementation the clamping circuit will raise the signal amplitude to allow the peak detector to detect the maximum number of peaks. The output is then level shifted to bring the low level voltage back to 0V and then the integrator would be able to provide the averaged signal with respect to a 0V reference.

6.6.1.5 Peak Detector

The peak detector circuit is used to amplify any peaks that occur in the waveform. By accentuating the peaks of the input wave, the windows of activity would be far more obvious and easier to condition. A basic peak detector circuit is shown in Fig. 6.29. The signal is passed through an op-amp with a negative feedback loop. The output of the op-amp is passed through a diode and is used to charge a capacitor, this capacitor then holds the peak value of the input signal and when the waveform drops the capacitor will discharge slowly through the load. Fig. 6.30 shows the time domain response of this circuit is shown.
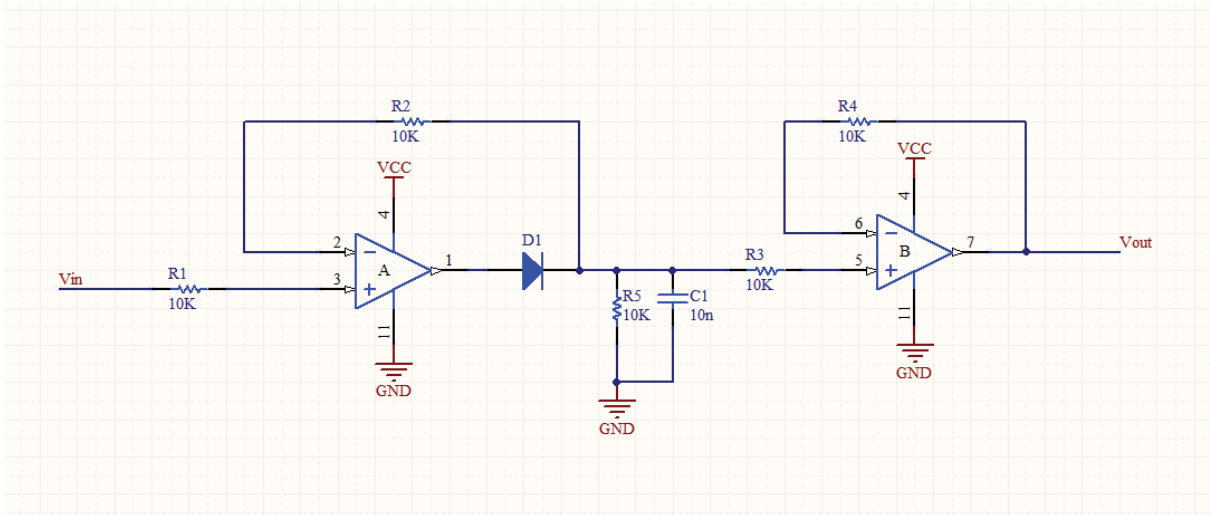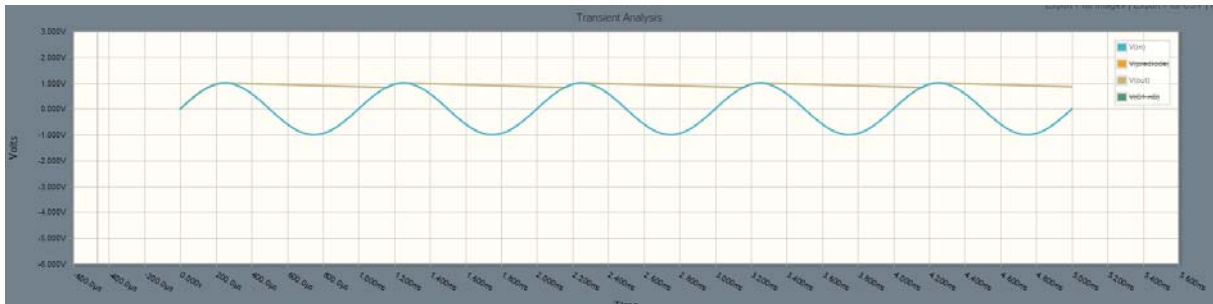
Fig. 6.29 - Peak Detector Schematic

Fig. 6.30 - Peak Detector Time Domain Response

Changing the value of the capacitor and resistor in this circuit will change the peak height and the discharge rate of the held peak, choosing a large capacitor will reduce the height of the peak as it does not have time to completely charge. The discharge time can be calculated by using the RC time constant. This constant is the amount of time it will take for the capacitor in the circuit to either charge to 63% or discharge to 37% of the maximum voltage. The equation for the RC Time constant is:

$$\tau = RC \qquad\qquad [6.2]$$

Where τ is the discharge time constant, R is the resistance and C is the capacitance.

6.6.1.6 Clamper Circuit

A clamping circuit is used to shift an entire waveform in either a positive or negative direction to clamp the peaks of the waveform to a specified voltage. This is done by raising the DC offset of the waveform and does not affect the shape of the waveform within the specified frequency ranges. A clamping circuit will not prevent the waveform from becoming negative if the negative peaks exceed the DC offset that the clamp provides. There are many different clamping circuit types: the positive biased, the negative biased, positive unbiased and the negative unbiased. The two unbiased types of clamp have a maximum peak value of 2x the input voltage while the two types with bias are able to have a maximum peak value of 2x the input plus the bias reference. A basic clamping circuit can be realised by using a diode across the signal rails in conjunction with a RC circuit. This can pose a problem as there is a 0.7V drop over the diode making the clamping circuit less efficient. A way to overcome this voltage drop is to use an op-amp in the circuit. The voltage drop is compensated for within the amplifier gain, making this a far more stable circuit design.

The design that was considered for the EMG applications shown in Fig. 6.31 is a positive biased op-amp based clamping circuit. Using this circuit topology, the waveform is able to be lifted above the ground reference and the activity envelope is able to be identified far easier. Equation 6.3 shows the calculation to find the required capacitance with F_{low} being the lowest required frequency.
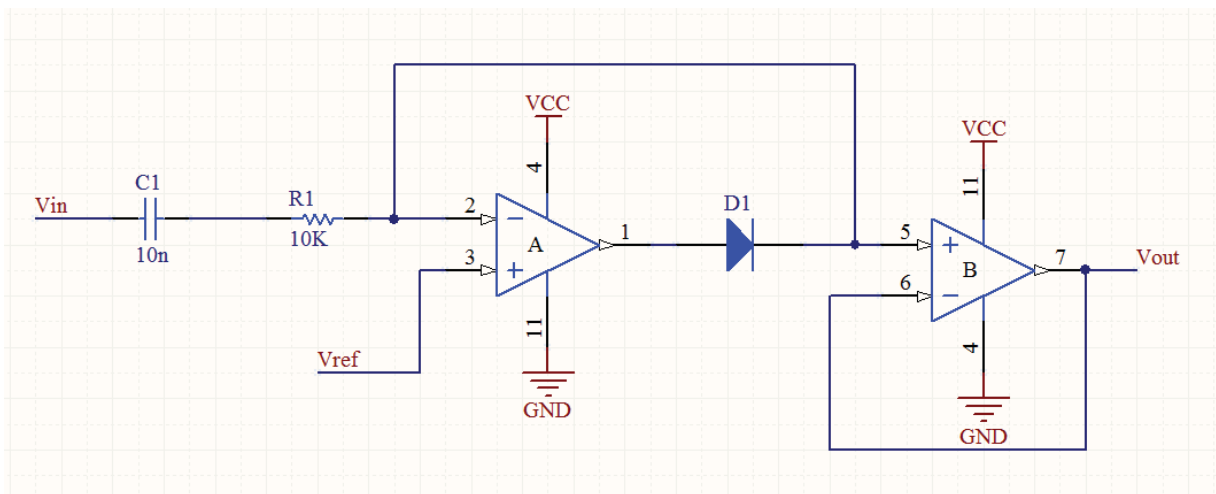
Fig. 6.31 - Clamping Circuit Schematic

$$C_1 = \frac{16.7}{R_1 F_{low}}$$ [6.3]

6.6.1.7 Integration Circuit

The integrator circuit is essential to making a slower moving waveform suitable for input into the microcontroller. The primary purpose of the integrator is to smooth out the highly changing signal and to make it into an activation envelope. The op-amp integrator averages the area under the waveform and creates a moving average that shows the activation periods clearly and smoothly. A simple integration circuit is shown below.

Fig. 6.32 - Basic Op-Amp Integration Circuit
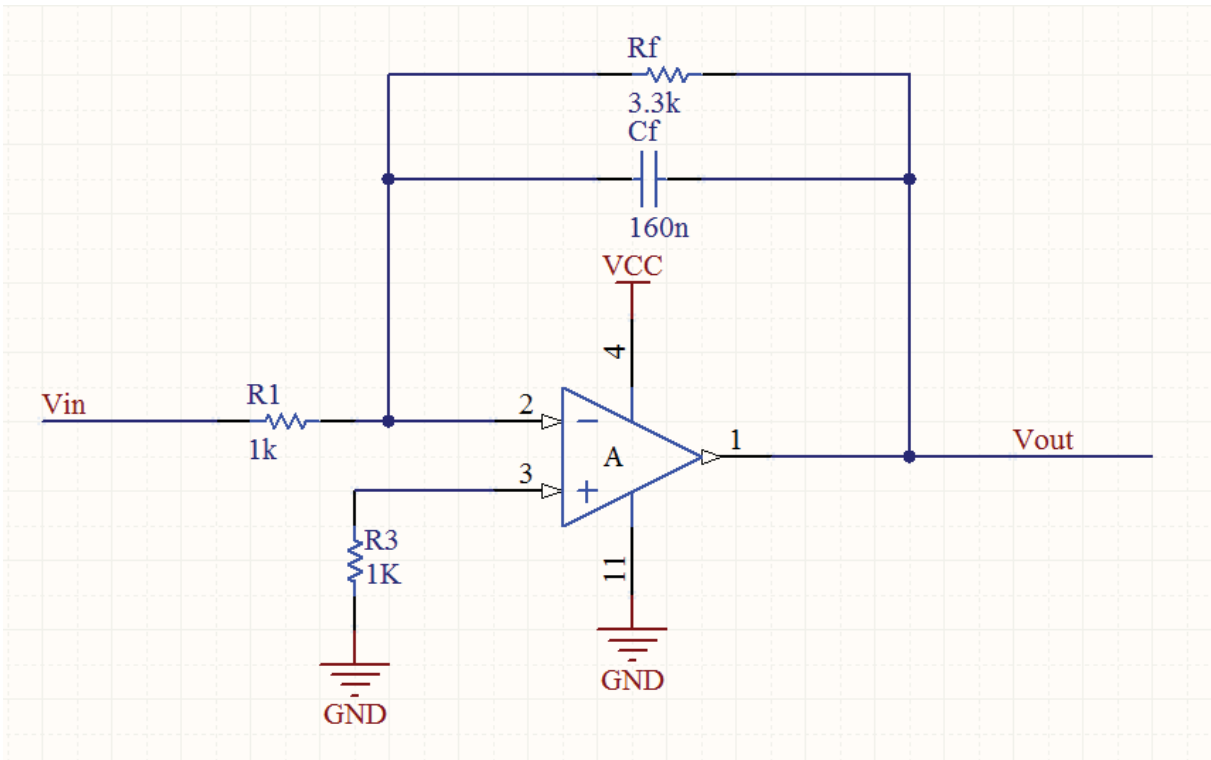
The integration circuit response is governed by the following equations:

$$F_b = \frac{1}{2\pi R_1 C_f}$$ [6.4]

$$F_a = \frac{1}{2\pi R_f C_f}$$ [6.5]

Where F_b and F_a are the crossover and 3dB cutoff frequency respectively.

6.6.1.8   Level Shifter

The purpose of the level shifter shown in Fig. 6.33 is to raise the level of the waveform to a more useable level. This circuit adds a predetermined DC offset to the waveform. This is generally used to raise the waveform above the ground reference or to condition the waveform to fit between a specific set of voltages.
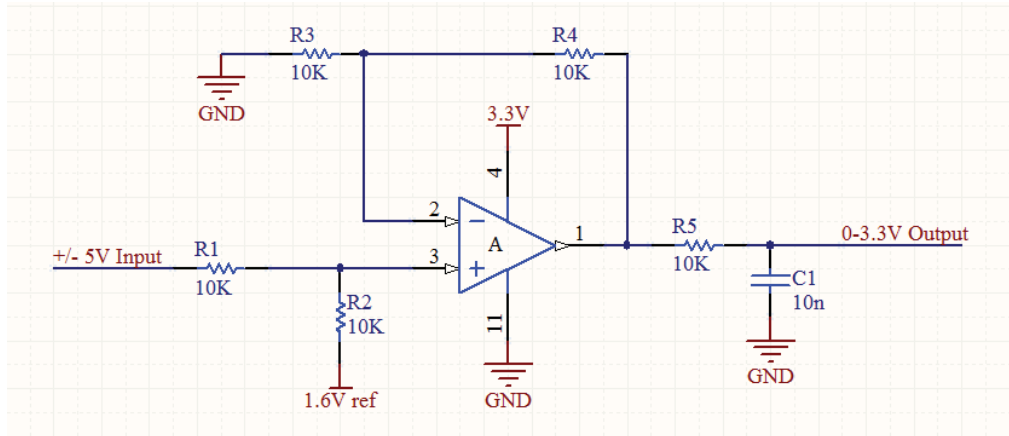
Fig. 6.33 - +/-5V to 0-3.3V Level Shiting Circuit

6.6.1.9   Clipping Circuit

The clipping circuit shown in Fig. 6.34 is similar to the clamping circuit except that instead of refitting the whole waveform to the reference voltage, the peaks are clipped at the reference voltage. This circuit is used if the amplitude of the waveform peaks is not important. This is especially useful for clipping the voltages of the waveform to protect inputs of microcontrollers and other integrated circuits.

Fig. 6.34 - Clipping Circuit Schematic

6.6.1.10 *Comparator Circuit*

Comparator circuits are primarily used to compare two waveforms and output an on/off or digital signal when waveform 1 is greater than waveform 2. It is common practice to use a ste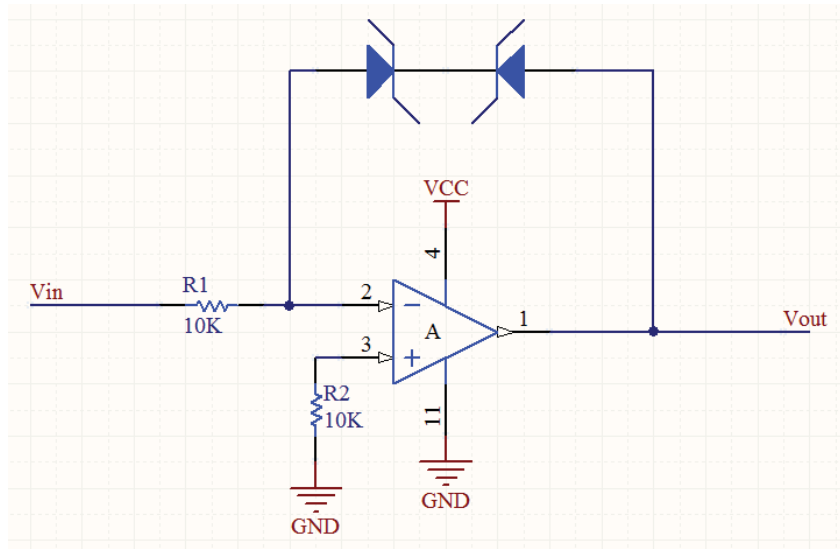ady DC reference voltage to set a threshold and use the comparator to identify when the signal passes the reference voltage thereby amplifying the peaks. These peaks can then be used as a reliable input into a control system. For adjustable sensitivity and possible calibration, a variable resistor can be used in a voltage divider to change the reference DC voltage to include or exclude the correct peaks of the signal waveform.
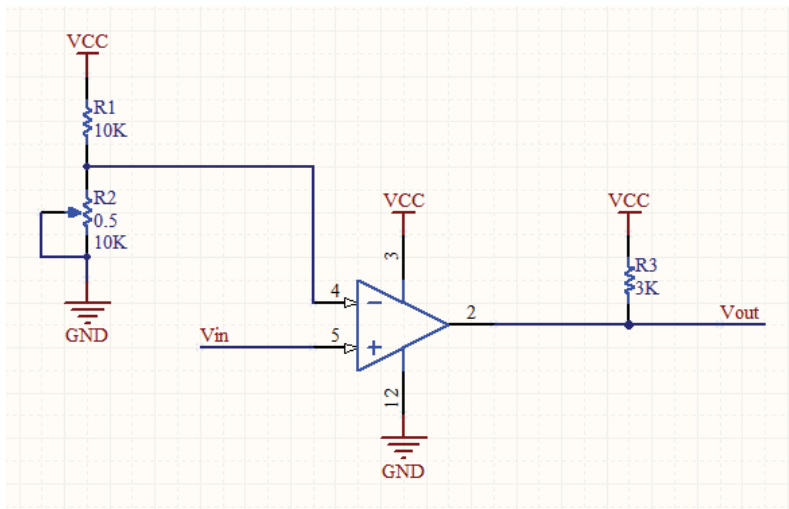
Fig. 6.35 - Comparator Schematic

6.6.2   Comparator Based Conditioning

Instead of using a MAV method of conditioning the signal, an alternate conditioning method was developed. The comparator based signal conditioning circuitry uses an amplifier to boost the signal waveform to compensate for the 1.2V drop over the full wave rectifier prior to passing the waveform through two comparators and an integration circuit. The comparators and integrator are designed so the waveform passes through the first comparator to produce a different type of peak detector effect. This is followed by the integrator to help smooth the peaks out and then the third comparator is used to make a slow moving waveform which is suitable for control input to the microcontroller. Shown below is the circuit schematic for this conditioning method.

Fig. 6.36 - Comparator Based Conditioning Schematic

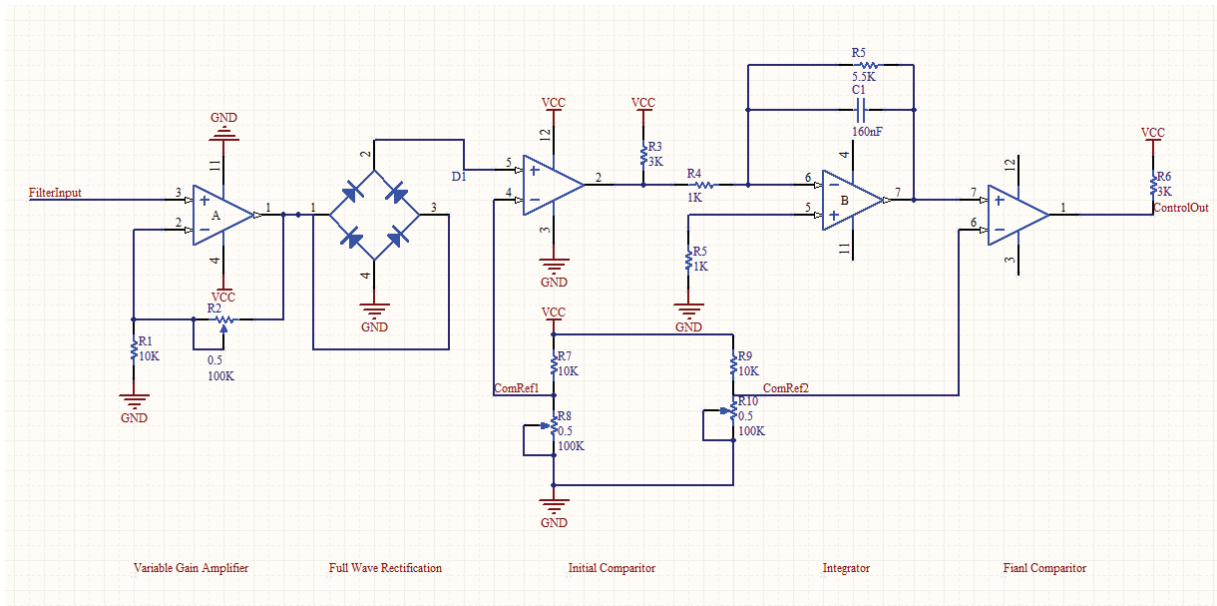The components of the conditioning circuit needed to be tailored to the signal type. The initial amplification stage needed to have a variable gain set so that the input signal could be adjusted above the 1.2V drop of the full wave rectifier induces. The comparators both require a variable voltage reference so the low level peaks of the input signal are able to be excluded if they are too large and increase the sensitivity if the input signal is too low. Finally the integrator required the passive component values to be calculated in regards to the crossover frequency and the 3dB frequency. The outcome of the component calculations are:

Amplifier:

$$Amplification\ Required: 1\ to\ 30$$

$$R_1 = 1K\Omega \qquad R_2 = 30K\Omega$$

Comparator:

$$Required\ Voltage\ Range: 0\ to\ 5V$$

$$R_1 = 1K\Omega \qquad R_2 = 100K\Omega$$

Integrator:

$$F_a = 180Hz \qquad F_b = 1000Hz$$

$$F_a = \frac{1}{2\pi R_f C_f} \qquad F_b = \frac{1}{2\pi R_1 C_f}$$

Crossover Frequency

$$R_1 = 1K\Omega \qquad 1000 = \frac{1}{2\pi \times 1000 \times C_f}$$

$$C_f = \frac{1}{2\pi \times 1000 \times 1000} \qquad C_f = 1.59 \times 10^{-7}$$

$$C_f = 160nF$$

3dB Frequency

$$F_a = \frac{1}{2\pi R_f C_f} \qquad 120 = \frac{1}{2\pi \times R_f \times 1.59 \times 10^{-7}}$$

$$R_f = \frac{1}{2\pi \times 120 \times 1.59 \times 10^{-7}} \qquad R_f = 5555.5\Omega \qquad R_f = 5.5K\Omega$$

The output of the comparator based conditioning circuit can be tested in a series of points. As time did not allow these circuits to be implemented the expected output of the circuit has been simulated through LabView. Fig 6.37 shows the signal waveform simulated through LabView at each of the major points of the circuit.
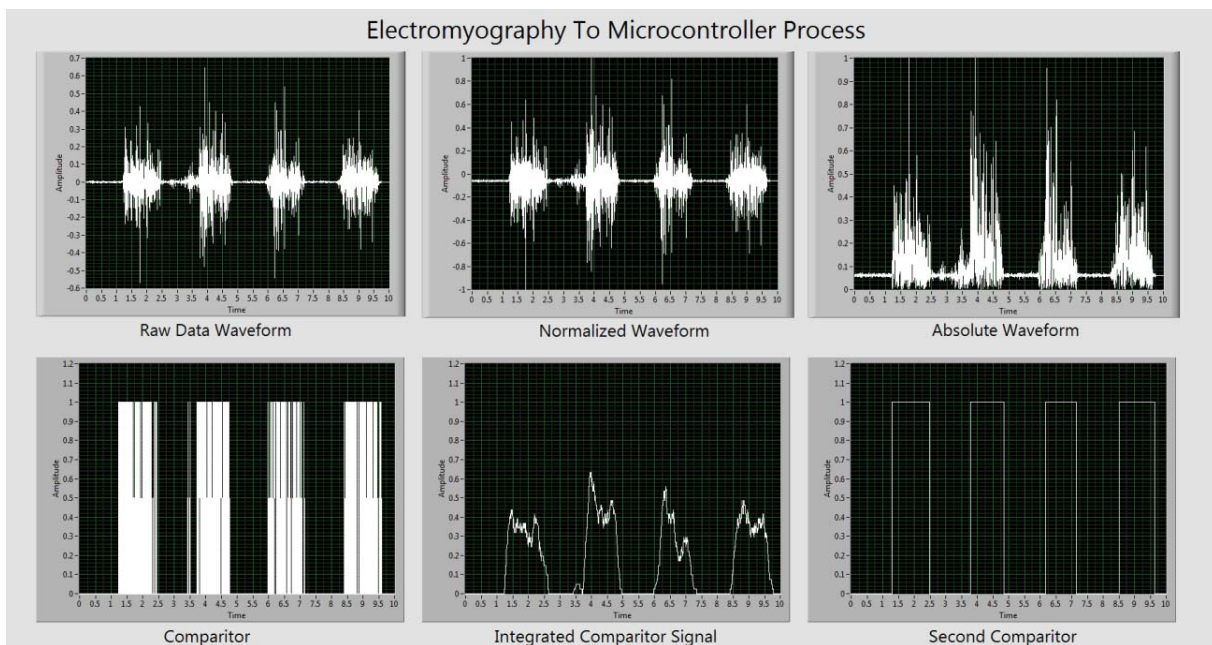

Fig. 6.37 - Comparator Simulation Output

The LabView program is shown in Fig. 6.38. The program reads captured EMG data from an excel file, passes the data through a filer, amplifies the signal to a normalized level, performs an absolute operation so no signal is lost, compares with a reference voltage to produce a pseudo digital comparator, passes through an average time envelope to imitate an integrator and finally passed through another comparison to make a digital on/off signal. This confirmed the usability of this method for control of the prosthetic device.
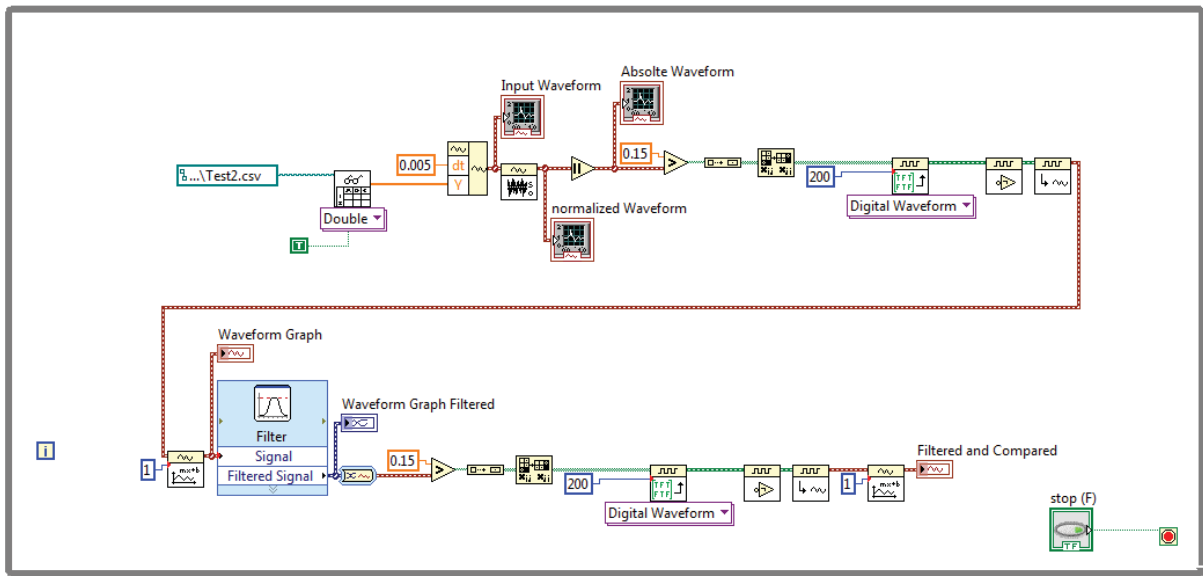

Fig. 6.38 - Block Diagram for Comparitor Conditioning

6.7 Motor Selection

The motor for this application was chosen based on the torque requirements of the fingers, the current draw, the speed and the physical dimensions. The physical dimensions were the most restrictive criteria for the selection process because the palm design heavily restricted the size and therefore type of the motor. The only motors that were found to be suitable were micro gearbox DC motors. The current draw from this motor was a maximum of 1.6A and had a free running speed of between 14 and 6000rpm, both of which are allowable in the design. The final selection criteria was torque, the micro gearbox DC motors are limited in their output of high torque. For this reason, the highest possible torque motor was chosen with a gear ratio of 1000:1 and a free running speed of 32rpm. The torque requirement calculations and the comparison to the micro motor's specifications were made to confirm the motor meets the requirements.

$$T_{req} = F_{finger} \times r_{MaxPulley} \qquad [6.6]$$

$$T_{req} = 13 \times 0.9 = 11.2 \ Kgcm$$

Where T_{req} is the required force, F_{finger} is the force from the finger and $r_{maxpulley}$ is the maximum radius of the pulley. The numbers used in equation [6.6] were taken from sections 4.2 and 4.4 respectively.

The specification of the 1000:1 motor gives the maximum torque as 9Kgcm which is not quite enough for the basic lift. The basic lift can still be achieved by lifting objects in the middle of the finger rather than in the worst case scenario at the ends of the fingers. The maximum radius of the pulley attached to this motor to achieve this worst case scenario lift is therefore:

$$r_{max} = \frac{9}{13} = 7mm$$

This means that 14mm is the maximum diameter of the pulley to achieve the maximum lift of 2Kg as set out in the torque requirement previously. There are some pulleys however that are larger than this diameter due to the requirement of the cable channels. This is allowable because the torque calculations are made in the worst case scenario as well as equalling the socket limit load. All of the tensing pulleys are slightly larger than this diameter but due to the high gear ratio the motors are near self-locking. This means that the fingers could be closed around a heavy object and then lock in place, enabling the object to be lifted regardless if the fingers were able to lift it by themselves.

6.8 Motor Driver

The motors are driven by a dual H bridge integrated circuit, the NJM2670D2. This circuit contains an output suitable for driving one stepper motor or two DC motors. Initially a test was performed by directly connecting a DC motor to a bench top power supply and set it to forward direction with limited current as to not harm the motor. The running current of the motor was recorded and then the motor was stalled by stopping the finger. The peak stalling current on the bench top power supply was then recorded by restraining the finger and watching the current output display on the power supply. This demonstrated the maximum current needed by the motor and this was one of the criteria used in deciding the motor driver circuit.

Initially the L293DD was used to start driving the motors as it is a basic dual H-Bridge circuit with the correct voltage and current outputs. This Integrated Circuit (IC) allowed the initial interfacing with the microcontroller to allow for basic control. The first type of control by the microcontroller was a direct forward and reverse action controlled by a timer. The second type of control involved using Pulse Width Modulation (PWM) to control the speed of the motor. After the motors were confidently able to be driven by the microcontroller, the control system needed a way to tell if there was an object in the prosthetic's grasp. This is where the idea of current sensing to determine torque was introduced. The L293DD does not include a "sense pin" which makes the current used in each circuit in the IC available to external sources. The NJM2670D2 was then discovered as a suitable replacement for the L293DD as it met the requirement of voltage, current and sensing.

6.9   Current Feedback using Current Sensing

A motor prototype circuit was designed on breadboard to check the functionality and viability of the circuit idea. This prototype circuit used one NJM2670D2, two motors and a bench top power supply. The Motor driver IC was connected up in the configuration shown in the schematic below.
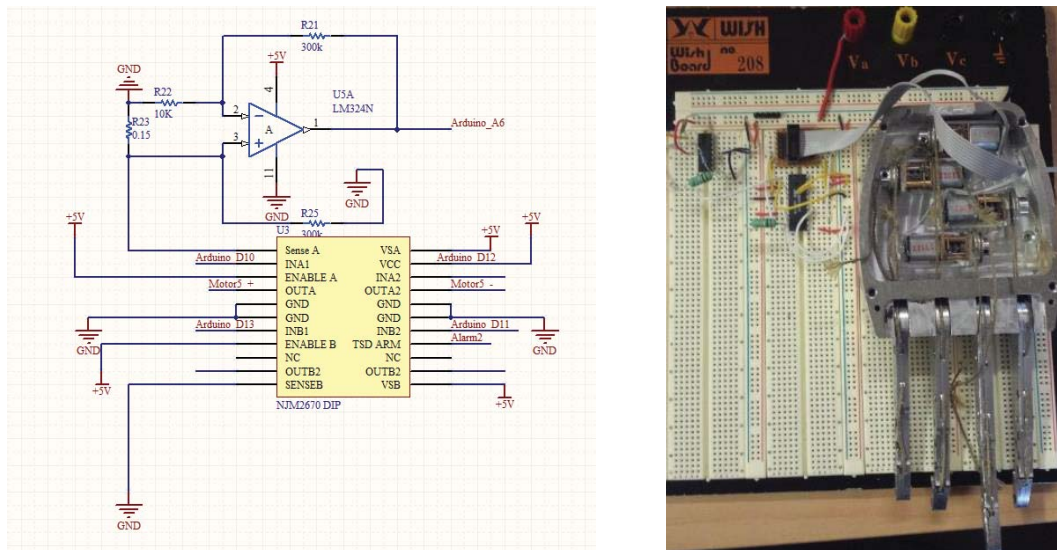

Fig. 6.39 - Motor Driving Current Sense Schematic (Left), Breadboard Prototype Testing Setup (Right)

The motors were initially tested by activating the motors in the forward direction and then in the reverse. The bench top power supply was limited to an output of 1 amp to protect the motors in the event of stalling. The limited current did not allow the motor's gearbox to slip a tooth or risk breakages. Knowing that the motors would come to no harm, a pulley was attached to the testing motor and attached to the finger design. This setup allowed forces to be set in opposition to the finger designed to bring the motor to a stalling point. When it was proved that the motor was able to be stalled safely, a sense resistor and op amp non-inverting amplifier were added to the circuit prototype. Measuring the voltage across the sense resistor with an oscilloscope and monitoring the bench top power supply, the change in voltage was easily observed when the motor transitioned from free running into a stalled state. The transition is shown below in an oscilloscope capture.
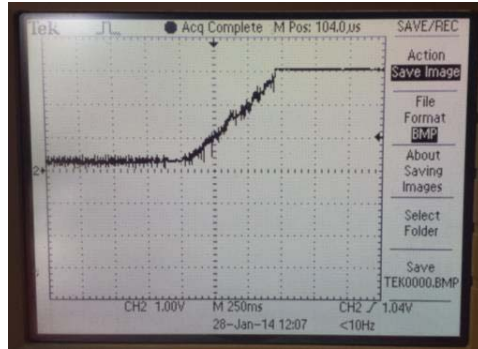
Fig. 6.40 - Oscilloscope Current Sensing Waveform at Motor Stall Transition

Chapter 7 - Control System

The control system of a robotic prosthesis is like the central nervous system of the human body, the designed prototype would be useless without a robust system to process the incoming EMG signal and to control the movement of the fingers. The control system in most current prosthetic devices is highly powered and expensive in features as well as price. For the control system of this prototype the aim is for an "accurate enough" control system such that adequate control is provided without incurring extra expense. Doing the majority of the signal processing in hardware allowed for a much lower powered microcontroller due to the reduced need for a high clock speed and memory.

7.1 Required Features

The control system for this prototype required the ability to control 5 motors simultaneously in forward and reverse, preferably with the ability to actuate them individually. The microcontroller needed to be able to receive two channels of EMG signal for the input as well as a feedback signal from the motor driver current sensing circuit. Last of all the control system needed to be able to output a PWM signal for each of the motors to allow for the slower actuation of the fingers in case the amputee is doing a delicate motion. Fig. 7.3 shows the required input output (I/O) pins.

Required Function	Type Of Pin	# of pins
Receive EMG Input	Analogue	2
Drive Motors	Digital	5
Drive Motors	PWM	5
Current Sense Feedback	Analogue	5
Totals	Number of Pins	
Analogue	7	
Digital	10	

Fig. 7.1 - Table of Required Microcontroller Pins

7.2 Micro-controller Comparisons

With the conditioning being implemented in hardware the specifications for the microcontroller were clarified and the selection process could begin. The optimal microcontroller needed to have a minimum of 7 analogue input pins and 10 digital output pins for the required functionality. The power supply for the microcontroller is preferred to be 5V input so it is the same as the rest of the electrical circuits. Fig. 7.1 is a table showing the differences between a number of microcontrollers and the respective selection criteria.

Microcontroller	Price	# of analogue Pins	# of digital pins	Speed of Processor
Arduino Uno	$46.00	8	16	20MHz
Arduino Nano	$76.00	8	16	20MHz
Arduino Mega	$78.00	16	54	16MHz
Silabs 8051	$120.00	16-32	32-64	25MIPS
CY8CKIT-030 PSoC® 3	$99.00	18	32-64	32KHz

Fig. 7.2 - Micro-Controller Comparison Table

The microcontrollers that were considered all came with a breakout board for ease of prototyping. The reason these microcontrollers were chosen to compare over others is because of their common usage in robotics and prototyping applications. Out of the microcontrollers compared, the Arduino Uno and Nano both use the Atmega 328 controller and therefore have the same specifications apart from the physical dimensions. The Arduino Mega in contrast uses the Atmega 1280, this microcontroller trades processing speed for a larger number of I/O pins. The Silabs 8051 is a higher powered microcontroller with a higher processing speed and a large increase in I/O pins. Finally the CY8CKIT microcontroller has the highest processing speed of all considered however it has less I/O pins than the 8051.

When considering these microcontrollers extra considerations were made, not only the raw hardware was considered. Things like ease of use, online support, familiarity with the IDE and physical dimension were taken into account. The Silabs 8051 uses a proprietary Integrated Development Environment (IDE) and uses C as a programming language. All Arduino microcontrollers share the same programming language, IDE and online support. The large amount of online resource to help with development and the familiar programming language lead to the decision to use the Arduino IDE. Out of the three Arduino microcontrollers there were two with acceptable processing power and pin I/O, the Uno and the Nano. Finally the Nano was chosen due to the smaller form factor, making it easier to integrate into the prototype.

7.3   Choice of micro-controller

The Arduino Nano microcontroller board was chosen for the number of digital outputs, analogue inputs and low cost factor. Other deciding factors for the Arduino were the programming environment, the language is simple to learn and it has a large support base online. Along with the large support base there are many downloadable libraries for a multitude of different applications. Due to the Arduino's requirement for 5V supply for power, there was no need to add additional voltage dividers or regulators to provide the microcontroller with the correct supply voltage. The Arduino Nano features an on-board ATmega 168 for processing.
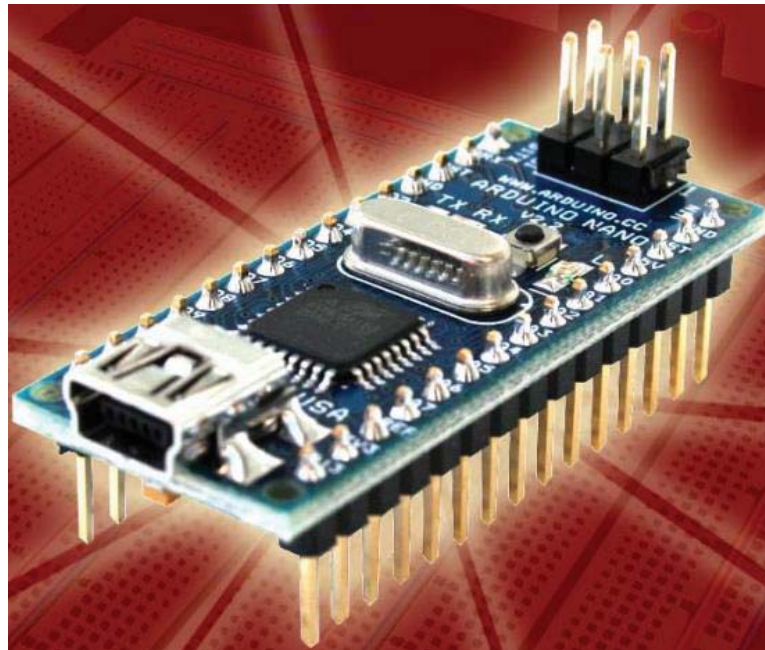

Fig. 7.3 - Arduino Nano

7.4   Feature Programming

Once the required features were decided on, they needed to be programmed into the Arduino Nano. The primary step in the programming of the Arduino was to set all of the input/output pins to be in their respective mode such as analogue input/output and digital input/output. The next step in the setup of the program was to initialize the necessary variables and constants for the functions to work. After all of the pins had been set to their respective modes and the variables were initialized, the movement functions were able to be programmed. Each of the motors are capable of moving independently of the other 4, therefore each motor has a separate move, sense and stop function written into the software to enable increased functionality.

The forward movement function makes use of the PWM output of the digital output pins so the speed of contraction is fully adjustable, either speeding up or slowing down depending on the user's preference. The reverse movement does not need to use PWM to modulate the speed of the fingers in the reverse direction because this function is only used in a resetting application. Once the forward and reverse movement functions were complete, a method of sensing the end of movement needed to be developed to prevent the motors stalling and damaging themselves. The current sensing functions were written separately from the movement functions so they could be easily identified and changed if necessary. This is because the threshold for the current limit is software dictated, making the threshold easier to locate makes for easier debugging and faster changing in the prototyping process. The final step in the control programming was to write the activity loop.

The activity loop consisted of running a set of checks against the threshold values for EMG input and current sensing. Every iteration of the activity loop starts with the EMG input signals being checked to determine whether any action was needed based on the signal input. If this was determined to be no, then the stop function was called for all motors to bring the hand to a stop if it was in motion, or to leave the hand at rest. However if there was action needing to be taken due to either the forward channel or reverse channel further checks were run. The first check to be run is the current sense check on each motor to ensure that they are not stalling and have reached their destination. If there are one or more channels that are showing stalled motors, the stop function for each channel is called. If for the non-stalled channels the forward function for the finger is called for the respective direction. If all channels have been stalled then a flag is set so that the motors will not move in the forward direction again until the fingers have been reversed and the flag is reset. The reverse function has an inbuilt forward stall flag clear built into the function for such occasions. The activation functions include a failsafe check so if both of the EMG channels are activated at the same time no motors will move and there will be no danger of motor damage. Fig. 7.4 and 7.5 show the state diagram for activation of a motor in either direction. The Arduino code is included in the appendix 3.
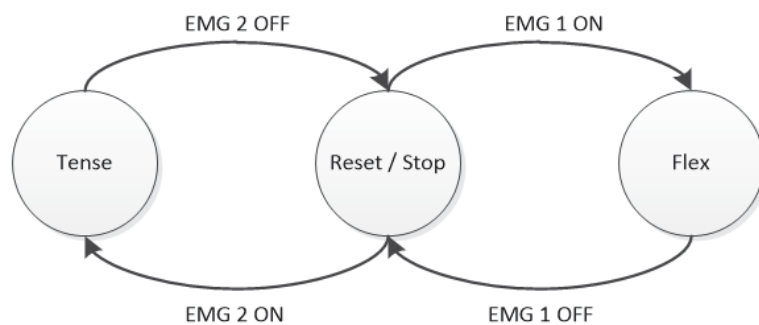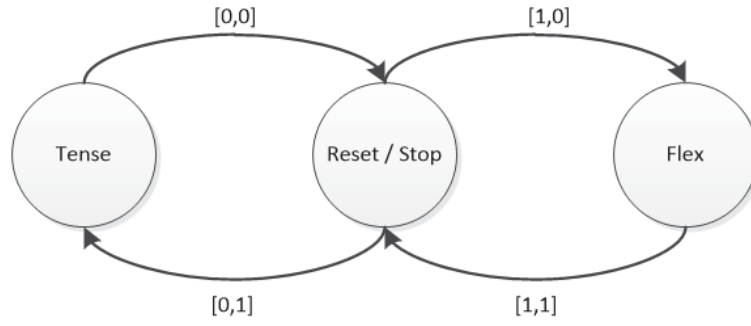

Fig. 7.4 - Microcontroller State Diagram

Fig. 7.5 - Microcontroller State Output Diagram for One Motor

Chapter 8 - Cost Analysis

It has been shown through this research that it is possible to create a low-cost biometrically controlled prosthetic hand. In this section a detailed cost analysis has been conducted to show the cost of producing the initial prototype, the probable cost of taking this design to manufacture and the cost of producing the prototype in alternative manufacturing methods.

8.1.1 Current Prototype

The current prototype has been manufactured in house at Massey University using the workshop and materials from the university stores. This reduced the cost of producing the initial prototype to material costs. However a full cost analysis has been undertaken to investigate the cost of this prosthetic device as if it was produced via outside contractors and businesses. The following table shows the total cost for developing the mechanical prototype prosthetic hand.

Part	Quantity	Price	Total
CNC Technician Hourly Rate	22	$120.00	$2,640.00
Workshop Technician Hourly Rate	10.5	$60.00	$630.00
Aluminium Plate 12.5mm	0.033	$390.63	$12.89
Aluminium Plate 5mm	0.0039	$81.60	$0.32
Aluminium Plate 4mm	0.05605	$80.90	$4.53
Aluminium Plate 2mm	0.04345	$59.72	$2.59
Aluminium Bar 20mm	0.06	$12.60	$0.76
Silver Steel 500x3mm	1	$12.00	$12.00
M2 Screws	41	$0.25	$10.25
M3 Screws	19	$0.17	$3.23
Polycarbonate Sheet 1500x800	0.00075	$177.00	$0.13
Pololulu 1000:1 Micromotors	5	$28.33	$141.65
Kevlar String	0.7	$20.00	$14.00
Total			$3,472.36

Fig. 8.1 - Cost of Mechanical Prototype Prosthetic

The total cost of manufacturing the mechanical prototype is shown by Fig. 8.1 to be $3472.36 NZD with Labour included. The material costs were calculated by acquiring quotes from the university purchasing, breaking each material down into a dollar per unit amount and then working out the amount of stock needed to manufacture each part in the hand. Once the stock material was known for each part in the prototype was known, the similar material parts were added together and then the price per unit was multiplied by the amount of stock used. This gave a final cost of each material used in the prototype.

Material Cost Total	$202.36
Labour Cost Total	$3,270.00

Fig. 8.2 - Breakdown of Material Costs Vs. Labour Costs

The ratio of material compared to labour used in this research is shown in Fig. 8.2. The large bias toward labour is due to the relatively low cost nature of the materials chosen and the necessary complexity of the design of a hand. An investigation was then performed to break down the labour costs into individual mechanical parts to allow for further cost reduction in the future by redesigning time consuming parts. Because the material costs were not significant in this comparison some material could be added to reduce the amount of time spent by the CNC Mill shaping these parts.

Part	CNC - $120/h	Workshop - $60/h	Electrical - $60/h	Total cost of time
Fingers	10	3	0	1380
Thumb Bust	5	2	0	720
Palm	2	2	0	360
Palm Middle	2	2	0	360
Palm Top	1	0	0	120
Motor Brackets	1	1	0	180
String Guide	0.5	0	0	60
Polycarbonate Bushings	0.5	0	0	60
PCB Printing	0	0	0.5	30
Total Labour Cost	22	10	0.5	3270

Fig. 8.3 - Breakdown of Labour Time for Entire Prototype Manufacture

The most expensive part to produce in terms of labour was the thumb bust. Although the fingers were the highest total time spent on a part, there are twenty eight separate parts that make up the finger set whereas the thumb bust is a single part which took slightly more than half the time as compared to the entire set of fingers. The CNC machine had an hourly rate twice that of the other two workshops however it has been proven before to be more than twice as fast in complex operations, thereby justifying the number of hours spent on the CNC instead of the alternate workshop.

8.1.2   3D Printing Prototype

As an alternative manufacturing method, 3D printing was considered to produce the prototype in the same state as the one created in house. The main differences between these two manufacturing methods are the materials used and the manufacturing methodology. 3D printing in this case uses titanium alloy to manufacture the main hand, this was ruled out of the initial material selection due to being too expensive in both monetary and machinability. 3D printing however overcomes the machinability problems by using a "material adding" manufacturing technology as compared to the

conventional machinery which uses a "material removal" technology. The advantages of having a 3D printed prototype are that it will be both stronger and lighter than the aluminium counterpart while still being mass-producible. To make a fair comparison between the costs of each manufacturing technology, the same form factor was used to gain a quote from the 3D printing company. However only the largest parts were sent to quote to reduce the load on the printing company, from these numbers a total figure was able to be calculated for the current hand design. Fig. 8.4 below shows the extrapolated total cost for a 3D printed titanium prototype. The actual quote has been included in appendix 5.

Part	Quantity	Price	Total
Palm	1	$800.94	$800.94
Palm Middle	1	$428.92	$428.92
Part 7 (Thumb Bust)	1	$529.25	$529.25
Finger J1 Bottom	5	$81.05	$405.25
Finger J1 Top	5	$62.85	$314.25
Extrapolated Estimates			
Finger J2 Bottom	4	$60.79	$303.94
Finger J2 Top	4	$47.14	$235.69
Finger Tip Bottom	5	$32.42	$162.10
Finger Tip Top	5	$25.14	$125.70
Total			$3,306.04

Fig. 8.4 - Expected Cost of 3D Printing in Titanium

The quoted prices for each part from Titanium Industry Association Incorporated (TiDA) are shown in the top portion of Fig. 8.4, the full quote is attached in the appendices. It appears that as the parts get larger volumetrically the price drops as there is less setup time. This makes the finger parts slightly more expensive than they were to produce in the conventional milling method, but the palm and thumb bust are cheaper. Comparing the cost of the conventional milling and the 3D printing, the prices come out very comparable. $3472.36 for conventional milling and $3306.04 for 3D printing, the advantage of 3D printing materials however do contribute to the consideration of 3D printing for future designs. The increases in material costs are offset by the reduced labour costs incurred by this manufacturing technology as well as the ability to use more intricate and complex designs for 3D printing proves 3D printing is worth investigating for future designs.

8.1.3 Electrical Costs
In this section the costs for the electrical circuits in this prototype are outlined on a per circuit basis. This starts with EMG input circuits, filtering, signal conditioning and control. These are then collated into a total cost of the electrical portion of this research. All prices used in the cost analysis are using common consumer vendors at market price.

8.1.3.1 *EMG Circuit Costs*

The EMG circuit used in this research is made in-house and as Fig. 8.5 shows, it costs only $62.55 as compared to over $200 for commercial sensing equipment. The EMG cost analysis does not include the disposable sensing pads because these are needed in both sensing applications and therefore would not impact the overall cost analysis.

Part	Quantity	Price	Total
INA2128	1	$32.88	$32.88
OPA2604	2	$9.60	$19.20
390KΩ	4	$0.80	$3.20
10KΩ	2	$0.80	$1.60
100nF	2	$1.40	$2.80
10pF	2	$0.90	$1.80
3 Pin Header	1	$0.03	$0.03
2 Pin Header	2	$0.02	$0.04
4 Pin Input EMG Header	2	$0.50	$1.00
Total			$62.55

Fig. 8.5 - EMG Sensing Circuit Cost Analysis

The major component of the EMG sensing input is the INA2128 and the two OPA2604 Integrated Circuits. Together these make up slightly over 80% of the total circuit cost.

8.1.3.2 *Filtering Cost*

The filtering is usually performed inside the proprietary sensing circuits used by medical applications, in this prototype the filter has been separated for a more modular design. Due to the nature of filtering circuits, there are many off-the-shelf options available to the consumer market so these were not developed for the initial prototype but would be for further iterations of the design. The expected cost of the purchased filters is $70.00

8.1.3.3 *Signal Conditioning Cost*

Only the final signal conditioning circuit has been analysed for this section as the development of the initial circuits would not be included in a manufacturing cost quote. The conditioning circuitry is by far the most expense inducing circuit for proprietary EMG solutions, usually requiring a bench top analysis device or advanced probes with on-board conditioning. This circuit costs substantially less, costing only $29.94.

Part	Quantity	Price	Total
Full Bridge Rectifier	1	$16.00	$16.00
LM339 Comparitor	1	$1.49	$1.49
LM324 Amplifier	1	$2.25	$2.25
3KΩ	2	$0.80	$1.60
10KΩ	3	$0.80	$2.40
1KΩ	2	$0.80	$1.60
5.5KΩ	1	$0.80	$0.80
100KΩ Variable Resistor	3	$0.80	$2.40
160nF	1	$1.40	$1.40
Total			$29.94

Fig. 8.6 - Conditioning Circuit Costing

8.1.3.4 Control Circuit Cost

The control circuitry is the heart of the prosthetic device; this is what makes the device perform at the required level of functionality. This is usually where the large sums of money are spent when dealing with a bio-robotic device, adding extra functionality and waveform analysis to push the device to the limit of intelligence thereby reducing the impact of the injury on the patient and increasing quality of life. This however was not the aim of this research, the purpose of this research was to create a control system that was "accurate enough" to allow the amputee some additional form of functionality over a hook or passive prosthesis. This shift in focus has shown a greatly reduced price in control system as shown in Fig. 8.7.

Part	Quantity	Price	Total
Arduino Nano	1	$76.54	76.54
10uF Capacitor	1	$0.30	$0.30
2 Pin Header	2	$0.02	$0.04
5 Pin Header	2	$0.05	$0.10
10 Pin Header	3	$0.10	$0.30
LM324N	2	$1.22	$2.44
NJM2670	3	$8.45	$25.35
0.15Ω Resistor	5	$3.48	$17.40
10KΩ Resistor	5	$0.80	$4.00
300KΩ Resistor	10	$0.80	$8.00
PCB Fabrication	1	$0.60	$0.60
Total			$135.07

Fig. 8.7 - Control System Circuitry Cost Analysis

The control system for this prototype only costs $135.07, this figure is far below expected and is a sign that the cost of current prosthesis are not the only way to provide amputees with increased quality of life.

8.1.3.5 Total Electrical Cost

As above figures show, the total cost of the electrical portion is $227.56, the cost breakdown is shown in Fig. 8.8.

Electrical Parts	Price
EMG	$62.55
Conditioning	$135.07
Motor Driver	$29.94
Total	$227.56

Fig. 8.8 - Electrical Cost Breakdown

8.1.4 Total Overall Costs

This brings the total cost of the project to $3769.92.

Part	Price
Mechanical	$3,472.36
Electrical	$227.56
Filtering	$70.00
Total	$3,769.92

Fig. 8.9 - Total Cost of Prototype

Chapter 9 – Results and Discussion

9.1 Final Mechanical System

The final mechanical system is at a level which is able to perform the functions that were set out in the aims of this research. The overall system design is sound and durable with a reasonable cost associated with the level of function provided. The use of aluminium as the base material has enabled fast and accurate prototyping to be achieved. The benefits of this system over other prosthetic devices in the market are the strength of the fingers due to their manufacturing process and materials as well as a simplistic actuation design to reduce possible fault factors.

Fig. 9.1 - Final Mechanical System

9.2 EMG Acquisition and Conditioning

The EMG acquisition circuitry works to a standard such that the data can be gathered reliably from the targeted muscle groups. This signal contains noise due to the body acting as an antenna for a wide spectrum of environmental noise. Much of the captured noise is the power line noise which occurs in the 50/60Hz frequency band as this is the most prevalent ambient environmental frequency. The proposed filtering cut-off frequencies worked to reduce and eliminate this ambient noise only keeping the major frequency components of the waveform.

The comparator conditioning method of converting the EMG input signal into a slowly moving control signal suitable for input into a control system is effective and enables the control system to be simplified. By using a set of readily available components to transform the input signal a low cost method of interpreting and applying the EMG signal has been achieved with enough accuracy for use.

9.3 Control System and Motor Driving

The control system for the prototype prosthetic device uses an "accurate enough" philosophy to achieve effective and low cost control. Due to the increased hardware processing, the cost of the microcontroller was able to be reduced to a level where it is affordable by the general public and as an added bonus of using open source software. The control system does suffer in the area of extra features due to the nature of the conditioning however. The method of conditioning is classed as "lossy" as some of the signal is lost in the process, therefore the features that are commonly detected in higher cost devices by pattern recognition techniques are no longer possible.

By enabling the control system to actuate each finger individually, the device is able to contour the fingers into a complex shape to grip a wide variety of objects. This ability to contour the fingers is achieved by allowing each motor to stop individually during the contraction process when enough force is reached on each digit. This ensures that the held object is always gripped with sufficient force to be held safely.

9.4 Suitability of First Prototype

The first prototype prosthetic design is a baseline functional prototype. This design was to be used to prove that a workable prosthetic device could be developed for a lower overall cost than the current prosthetic designs on the market. While aiming to reduce the cost of the overall prosthetic device a focus was also made to not sacrifice an undue amount of functionality. The criteria the prototype can be assessed against to gauge the suitability to the market and the end user are: the physical functionality, durability, aesthetic design and cost.

9.4.1 Physical Functionality

When considering the physical functionality of the initial prototype there are multiple factors that require consideration to completely evaluate the functionality. The factors that require attention are: the lifting capabilities, the day to day usability, level of normality returned to the end user and the control system reliability. When considering the lifting capabilities of the developed prosthetic, the carbon fibre socket maximum lifting capacity can be used as a benchmarking target. The prototype prosthetic device is capable of lifting and holding a weight similar to the maximum of the carbon mounting socket, therefore making it a suitable replacement to the hook type prosthetic and can be considered to be suitable for the proposed applications.

When considering the day to day usability, the grip pattern and weight need to be investigated. The gripping pattern of the prototype aims to mimic the natural hand in the closest way possible. With this goal in mind the fingers have been designed in likeness to natural fingers and the bend priority is the same. With the naturally inspired finger design the possible grip patterns of the prototype are wide ranging, enabling the effective grip of most objects. However, the fingers do have some limitations. Due to the limitations of the finger joint bend radius and the solid nature of the finger mounting points, the fingers are set very rigidly and therefore do not allow any sideways movement. This lack of sideways movement does make the grip on some items less effective as the fingers are not able to spread around the object like natural fingers. The overall weight of the physical prosthetic device is approximately 500g, this weight is not excessive and will not adversely affect a person using the device throughout the day. If the device were heavier than this the amputee may experience fatigue in the connected arm, shoulder and back muscles. The current harness mounting system for the hook prosthetic can cause long-term adverse medical effects, with the 500g prototype the need for the harness may be removed.

This leads into the next criterion, level of normality returned to the amputee. The aim for any prosthetic device is to give the amputee a better quality of life to the extreme of returning full functionality to the lost limb. This prosthetic device achieves a level where the amputee is able to interact with the environment with the ability to grip and hold rather than the limited push, pull and carry offered by hook prosthesis. The ability to hold an object such as a drink bottle goes a long way to bringing the quality of

life back to the amputee. Not only does this serve a purpose to allow the amputee to complete a task with the amputated arm but it frees up the able bodied arm to complete another task which would have previously been impossible.

The final criterion is the reliability of the EMG control system. The control system is the interpreter between the brain of the user and the actions of the device, for the user to be pleased by the device they are using it must function as the amputee wishes it to. The control system for this prototype is suitable as far as a prototype device is concerned, however there is much room left for improvement. The current control system is able to detect when a muscle is activated and when this activation is released. The microcontroller then acts on these signals to make the prosthetic device's fingers move forward and backward. This is a very basic interpretation of what the physical device is capable of. The current scheme of control only allows for a basic open and close grip with the fingers forming around the object, in future the capabilities of this device could be expended for a series of different grip types and intuitive actuation methods.

9.4.2 Durability

For a prosthetic device to be desirable to both the end user and the purchasing interest it must be durable. If a prosthetic device is fragile and is used in a hard wearing environment it will be prone to breakages, this will reduce the enjoyment and functionality of the amputee and will cost the purchasing interest more as they will be required to pay for additional parts and labour to fix the device. When a prosthetic device breaks, the user is inconvenienced by not being able to perform the functions they have become accustomed to and therefrom their quality of life is reduced to the level of amputation again. For this reason the initial prototype was constructed with all metal structural parts, thereby reducing the possibility of breakages. The all-aluminium design of the prototype is suitable as a testing platform; however in long term use this would not be suitable due to the soft nature of aluminium. If the prototype was to be used in day to day use for the next three years there would be a series of issues that would become prevalent. The first issue with the all-aluminium design is that in the day to day usage it is not kind to the environment around it, the corners of the fingers would scratch the objects that would be interacting with the prosthetic. The second issue is the bearing of the steel shafts on the aluminium finger joints, because steel is the harder of the materials it will wear out the joints and make the fingers become sloppy and inaccurate. On top of the finger joints wearing and becoming sloppy, the Kevlar string would wear out the cable channels over time. This would affect the bend radius, the friction surface and string travel length. With the string length changing and the fingers becoming sloppy, this would put undue stress on the motors causing them to eventually fail as well.

9.4.3 Aesthetic Design

For the prosthetic to be desirable to the maximum market sector it must look pleasing. Discussed earlier is the ratio of males to females requiring prosthetic devices being heavily sided in the male's direction. This indicates that the larger majority of the market would prefer a device that works well over one that looks good, however they would be happier if the device did look good as well. The current design leaves much to be desired when it comes to aesthetics, this is because it is used as a primarily as a testing platform. The prototype design at this point is purely functional and with a focus being put on machinability and time-saving. The design is therefore large and chunky to accommodate all of the non-

optimised parts. The palm shape is the least aesthetically pleasing part of the prototype, the palm is suitable for large handed males as it is designed for a male amputee. This however will not suit all amputees and especially not female amputees. This however could be addressed in future designs when the manufacturing techniques have been further investigated. The second aesthetic issue with the prototype are the fingers, they are very square and the parts themselves serve a purely functional end. These fingers would not be able to be covered by a glove due to their geometry and the square profile would give away their fake nature. This would need to be redesigned if this prototype were to go into production with a more rounded outside profile.

9.4.4 Cost

The prototype needed to be lower cost than the current market models with a comparable functionality to be deemed a successful outcome. As the results show, the prototype that has been constructed does in fact cost less than the current market models and this cost would be expected to decrease further if economics of scale were introduced. With the total cost of this project coming to $3,769.92 and the closest market model coming to $4094.00 this research takes a further step into reducing the cost of bio-controlled prosthetic devices for use by the general public. The saving of $300 seems small in the scheme of things, however this prototype is made with strong materials that will not break in the normal use of the amputee. It provides an "accurate enough" control method for the user to be able to complete most of the activities they would attempt in a normal day and it has a large room for expansion in features. This $300 saving is only the prototype saving, if this research was continued into the future and was designed to mass producible scale, the savings would increase further.

9.5 Future Work (Improvements)

This initial prototype is far from finished, the study that has been conducted was to begin the process and prove that it is possible to create prosthesis with similar features for a reduced price. From this point there are many possible improvement avenues which can be explored while not increasing the cost of the prototype to an inflated price. There are possibilities for improvement in the following areas: Mechanical design, aesthetics and the EMG circuitry.

9.5.1 Mechanical

The mechanical design of the initial prototype was used as a testing platform and had strict time constraints. Going into the future the primary focuses for improvements would be the finger design, palm design, manufacturing method and finger actuation method. With these mechanical factors improved, other mechanical features would be able to be considered. Features such as soft knuckle joints and moveable motor mounts could be considered for inclusion to the design.

The finger design currently is very crude and considers only the function to curl around an object and hold it in place with force and friction. These square edged designs were convenient for manufacture by the conventional methods available at Massey, however they are liable to damage held objects with their edges and they look aesthetically unpleasant. To improve this in the future, the external finger design could be made rounded like a natural finger bone. This change to the external profile would reduce the damage caused as well as making the finger itself look better. If the manufacturing

technology was changed to 3D printing, the screw holes on the side of the finger would become unnecessary, further increasing aesthetic appeal.

The design of the palm in the current prototype is made with conventional machining and ease of prototyping in mind. For any future prototypes this design would be changed to become more representative of a natural human hand in both size and shape. Currently the palm has a flat bottom to allow for easy mounting of the motors and thumb bust. This makes holding objects between the fingers and the palm difficult, in future revisions of the palm design the bottom surface would be made to adopt a curve like a natural hand. This would provide a groove for held objects to rest in, reducing the possibility of the object moving within the process of gripping it with the fingers. This would increase the manufacturing time and ease of motor mounting if the palm was to continue to be manufactured with conventional manufacturing methods. Another improvement to the palm design would be to continue the theme of curvature through the knuckles at the front of the design to make the whole prototype able to fit into a covering glove.

The current method of manufacturing the prototype is by using conventional milling machines to remove stock material to achieve the desired shapes. Moving forward the prototype would benefit from adopting a newer form of manufacturing, 3D printing is a newer manufacturing method which would benefit the curved designs of the fingers and palm in the future. With the ability to manufacture parts out of superior materials for similar or less cost, 3D printing is a logical progression and will open up many new opportunities to develop less conventional shapes and actuation methods. Using titanium alloy laser sintering to develop the prosthetic devices shape allows for smaller, lighter and more complex parts to be constructed due to the stronger and more durable nature of the titanium. This improvement is the largest advancement opportunity for the mechanical design due to the large number of improvements that can be made if titanium 3D printing is adopted.

The final improvement opportunity for the mechanical design side of the prosthetic device is to improve the finger actuation method. At the current point the fingers are actuated through a rotary motor with a pulley providing the driving power to the finger. The motors in this application provide sufficient torque to achieve the target lifting weight, however the mounting system and cable path leaves room for improvement. The motor mounts could be improved by introducing a better pulley and string mounting system, the current version relies on the string being fed through the pulley and then tied off in a knot on the face of the pulley. To improve on this design the string could be fixed internally without the knot on the face of the pulley and build in a string tensioning system to enable the tensioning of the actuation cables in the case of wear. To improve the cable actuation channels, more of the cable needs to be internalised so there is less chance of damage on to the cable while in use. The cable is currently exposed at the radius of each joint in the finger, if the user were to grasp something sharp there is a possibility that this could either damage or sever the actuation cable. This is a weakness of the finger design and should be compensated for in future revisions.

9.5.2 Aesthetics

The aesthetic design of this prototype is a secondary concern, however it is not to be disregarded altogether. The functionality of the prototype is the primary selling point of this device, however a higher market share would be inclined to purchase an attractive design rather than a purely functional one. To improve the aesthetics of the design the prototype would need to imitate a human hand more closely. The palm and fingers would become more rounded than they are in the current design, the entire prototype would become smaller and more manageable.

9.5.3 EMG Circuit

The EMG circuitry in this prototype is at a basic level. To get more out of this prosthetic device the EMG circuit sensitivity could be increased and the conditioning could be further tailored to suit the application. A future opportunity for the EMG circuitry is the use of active sensors instead of the passive ones currently used for the prototype. Using active electrodes will allow reduce the amount of noise gathered by the EMG signal as it is captured and transported to the control system. The cleaner signal may enable the use of a higher level of signal processing for a similar price. A further possible development would be to enable a mode choice to change the prosthetic gripping pattern. Modes like: power, delicate, point and two finger modes would allow for some specialist actions to be performed by the prosthetic further increasing the overall functionality restored to the amputee.

9.5.4 Human Testing and Comparison

This prototype is just reaching the point where human trials can begin. To further this research the prototype would need to be tested in a day to day environment to allow any bugs to become apparent and removed from future revisions. This includes but is not limited to speed of wear, material suitability and reliability of electronic and control circuits. When the prototype is at an acceptable level, a set of evaluation parameters would need to be agreed upon and then a comparison with other prostheses could occur. This comparison would be used as the measure for functional success.

9.6 Other Work Opportunities from this Project

During the course of this research a further research opportunity was brought to light that is not related directly to the research. While designing the finger form an interest was shown in the further applications of the bending method and grasping strength. The design incorporating the cable channels inside the gripping mechanism was seen to be somewhat novel and could be used in other applications. These additional applications were theorised to possibly include wall mounting systems and quick release gas bottle clamps. Further research could be used to validate these ideas and prove their effectiveness.

Chapter 10 - Conclusions

This research has shown that it is possible to make a low cost biometrically controlled prosthetic device. The prosthetic device maintains a sufficient amount of functionality to be competitive with the prosthetic devices in the current market. The mechanical design of the prototype is sufficient for a testing platform and a proof of concept, this design however can be greatly improved by changing the manufacturing techniques and processes. Moving to 3D titanium printing would improve the structural design, the aesthetic design and the durability of the entire prototype for a similar cost. The overall viability of this first prototype is less than optimal due to some mechanical manufacturing issues, however once the mechanical design and manufacturing technologies have been changed this prototype could be very competitive in the prosthetic hand market.

Currently this prosthetic is able to be manufactured for $300 less than the next cheapest device on the market and it offers a high durability as well as a good level of functionality. This does not include any discount for mass production, one-off prototypes are more costly than a design that will be produced in a run of 100+. Therefore the prototype could be expected to further decrease in price and widen the gap between it and the current market devices. This reduction in price for similar features and a more durable device would translate into a more desirable device for both the amputee user community but also for the purchasing interests such as the government departments covering medical accidents.

The EMG side of this prosthetic device is of a basic level and leaves a lot of room for improvement, currently it only allows for a simple forward and reverse. For this prototype to exceed in the market a more advanced EMG system would need to be developed. Currently the signal from the EMG is converted in a "lossy" manner where much of the information in the waveform is lost. If this were to change and the waveform were to become cleaner and additional tailored conditioning to remove additional noise got implemented, higher level recognition could be used. Having this higher level of recognition would allow for a greater control of the device and finer motor movements to be performed. By then including a mode select option for the amputee, the functionality of the device would be far increased and the level of normality returned to the amputee would further increased. It is another attempt to actuate the fingers by bypassing the complicated and costly EMG waveform pattern recognition.

In conclusion, the prototype that was developed by this research is a proof of concept that biometrically controlled prosthetic devices can be developed for less money than the current market designs to a point where they are far more affordable to the general amputee community. The initial prototype that has been developed is a basic representation of what could be possible and with further work it could become a viable low-cost alternative to the current marketed devices with equal functionality and higher durability.

References

Amputee Coalition. (2013). *Shoulder Disarticulation or Forequarter Amputation*. Retrieved March 25, 2013, from Amputee Coalition: http://www.amputee-coalition.org/limb-loss-resource-center/resources-by-amputation-level/shoulder-disarticulation/index.html

Birglen, L., & Gosselin, C. (2006). Geometric design of three-phalanx underactuated fingers. *Journal of Mechanical Design*, 356-364.

Burns, M. T., & M.D. (2011, Febuary 01). *Extremity Soft Tissue Care and Amputation in an Austere Environment*. Retrieved March 25, 2013, from Wheeless' Textbook of Orthopaedics: http://www.wheelessonline.com/ortho/12787

Daley, H., Englehart, K., Hargrove, L., & Kuruganti, U. (2012). High density electromyography data of normally limbed and transradial amputee subjects for multifunction prosthetic control. *Journal of Electromyography and Kinesiology*, 478-484.

Fukuda, O., Bu, N., & Ueno, N. (2010). Training of grasping motion using a virtual prosthetic control system. *2010 IEEE International Conference on Systems Man and Cybernetics (SMC)*, (pp. 1793 - 1798). Saga.

HARDING, H. E., & LANGDALE-KELHAM. (1957). Amputation Stumps. *The Journal of Bone and Joint Surgery*, 221-223.

Heikki Uustal, M., & Edgardo Baerga, M. (2004). *Physical Medicine and Rehabilitation Board Review.* New York: Demos Medical Publishing.

Hochberg, L. R., Serruya, M. D., Friehs, G. M., Mukand, J. A., Saleh, M., Caplan, A. H., et al. (2006). Neuronal ensemble control of prosthetic devices by a human with tetraplegia. *Nature*, 164-171.

Jamal, M. Z. (2012). Signal Acquisition Using Surface EMG and Circuit Design Considerations for Robotic Prosthesis . In Intech, *Computational Intelligence in Electromyography Analysis – A Perspective on Current Applications and Future Challenges* (pp. 427-448). Intech.

Leon, M., Gutierrez, J., Leija, L., & Munoz, R. (2011). EMG pattern recognition using Support Vector Machines classifier for myoelectric control purposes. *2011 Pan American Health Care Exchanges (PAHCE)*, (pp. 175 - 178). Mexico City.

Lipschutz, R., & Lock, B. (2011). A Novel Research And Clinical Approach To Using Gel Liners For Collection Of Surface Myoelectric Signals For Prosthetic Control. *Proceedings of the Myoelectric Controls Symposium'11 conference, University of New Brunswick; 2011.* Myoelectric Symposium.

Lock, B. A., Simon, A. M., Stubblefield, K., & Hargrove, L. J. (2011). Prosthesis-Guided Training For Practical Use Of Pattern Recognition Control Of Prostheses. *Proceedings of the Myoelectric Controls Symposium'11 conference, University of New Brunswick; 2011.*

Matrone, G., Cipriani, C., Carrozza, M., & Magenes, G. (2011). Two-channel real-time EMG Control of a Dexterous Hand Prosthesis. *Proceedings of the 5th international IEEE EMBS Conference on Neural Engineering*, (pp. 554-557). Cancun.

Michigan, U. o. (2012, January 1). *Upper Extremity Amputation*. Retrieved March 25, 2013, from University of Michigan Health System: http://www.uofmhealth.org/medical-services/upper-extremity-amputation

Murdoch, G. (1967). Levels of Amputation and Limiting Factors. *Annals of the royal college of surgeons of England*, 204-216.

Potluri, C., Yihun, Y., Kumar, P., Molitor, J., Chru, S., Naidu, D., et al. (2011). sEMG Based Real-Time Embedded Force Control Strategy for a Prosthetic Hand Prototype. *Electro/Information Technology (EIT), 2011 IEEE International Conference on* (pp. 1-6). IEEE.

Rouse, E., Nahlik, D., Peshkin, M., & Kuiken, T. (2011). Development of a Model Osseo-Magnetic Link for Intuitive Rotational Control of Upper-Limb Prostheses. *IEEE Transactions on Neural Systems and Rehabilitation Engineering*, 213-220.

Scott, C. G., Tang, L., & Gupta, G. S. (2012). *Smart Prosthetc Hand.* Palmerston North: SEAT. Massey University.

Siriprayoonsak, S. (2005). *Real-time Measurement of Prehensile EMG Signals*. Retrieved April 2012, from San Diego State University.

Texas Instruments. (2007, April). *INA2128 Instrumentation amplifier.* Retrieved April 15, 2013, from Texas Instruments: http://www.ti.com/product/ina2128

University of California, San Francisco. (2011, January 1). *Shoulder Disarticulation Amputation / interscapulothoracic Amputation*. Retrieved March 25, 2013, from University of California, San Francisco Orthopaedic Trauma Institute: http://orthosurg.ucsf.edu/oti/patient-care/divisions/orthotics-and-prosthetics/services/upper-extremity-prosthetics/shoulder-disarticulation-amputation-interscapulothoracic-amputation/

Zecca, M., Micera, S., Carrozza, M., & Dario, P. (2002). control of multifunctional prosthetic hands by processing the electromyographic signal. *Critical Reviews™ in Biomedical Engineering*, 459-485.

Zhao, J.-S., Chu, F., & Feng, Z.-J. (2008). *Mobility of Spatial Parallel Manipulators, Parallel Manipulators, towards New Applications.* (H. Wu, Ed.) InTech.

Appendices

10.1 Appendix 1 - INA 2128 Datasheet

BB | **Burr-Brown Products**
from Texas Instruments

INA2128

Dual, Low Power
INSTRUMENTATION AMPLIFIER

FEATURES

- LOW OFFSET VOLTAGE: 50μV max
- LOW DRIFT: 0.5μV/°C max
- LOW INPUT BIAS CURRENT: 5nA max
- HIGH CMR: 120dB min
- INPUTS PROTECTED TO ±40V
- WIDE SUPPLY RANGE: ±2.25V to ±18V
- LOW QUIESCENT CURRENT: 700μA / IA
- 16-PIN PLASTIC DIP, SOL-16

APPLICATIONS

- SENSOR AMPLIFIER
  THERMOCOUPLE, RTD, BRIDGE
- MEDICAL INSTRUMENTATION
- MULTIPLE-CHANNEL SYSTEMS
- BATTERY OPERATED EQUIPMENT

DESCRIPTION

The INA2128 is a dual, low power, general purpose instrumentation amplifier offering excellent accuracy. Its versatile 3-op amp design and small size make it ideal for a wide range of applications. Current-feedback input circuitry provides wide bandwidth even at high gain (200kHz at G = 100).

A single external resistor sets any gain from 1 to 10,000. Internal input protection can withstand up to ±40V without damage.

The INA2128 is laser-trimmed for very low offset voltage (50μV), drift (0.5μV/°C) and high common-mode rejection (120dB at G ≥ 100). It operates with power supplies as low as ±2.25V, and quiescent current is only 700μA per IA—ideal for battery-operated and multiple-channel systems.

The INA2128 is available in SOL-16 packages, specified for the –40°C to +85°C temperature range.

$$G_A = 1 + \frac{50k\Omega}{R_{GA}}$$

$$G_B = 1 + \frac{50k\Omega}{R_{GB}}$$
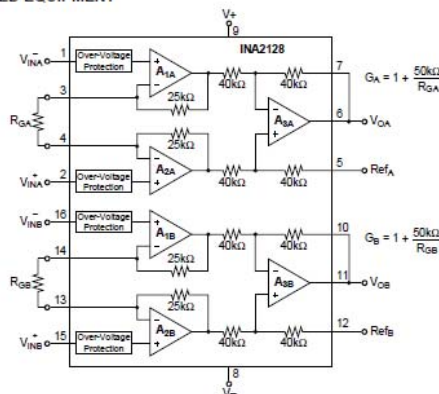
Please be aware that an important notice concerning availability, standard warranty, and use in critical applications of Texas Instruments semiconductor products and disclaimers thereto appears at the end of this data sheet.

All trademarks are the property of their respective owners.

TEXAS INSTRUMENTS
www.ti.com

ABSOLUTE MAXIMUM RATINGS[1]

Supply Voltage	±18V
Analog Input Voltage Range	±40V
Output Short-Circuit (to ground)	Continuous
Operating Temperature	–40°C to +125°C
Storage Temperature	–55°C to +125°C
Junction Temperature	+150°C

NOTE: (1) Stresses above these ratings may cause permanent damage. Exposure to absolute maximum conditions for extended periods may degrade device reliability.

PIN CONFIGURATION

Top View   **SOIC**

V_{INA}	1		16	V_{INB}
V_{INA}^+	2		15	V_{INB}^+
R_{GA}	3		14	R_{GB}
R_{GA}	4		13	R_{GB}
Ref_A	5		12	Ref_B
V_{OA}	6		11	V_{OB}
$Sense_A$	7		10	$Sense_B$
$V-$	8		9	$V+$
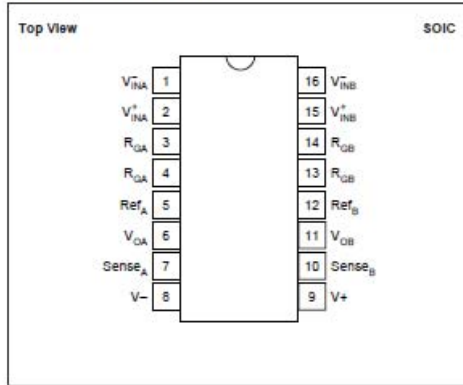
⚠ ELECTROSTATIC DISCHARGE SENSITIVITY

This integrated circuit can be damaged by ESD. Texas Instruments recommends that all integrated circuits be handled with appropriate precautions. Failure to observe proper handling and installation procedures can cause damage.

ESD damage can range from subtle performance degradation to complete device failure. Precision integrated circuits may be more susceptible to damage because very small parametric changes could cause the device not to meet its published specifications.

ORDERING INFORMATION[1]

PRODUCT	PACKAGE-LEAD	PACKAGE DESIGNATOR	TEMPERATURE RANGE
INA2128UA	SOIC-16	DW	–40°C to +85°C
INA2128U	SOIC-16	DW	–40°C to +85°C

NOTES: (1) For the most current package and ordering information, see the Package Option Addendum at the end of this document, or see the TI web site at www.ti.com.

ELECTRICAL CHARACTERISTICS

At T_A = +25°C, V_S = ±15V, R_L = 10kΩ, unless otherwise noted.

PARAMETER	CONDITIONS	INA2128U			INA2128UA			UNITS
		MIN	TYP	MAX	MIN	TYP	MAX	
INPUT								
Offset Voltage, RTI								
Initial	T_A = +25°C		±10 ±100/G	±50 ±500/G		±25 ±100/G	±125 ±1000/G	µV
vs Temperature	T_A = T_{MIN} to T_{MAX}		±0.2 ± 2/G	±0.5 ± 20/G		±0.2 ± 5/G	±1 ± 20/G	µV/°C
vs Power Supply	V_S = ±2.25V to ±18V		±0.2 ±20/G	±1 ±100/G		*	±2 ±200/G	µV/V
Long-Term Stability			±0.1 ±3/G			*		µV/mo
Impedance, Differential			10^{10} ‖ 2			*		Ω ‖ pF
Common-Mode			10^{11} ‖ 9			*		Ω ‖ pF
Common-Mode Voltage Range[1]	V_O = 0V	(V+) − 2	(V+) − 1.4		*	*		V
		(V−) + 2	(V−) + 1.7		*	*		V
Safe Input Voltage				±40			*	V
Common-Mode Rejection	V_{CM} = ±13V, ΔR_S = 1kΩ							
G=1		80	86		73	*		dB
G=10		100	106		93	*		dB
G=100		120	125		110	*		dB
G=1000		120	130		110	*		dB
BIAS CURRENT			±2	±5		*	±10	nA
vs Temperature			±30			*		pA/°C
Offset Current			±1	±5		*	±10	nA
vs Temperature			±30			*		pA/°C
NOISE VOLTAGE, RTI	G = 1000, R_S = 0Ω							
f = 10Hz			10			*		nV/√Hz
f = 100Hz			8			*		nV/√Hz
f = 1kHz			8			*		nV/√Hz
f_B = 0.1Hz to 10Hz			0.2			*		µV_pp
Noise Current								
f=10Hz			0.9			*		pA/√Hz
f=1kHz			0.3			*		pA/√Hz
f_B = 0.1Hz to 10Hz			30			*		pA_pp
GAIN								
Gain Equation			1 + (50kΩ/R_G)			*		V/V
Range of Gain		1		10000	*	*	*	V/V
Gain Error								
G=1			±0.01	±0.024		*	±0.1	%
G=10			±0.02	±0.4		*	±0.5	%
G=100			±0.05	±0.5		*	±0.7	%
G=1000			±0.5	±1		*	±2	%
Gain vs Temperature[2]	G=1		±1	±10		*	*	ppm/°C
50kΩ Resistance[2, 3]			±25	±100		*	*	ppm/°C
Nonlinearity	V_O = ±13.6V, G=1		±0.0001	±0.001		*	±0.002	% of FSR
G=10			±0.0003	±0.002		*	±0.004	% of FSR
G=100			±0.0005	±0.002		*	±0.004	% of FSR
G=1000			±0.001	(Note 4)		*	*	% of FSR
OUTPUT								
Voltage: Positive	R_L = 10kΩ	(V+) − 1.4	(V+) − 0.9		*	*		V
Negative	R_L = 10kΩ	(V−) + 1.4	(V−) + 0.8		*	*		V
Load Capacitance Stability			1000			*		pF
Short-Circuit Current			+6/−15			*		mA
FREQUENCY RESPONSE								
Bandwidth, −3dB	G=1		1.3			*		MHz
	G=10		700			*		kHz
	G=100		200			*		kHz
	G=1000		20			*		kHz
Slew Rate	V_O = ±10V, G=10		4			*		V/µs
Settling Time, 0.01%	G=1		7			*		µs
	G=10		7			*		µs
	G=100		9			*		µs
	G=1000		80			*		µs
Overload Recovery	50% Overdrive		4			*		µs
POWER SUPPLY								
Voltage Range		±2.25	±15	±18	*	*	*	V
Current, Total	V_{IN} = 0V		±1.4	±1.5		*	*	mA
TEMPERATURE RANGE								
Specification		−40		85	*		*	°C
Operating		−40		125	*		*	°C
θ_{JA}			80			*		°C/W

* Specification same as INA2128P, U.

NOTE: (1) Input common-mode range varies with output voltage—see Electrical Characteristics.
    (2) Ensured by wafer test.
    (3) Temperature coefficient of the *50kΩ* term in the gain equation.
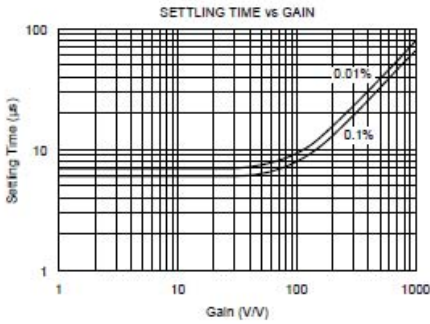   (4) Nonlinearity measurements in G = 1000 are dominated by noise. Typical nonlinearity is ±0.001%.

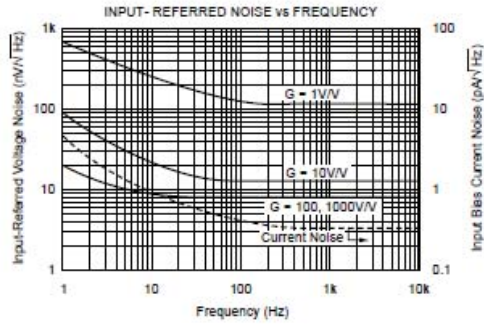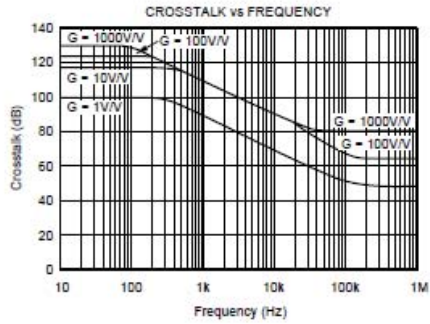# TYPICAL CHARACTERISTICS

At $T_A = +25°C$, $V_S = \pm15V$, unless otherwise noted.
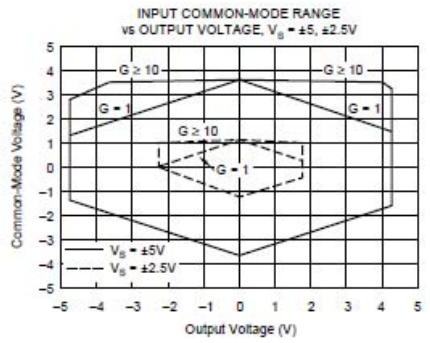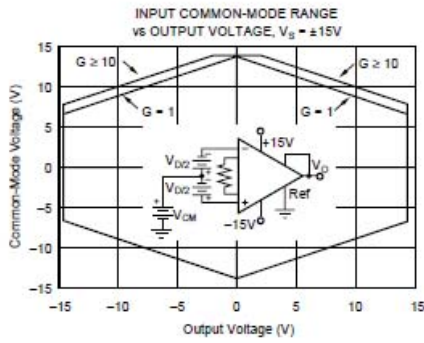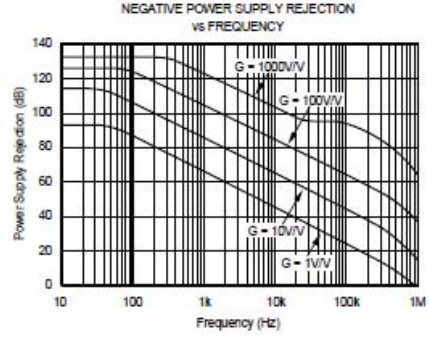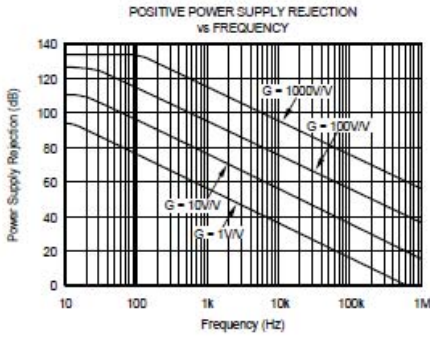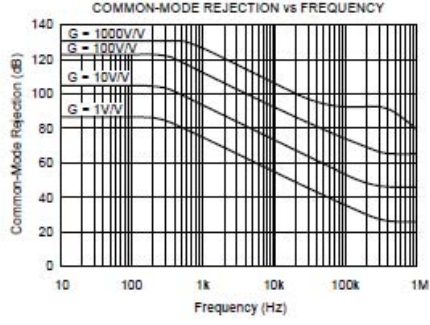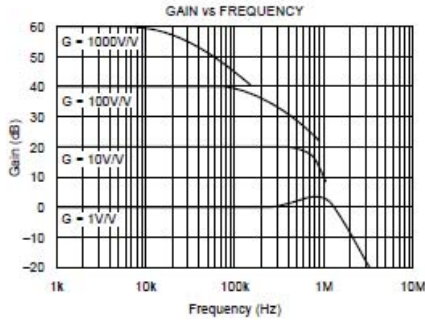
GAIN vs FREQUENCY
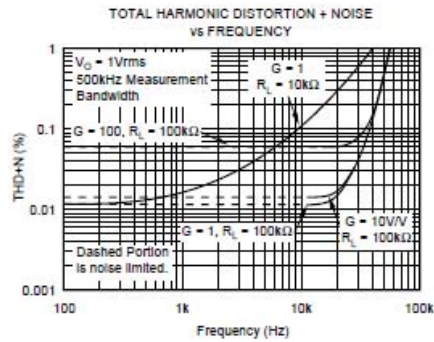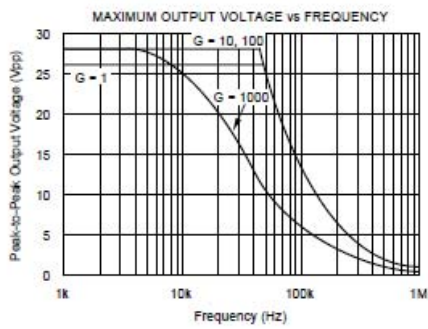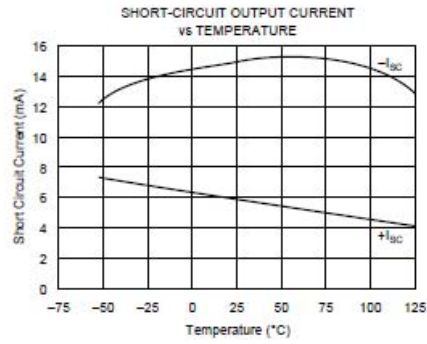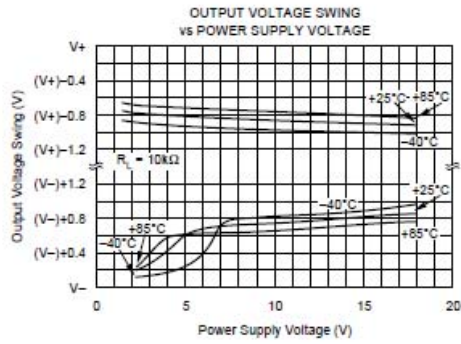

COMMON-MODE REJECTION vs FREQUENCY

POSITIVE POWER SUPPLY REJECTION vs FREQUENCY

NEGATIVE POWER SUPPLY REJECTION vs FREQUENCY

INPUT COMMON-MODE RANGE vs OUTPUT VOLTAGE, $V_S = \pm15V$

INPUT COMMON-MODE RANGE vs OUTPUT VOLTAGE, $V_S = \pm5, \pm2.5V$

TEXAS
INSTRUMENTS
www.ti.com

INA2128
SBOS035A

TYPICAL CHARACTERISTICS (Continued)

At T_A = +25°C, V_S = ±15V, unless otherwise noted.

CROSSTALK vs FREQUENCY

INPUT- REFERRED NOISE vs FREQUENCY

SETTLING TIME vs GAIN

QUIESCENT CURRENT and SLEW RATE vs TEMPERATURE

INPUT OVER-VOLTAGE V/I CHARACTERISTICS

OFFSET VOLTAGE WARM-UP
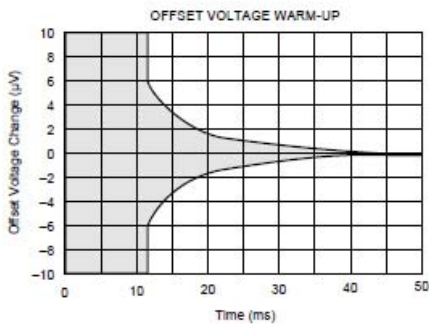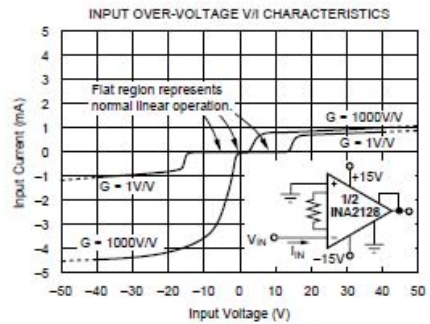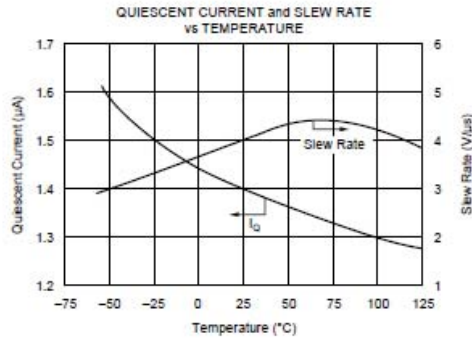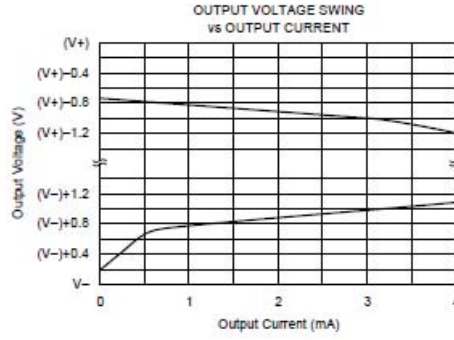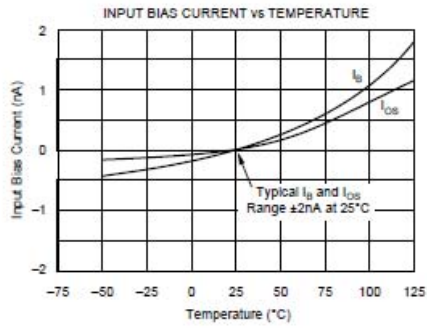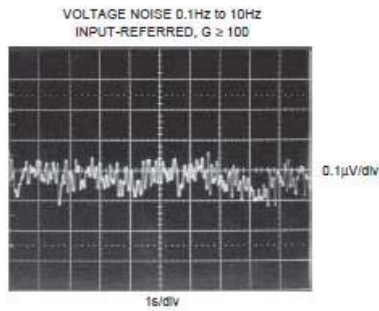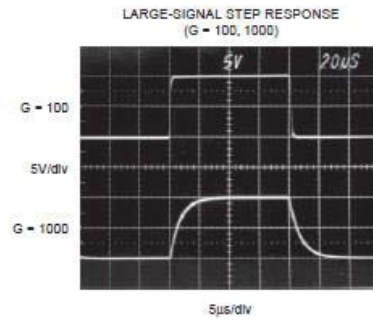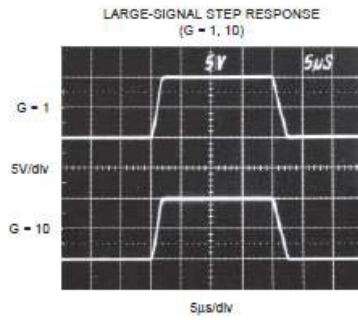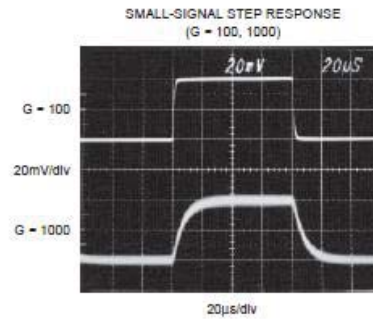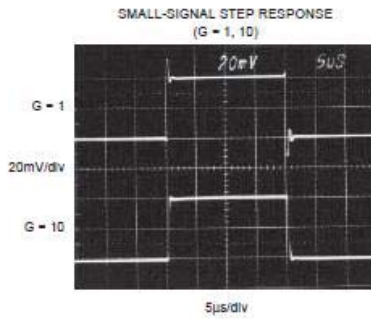
INA2128
SBOS035A

TEXAS
INSTRUMENTS
www.ti.com

5

126

TYPICAL CHARACTERISTICS (Continued)

At T_A = +25°C, V_S = ±15V, unless otherwise noted.

INPUT BIAS CURRENT vs TEMPERATURE

OUTPUT VOLTAGE SWING vs OUTPUT CURRENT

OUTPUT VOLTAGE SWING vs POWER SUPPLY VOLTAGE

SHORT-CIRCUIT OUTPUT CURRENT vs TEMPERATURE

MAXIMUM OUTPUT VOLTAGE vs FREQUENCY

TOTAL HARMONIC DISTORTION + NOISE vs FREQUENCY

TEXAS INSTRUMENTS
www.ti.com

INA2128
SBOS035A

127

TYPICAL CHARACTERISTICS (Continued)

At $T_A = +25°C$, $V_S = ±15V$, unless otherwise noted.

SMALL-SIGNAL STEP RESPONSE
(G = 1, 10)

SMALL-SIGNAL STEP RESPONSE
(G = 100, 1000)

LARGE-SIGNAL STEP RESPONSE
(G = 1, 10)

LARGE-SIGNAL STEP RESPONSE
(G = 100, 1000)

VOLTAGE NOISE 0.1Hz to 10Hz
INPUT-REFERRED, G ≥ 100

128

APPLICATION INFORMATION

Figure 1 shows the basic connections required for operation of the INA2128. Applications with noisy or high impedance power supplies may require decoupling capacitors close to the device pins as shown.

The output is referred to the output reference (Ref) terminals (Ref$_A$ and Ref$_B$) which are normally grounded. These must be low-impedance connections to assure good common-mode rejection. A resistance of 8Ω in series with a Ref pin will cause a typical device to degrade to approximately 80dB CMR (G = 1).

The INA2128 has separate output sense feedback connections, Sense$_A$ and Sense$_B$. These must be connected to their respective output terminals for proper operation. The output sense connection can be used to sense the output voltage directly at the load for best accuracy.

SETTING THE GAIN

Gain of the INA2128 is set by connecting a single external resistor, R$_G$, connected as shown:

$$G = 1 + \frac{50k\Omega}{R_G} \qquad (1)$$

Commonly-used gains and resistor values are shown in Figure 1.

The 50kΩ term in Equation 1 comes from the sum of the two internal feedback resistors, A$_1$ and A$_2$. These on-chip metal film resistors are laser-trimmed to accurate absolute values. The accuracy and temperature coefficient of these resistors are included in the gain accuracy and drift specifications of the INA2128.

The stability and temperature drift of the external gain setting resistor, R$_G$, also affects gain. R$_G$'s contribution to gain accuracy and drift can be directly inferred from the gain equation (1). Low resistor values required for high gain can make wiring resistance important. Sockets add to the wiring resistance which will contribute additional gain error in gains of approximately 100 or greater.

DYNAMIC PERFORMANCE

The typical performance curve "Gain vs Frequency" shows that despite its low quiescent current, the INA2128 achieves wide bandwidth, even at high gain. This is due to its current-feedback topology. Settling time also remains excellent at high gain—see "Settling Time vs Gain."

NOISE PERFORMANCE

The INA2128 provides very low noise in most applications. Low frequency noise is approximately 0.2μV$_{PP}$ measured from 0.1 to 10Hz (G ≥ 100). This provides dramatically improved noise when compared to state-of-the-art chopper-stabilized amplifiers.

DESIRED GAIN	R$_G$ (Ω)	NEAREST 1% R$_G$ (Ω)
1	NC	NC
2	50.00k	49.9k
5	12.50k	12.4k
10	5.556k	5.62k
20	2.632k	2.61k
50	1.02k	1.02k
100	505.1	511
200	251.3	249
500	100.2	100
1000	50.05	49.9
2000	25.01	24.9
5000	10.00	10
10000	5.001	4.99
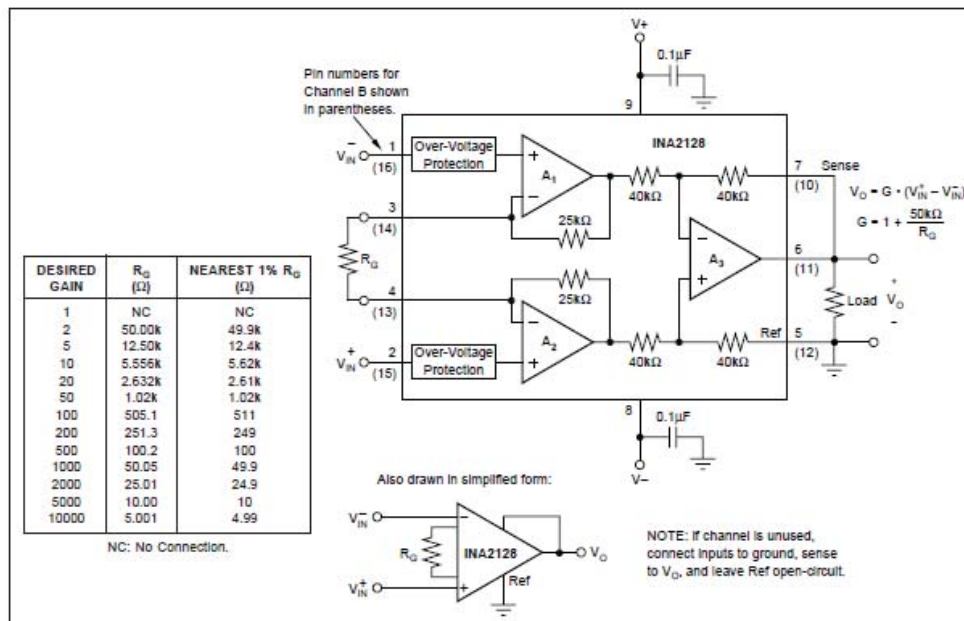
NC: No Connection.

FIGURE 1. Basic Connections.

Texas Instruments
www.ti.com

INA2128
SBOS035A

OFFSET TRIMMING

The INA2128 is laser-trimmed for low offset voltage and offset voltage drift. Most applications require no external offset adjustment. Figure 2 shows an optional circuit for trimming the output offset voltage. The voltage applied to Ref terminal is summed with the output. The op amp buffer provides low impedance at the Ref terminal to preserve good common-mode rejection.
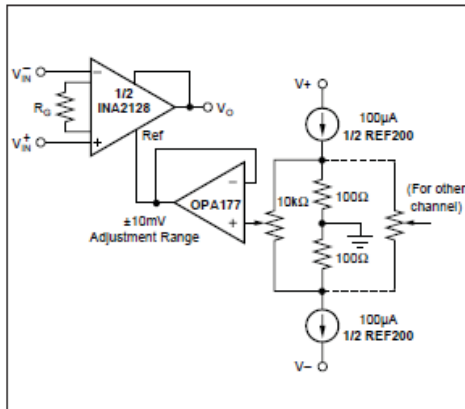
FIGURE 2. Optional Trimming of Output Offset Voltage.

INPUT BIAS CURRENT RETURN PATH

The input impedance of the INA2128 is extremely high—approximately $10^{10}\Omega$. However, a path must be provided for the input bias current of both inputs. This input bias current is approximately $\pm 2nA$. High input impedance means that this input bias current changes very little with varying input voltage.

Input circuitry must provide a path for this input bias current for proper operation. Figure 3 shows various provisions for an input bias current path. Without a bias current path, the inputs will float to a potential which exceeds the common-mode range of the INA2128 and the input amplifiers will saturate.

If the differential source resistance is low, the bias current return path can be connected to one input (see the thermocouple example in Figure 3). With higher source impedance, using two equal resistors provides a balanced input with possible advantages of lower input offset voltage due to bias current and better high-frequency common-mode rejection.

INPUT COMMON-MODE RANGE

The linear input voltage range of the input circuitry of the INA2128 is from approximately 1.4V below the positive supply voltage to 1.7V above the negative supply. As a differential input voltage causes the output voltage increase, however, the linear input range will be limited by the output
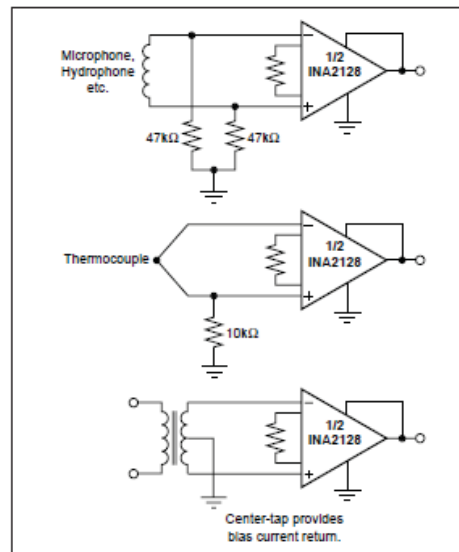
FIGURE 3. Providing an Input Common-Mode Current Path.

voltage swing of amplifiers A_1 and A_2. So the linear common-mode input range is related to the output voltage of the complete amplifier. This behavior also depends on supply voltage—see performance curves "Input Common-Mode Range vs Output Voltage."

Input-overload can produce an output voltage that appears normal. For example, if an input overload condition drives both input amplifiers to their positive output swing limit, the difference voltage measured by the output amplifier will be near zero. The output of the INA2128 will be near 0V even though both inputs are overloaded.

LOW VOLTAGE OPERATION

The INA2128 can be operated on power supplies as low as $\pm 2.25V$. Performance remains excellent with power supplies ranging from $\pm 2.25V$ to $\pm 18V$. Most parameters vary only slightly throughout this supply voltage range—see typical performance curves. Operation at very low supply voltage requires careful attention to assure that the input voltages remain within their linear range. Voltage swing requirements of internal nodes limit the input common-mode range with low power supply voltage. Typical performance curves, "Input Common-Mode Range vs Output Voltage," show the range of linear operation for $\pm 15V$, $\pm 5V$, and $\pm 2.5V$ supplies.

130

INPUT PROTECTION

The inputs of the INA2128 are individually protected for voltages up to ±40V. For example, a condition of –40V on one input and +40V on the other input will not cause damage. Internal circuitry on each input provides low series impedance under normal signal conditions. To provide equivalent protection, series input resistors would contribute excessive noise. If the input is overloaded, the protection circuitry limits the input current to a safe value of approximately 1.5mA to 5mA. The typical performance curve "Input Bias Current vs Common-Mode Input Voltage" shows this input current limit behavior. The inputs are protected even if the power supplies are disconnected or turned off.

CHANNEL CROSSTALK

The two channels of the INA2128 are completely independent, including all bias circuitry. At DC and low frequency there is virtually no signal coupling between channels. Crosstalk increases with frequency and is dependent on circuit gain, source impedance and signal characteristics.

As source impedance increases, careful circuit layout will help achieve lowest channel crosstalk. Most crosstalk is produced by capacitive coupling of signals from one channel to the input section of the other channel. To minimize coupling, separate the input traces as far as practical from any signals associated with the opposite channel. A grounded guard trace surrounding the inputs helps reduce stray coupling between channels. Run the differential inputs of each channel parallel to each other or directly adjacent on top and bottom side of a circuit board. Stray coupling then tends to produce a common-mode signal which is rejected by the IA's input.

FIGURE 4. Two-Axis Bridge Amplifier.
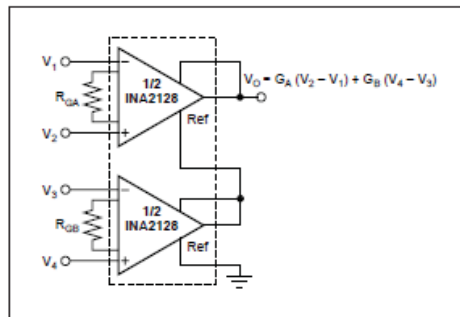
FIGURE 5. Sum of Differences Amplifier.
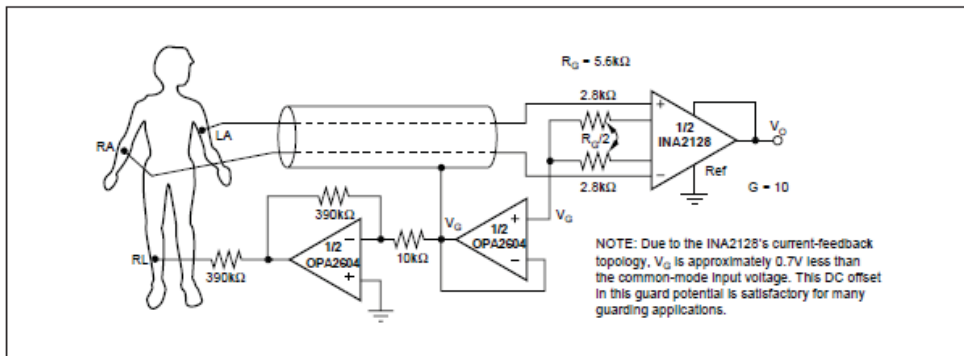
FIGURE 6. ECG Amplifier With Right-Leg Drive.

TEXAS
INSTRUMENTS
www.ti.com

INA2128
SBOS035A

PACKAGING INFORMATION

Orderable Device	Status (1)	Package Type	Package Drawing	Pins	Package Qty	Eco Plan (2)	Lead/Ball Finish	MSL Peak Temp (3)	Op Temp (°C)	Device Marking (4/5)	Samples
INA2128U	ACTIVE	SOIC	DW	16	40	Green (RoHS & no Sb/Br)	CU NIPDAU	Level-3-260C-168 HR	-40 to 85	INA2128U A	Samples
INA2128U/1K	ACTIVE	SOIC	DW	16	1000	Green (RoHS & no Sb/Br)	CU NIPDAU	Level-3-260C-168 HR		INA2128U	Samples
INA2128U/1KE4	ACTIVE	SOIC	DW	16	1000	Green (RoHS & no Sb/Br)	CU NIPDAU	Level-3-260C-168 HR		INA2128U	Samples
INA2128UA	ACTIVE	SOIC	DW	16	40	Green (RoHS & no Sb/Br)	CU NIPDAU	Level-3-260C-168 HR		INA2128U A	Samples
INA2128UA/1K	ACTIVE	SOIC	DW	16	1000	Green (RoHS & no Sb/Br)	CU NIPDAU	Level-3-260C-168 HR		INA2128U A	Samples
INA2128UA/1KG4	ACTIVE	SOIC	DW	16	1000	Green (RoHS & no Sb/Br)	CU NIPDAU	Level-3-260C-168 HR		INA2128U A	Samples
INA2128UAG4	ACTIVE	SOIC	DW	16	40	Green (RoHS & no Sb/Br)	CU NIPDAU	Level-3-260C-168 HR		INA2128U A	Samples
INA2128UG4	ACTIVE	SOIC	DW	16	40	Green (RoHS & no Sb/Br)	CU NIPDAU	Level-3-260C-168 HR	-40 to 85	INA2128U A	Samples

(1) The marketing status values are defined as follows:
ACTIVE: Product device recommended for new designs.
LIFEBUY: TI has announced that the device will be discontinued, and a lifetime-buy period is in effect.
NRND: Not recommended for new designs. Device is in production to support existing customers, but TI does not recommend using this part in a new design.
PREVIEW: Device has been announced but is not in production. Samples may or may not be available.
OBSOLETE: TI has discontinued the production of the device.

(2) Eco Plan - The planned eco-friendly classification: Pb-Free (RoHS), Pb-Free (RoHS Exempt), or Green (RoHS & no Sb/Br) - please check http://www.ti.com/productcontent for the latest availability information and additional product content details.
TBD: The Pb-Free/Green conversion plan has not been defined.
Pb-Free (RoHS): TI's terms "Lead-Free" or "Pb-Free" mean semiconductor products that are compatible with the current RoHS requirements for all 6 substances, including the requirement that lead not exceed 0.1% by weight in homogeneous materials. Where designed to be soldered at high temperatures, TI Pb-Free products are suitable for use in specified lead-free processes.
Pb-Free (RoHS Exempt): This component has a RoHS exemption for either 1) lead-based flip-chip solder bumps used between the die and package, or 2) lead-based die adhesive used between the die and leadframe. The component is otherwise considered Pb-Free (RoHS compatible) as defined above.
Green (RoHS & no Sb/Br): TI defines "Green" to mean Pb-Free (RoHS compatible), and free of Bromine (Br) and Antimony (Sb) based flame retardants (Br or Sb do not exceed 0.1% by weight in homogeneous material)

(3) MSL, Peak Temp. – The Moisture Sensitivity Level rating according to the JEDEC industry standard classifications, and peak solder temperature.

(4) There may be additional marking, which relates to the logo, the lot trace code information, or the environmental category on the device.

(5) Multiple Device Markings will be inside parentheses. Only one Device Marking contained in parentheses and separated by a "~" will appear on a device. If a line is indented then it is a continuation of the previous line and the two combined represent the entire Device Marking for that device.

Important Information and Disclaimer: The information provided on this page represents TI's knowledge and belief as of the date that it is provided. TI bases its knowledge and belief on information provided by third parties, and makes no representation or warranty as to the accuracy of such information. Efforts are underway to better integrate information from third parties. TI has taken and continues to take reasonable steps to provide representative and accurate information but may not have conducted destructive testing or chemical analysis on incoming materials and chemicals. TI and TI suppliers consider certain information to be proprietary, and thus CAS numbers and other limited information may not be available for release.

In no event shall TI's liability arising out of such information exceed the total purchase price of the TI part(s) at issue in this document sold by TI to Customer on an annual basis.
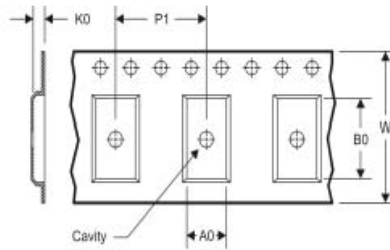
132

TAPE AND REEL INFORMATION

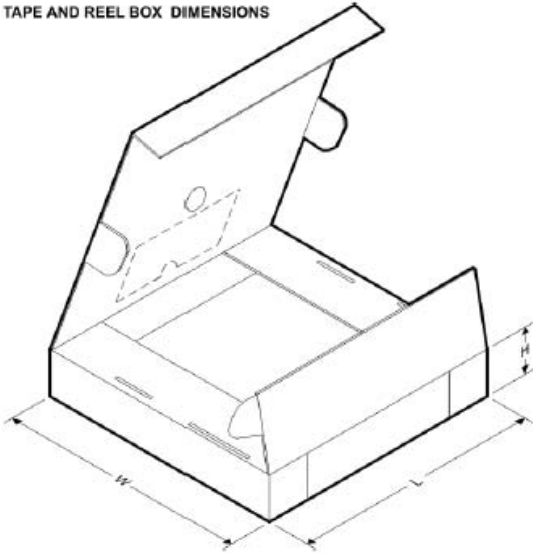**REEL DIMENSIONS**

TAPE DIMENSIONS

A0	Dimension designed to accommodate the component width
B0	Dimension designed to accommodate the component length
K0	Dimension designed to accommodate the component thickness
W	Overall width of the carrier tape
P1	Pitch between successive cavity centers

TAPE AND REEL INFORMATION

*All dimensions are nominal

Device	Package Type	Package Drawing	Pins	SPQ	Reel Diameter (mm)	Reel Width W1 (mm)	A0 (mm)	B0 (mm)	K0 (mm)	P1 (mm)	W (mm)	Pin1 Quadrant
INA2128U/1K	SOIC	DW	16	1000	330.0	16.4	10.75	10.7	2.7	12.0	16.0	Q1
INA2128UA/1K	SOIC	DW	16	1000	330.0	16.4	10.75	10.7	2.7	12.0	16.0	Q1

TAPE AND REEL BOX DIMENSIONS

*All dimensions are nominal

Device	Package Type	Package Drawing	Pins	SPQ	Length (mm)	Width (mm)	Height (mm)
INA2128U/1K	SOIC	DW	16	1000	367.0	367.0	38.0
INA2128UA/1K	SOIC	DW	16	1000	367.0	367.0	38.0

134

DW (R−PDSO−G16)   PLASTIC SMALL OUTLINE

0.413 (10,50)
0.398 (10,10)

16   9

0.419 (10,63)
0.393 (9,97)

0.299 (7,60)
0.291 (7,40)

1   8

Pin 1
Index Area

0.050 (1,27)

0.020 (0,51)
0.012 (0,31)

⊕ 0.010 (0,25) Ⓜ

0.104 (2,65) Max

0.012 (0,30)
0.004 (0,10)

0.013 (0,33)
0.008 (0,20)

Gauge Plane

0.004 (0,10)

Seating Plane

0.010 (0,25)

0°−8°

0.050 (1,27)
0.016 (0,40)

4040000−2/G 01/11
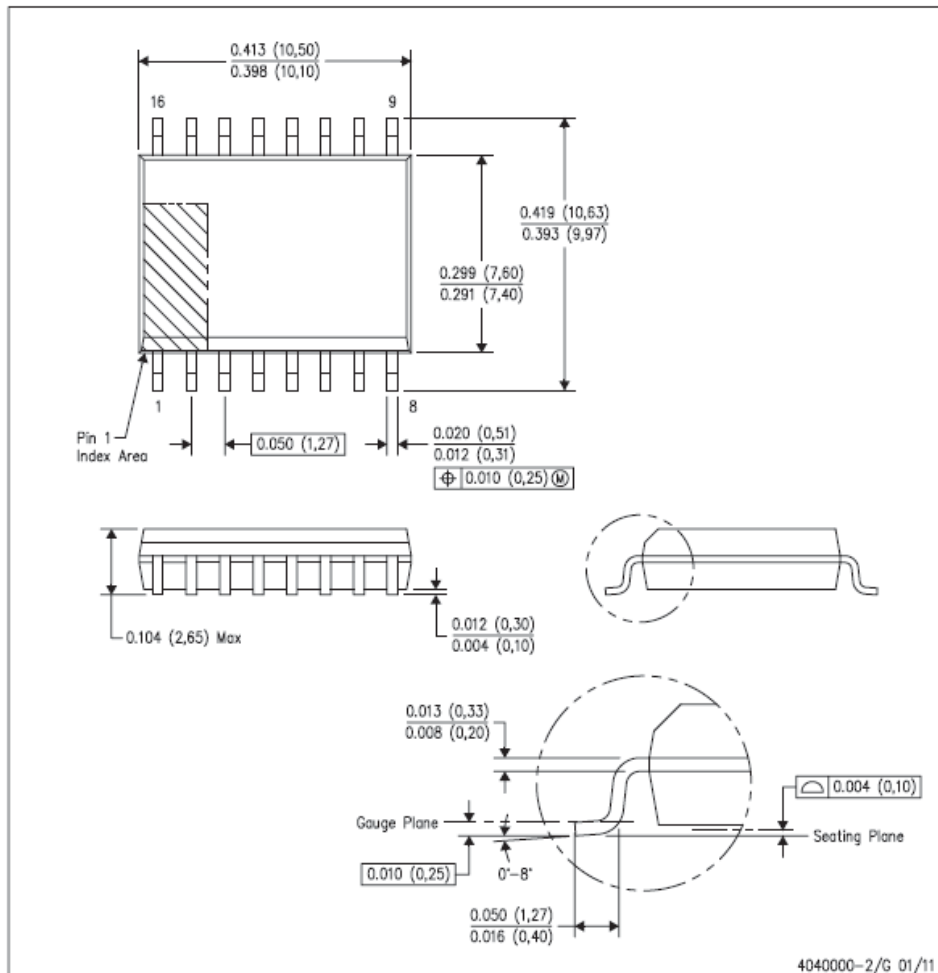
NOTES: A.   All linear dimensions are in inches (millimeters). Dimensioning and tolerancing per ASME Y14.5M−1994.
         B.   This drawing is subject to change without notice.
         C.   Body dimensions do not include mold flash or protrusion not to exceed 0.006 (0,15).
         D.   Falls within JEDEC MS−013 variation AA.

TEXAS INSTRUMENTS
www.ti.com

DW (R-PDSO-G16)   PLASTIC SMALL OUTLINE

Example Board Layout
(Note C)

Stencil Openings
(Note D)

14x1,27

16x0,55   14x1,27

16x1,95

9,4

9,4

Non Solder Mask Define Pad

0,6

Solder Mask Opening
(Note E)

2,0

Pad Geometry
(Note C)

0,07
All Around
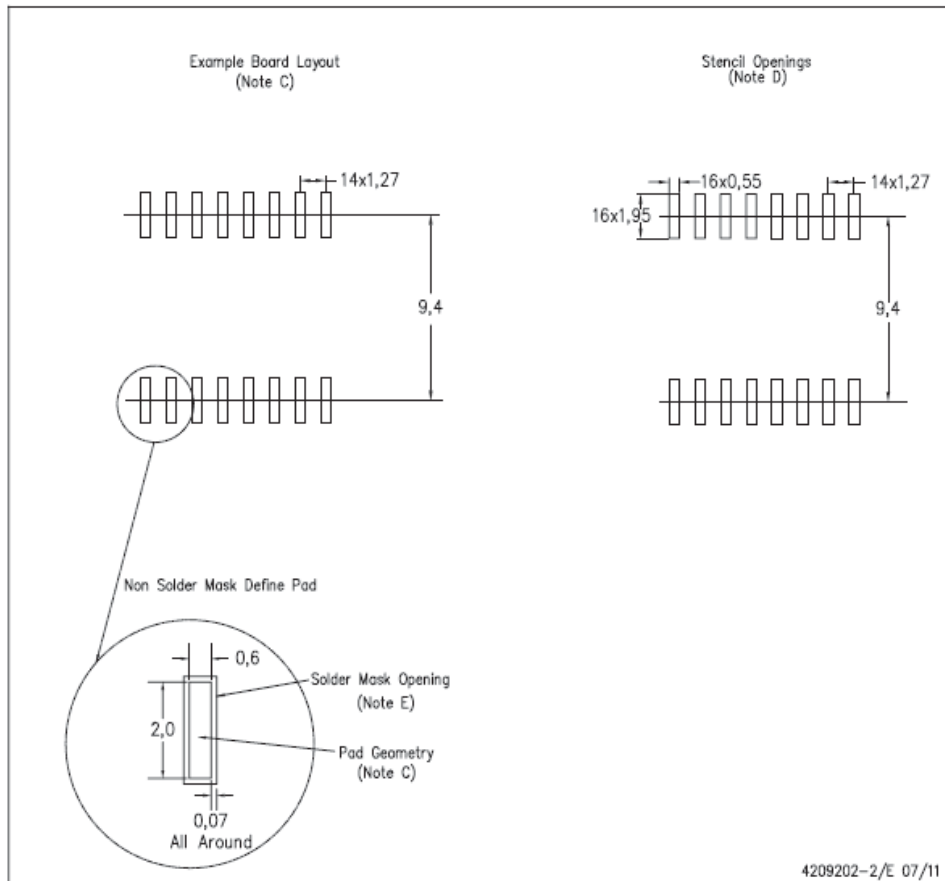
4209202-2/E 07/11

NOTES: A.   All linear dimensions are in millimeters.
         B.   This drawing is subject to change without notice.
         C.   Refer to IPC7351 for alternate board design.
         D.   Laser cutting apertures with trapezoidal walls and also rounding corners will offer better paste release. Customers should
              contact their board assembly site for stencil design recommendations. Refer to IPC-7525
         E.   Customers should contact their board fabrication site for solder mask tolerances between and around signal pads.

IMPORTANT NOTICE

10.2 Appendix 2 - OPA2604 Datasheet

BURR-BROWN®

OPA2604

www.burr-brown.com/databook/OPA2604.html

Dual FET-Input, Low Distortion
OPERATIONAL AMPLIFIER

FEATURES
- LOW DISTORTION: 0.0003% at 1kHz
- LOW NOISE: $10nV/\sqrt{Hz}$
- HIGH SLEW RATE: $25V/\mu s$
- WIDE GAIN-BANDWIDTH: 20MHz
- UNITY-GAIN STABLE
- WIDE SUPPLY RANGE: $V_S = \pm4.5$ to $\pm24V$
- DRIVES 600Ω LOADS

APPLICATIONS
- PROFESSIONAL AUDIO EQUIPMENT
- PCM DAC I/V CONVERTER
- SPECTRAL ANALYSIS EQUIPMENT
- ACTIVE FILTERS
- TRANSDUCER AMPLIFIER
- DATA ACQUISITION

DESCRIPTION

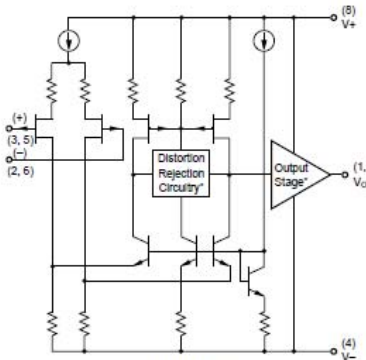The OPA2604 is a dual, FET-input operational amplifier designed for enhanced AC performance. Very low distortion, low noise and wide bandwidth provide superior performance in high quality audio and other applications requiring excellent dynamic performance.

New circuit techniques and special laser trimming of dynamic circuit performance yield very low harmonic distortion. The result is an op amp with exceptional sound quality. The low-noise FET input of the OPA2604 provides wide dynamic range, even with high source impedance. Offset voltage is laser-trimmed to minimize the need for interstage coupling capacitors.

The OPA2604 is available in 8-pin plastic mini-DIP and SO-8 surface-mount packages, specified for the $-25^\circ C$ to $+85^\circ C$ temperature range.

* Patents Granted:
#5053718, 5019789

PDS-1069E

SBOS006

SPECIFICATIONS

ELECTRICAL

At T_A = +25°C, V_S = ±15V, unless otherwise noted.

PARAMETER	CONDITION	OPA2604AP, AU MIN	OPA2604AP, AU TYP	OPA2604AP, AU MAX	UNITS
OFFSET VOLTAGE					
Input Offset Voltage			±1	±5	mV
Average Drift			±8		μV/°C
Power Supply Rejection	V_S = ±5 to ±24V	70	80		dB
INPUT BIAS CURRENT[1]					
Input Bias Current	V_{CM} = 0V		100		pA
Input Offset Current	V_{CM} = 0V		±4		pA
NOISE					
Input Voltage Noise					
Noise Density: f = 10Hz			25		nV/√Hz
f = 100Hz			15		nV/√Hz
f = 1kHz			11		nV/√Hz
f = 10kHz			10		nV/√Hz
Voltage Noise, BW = 20Hz to 20kHz			1.5		μVp-p
Input Bias Current Noise					
Current Noise Density, f = 0.1Hz to 20kHz			6		fA/√Hz
INPUT VOLTAGE RANGE					
Common-Mode Input Range		±12	±13		V
Common-Mode Rejection	V_{CM} = ±12V	80	100		dB
INPUT IMPEDANCE					
Differential			10^{12} ‖ 8		Ω ‖ pF
Common-Mode			10^{12} ‖ 10		Ω ‖ pF
OPEN-LOOP GAIN					
Open-Loop Voltage Gain	V_O = ±10V, R_L = 1kΩ	80	100		dB
FREQUENCY RESPONSE					
Gain-Bandwidth Product	G = 100		20		MHz
Slew Rate	20Vp-p, R_L = 1kΩ	15	25		V/μs
Settling Time: 0.01%	G = –1, 10V Step		1.5		μs
0.1%			1		μs
Total Harmonic Distortion + Noise (THD+N)	G = 1, f = 1kHz V_O = 3.5Vrms, R_L = 1kΩ		0.0003		%
Channel Separation	f = 1kHz, R_L = 1kΩ		142		dB
OUTPUT					
Voltage Output	R_L = 600Ω	±11	±12		V
Current Output	V_O = ±12V		±35		mA
Short Circuit Current			±40		mA
Output Resistance, Open-Loop			25		Ω
POWER SUPPLY					
Specified Operating Voltage			±15		V
Operating Voltage Range		±4.5		±24	V
Current, Total Both Amplifiers	I_O = 0		±10.5	±12	mA
TEMPERATURE RANGE					
Specification		–25		+85	°C
Storage		–40		+125	°C
Thermal Resistance[2], θ_{JA}			90		°C/W

NOTES: (1) Typical performance, measured fully warmed-up. (2) Soldered to circuit board—see text.

BURR-BROWN®
BB   OPA2604

PIN CONFIGURATION

Top View   DIP/SOIC

```
         Output A   1            8   V+
           –In A    2            7   Output B
           +In A    3            6   –In B
             V–     4            5   +In B
```
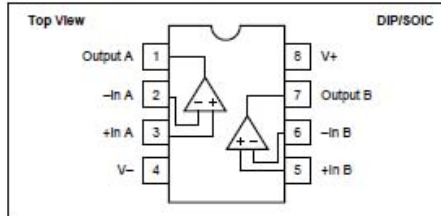
⚠ ELECTROSTATIC DISCHARGE SENSITIVITY

Any integrated circuit can be damaged by ESD. Burr-Brown recommends that all integrated circuits be handled with appropriate precautions. Failure to observe proper handling and installation procedures can cause damage.

ESD damage can range from subtle performance degradation to complete device failure. Precision integrated circuits may be more susceptible to damage because very small parametric changes could cause the device not to meet published specifications.

ABSOLUTE MAXIMUM RATINGS[1]

Power Supply Voltage	±25V
Input Voltage	(V–)–1V to (V+)+1V
Output Short Circuit to Ground	Continuous
Operating Temperature	–40°C to +100°C
Storage Temperature	–40°C to +125°C
Junction Temperature	+150°C
Lead Temperature (soldering, 10s) AP	+300°C
Lead Temperature (soldering, 3s) AU	+260°C

NOTE: (1) Stresses above these ratings may cause permanent damage.

ORDERING INFORMATION

PRODUCT	PACKAGE	TEMP. RANGE
OPA2604AP	8-Pin Plastic DIP	–25°C to +85°C
OPA2604AU	SO-8 Surface-Mount	–25°C to +85°C

PACKAGING INFORMATION

PRODUCT	PACKAGE	PACKAGE DRAWING NUMBER[1]
OPA2604AP	8-Pin Plastic DIP	006
OPA2604AU	SO-8 Surface-Mount	182

NOTE: (1) For detailed drawing and dimension table, please see end of data sheet, or Appendix C of Burr-Brown IC Data Book.

OPA2604   BURR-BROWN® **BB**

TYPICAL PERFORMANCE CURVES

At T_A = +25°C, V_s = ±15V, unless otherwise noted.

TOTAL HARMONIC DISTORTION + NOISE
vs FREQUENCY

TOTAL HARMONIC DISTORTION + NOISE
vs OUTPUT VOLTAGE

OPEN-LOOP GAIN/PHASE vs FREQUENCY

INPUT VOLTAGE AND CURRENT NOISE
SPECTRAL DENSITY vs FREQUENCY

INPUT BIAS AND INPUT OFFSET CURRENT
vs TEMPERATURE

INPUT BIAS AND INPUT OFFSET CURRENT
vs INPUT COMMON-MODE VOLTAGE

BURR-BROWN®
BB OPA2604

4

141

TYPICAL PERFORMANCE CURVES (CONT)

At $T_A = +25°C$, $V_S = ±15V$, unless otherwise noted.

INPUT BIAS CURRENT vs TIME FROM POWER TURN-ON

COMMON-MODE REJECTION vs COMMON-MODE VOLTAGE

POWER SUPPLY AND COMMON-MODE REJECTION vs FREQUENCY

A_{OL}, PSR, AND CMR vs SUPPLY VOLTAGE

GAIN-BANDWIDTH AND SLEW RATE vs SUPPLY VOLTAGE

GAIN-BANDWIDTH AND SLEW RATE vs TEMPERATURE

OPA2604   BURR-BROWN® BB

142

TYPICAL PERFORMANCE CURVES (CONT)

At T_A = +25°C, V_S = ±15V, unless otherwise noted.

SETTLING TIME vs CLOSED-LOOP GAIN

V_O = 10V Step
R_L = 1kΩ
C_L = 50pF

0.01%

0.1%

CHANNEL SEPARATION vs FREQUENCY

R_L = ∞

R_L = 1kΩ

V_O = 20Vp-p

Measured Output

MAXIMUM OUTPUT VOLTAGE SWING vs FREQUENCY

V_S = ±15V

SUPPLY CURRENT vs TEMPERATURE

Total for Both Op Amps

V_S = ±15VDC

V_S = ±24VDC

V_S = ±5VDC

LARGE-SIGNAL TRANSIENT RESPONSE

SMALL-SIGNAL TRANSIENT RESPONSE

TYPICAL PERFORMANCE CURVES (CONT)

At T_A = +25°C, V_S = ±15V, unless otherwise noted.

SHORT-CIRCUIT CURRENT vs TEMPERATURE

I_{SC+} and I_{SC-}

POWER DISSIPATION vs SUPPLY VOLTAGE

Worst case sine wave R_L = 600Ω (both channels)

Typical high-level music R_L = 600Ω (both channels)

No signal or no load

MAXIMUM POWER DISSIPATION vs TEMPERATURE

θ_{J-A} = 90°C/W Soldered to Circuit Board (see text)

Maximum Specified Operating Temperature 85°C

7   **OPA2604**

APPLICATIONS INFORMATION

The OPA2604 is unity-gain stable, making it easy to use in a wide range of circuitry. Applications with noisy or high impedance power supply lines may require decoupling capacitors close to the device pins. In most cases 1μF tantalum capacitors are adequate.

DISTORTION MEASUREMENTS

The distortion produced by the OPA2604 is below the measurement limit of virtually all commercially available equipment. A special test circuit, however, can be used to extend the measurement capabilities.

Op amp distortion can be considered an internal error source which can be referred to the input. Figure 1 shows a circuit which causes the op amp distortion to be 101 times greater than normally produced by the op amp. The addition of R_3 to the otherwise standard non-inverting amplifier configuration alters the feedback factor or noise gain of the circuit. The closed-loop gain is unchanged, but the feedback available for error correction is reduced by a factor of 101. This extends the measurement limit, including the effects of the signal-source purity, by a factor of 101. Note that the input signal and load applied to the op amp are the same as with conventional feedback without R_3.

Validity of this technique can be verified by duplicating measurements at high gain and/or high frequency where the distortion is within the measurement capability of the test equipment. Measurements for this data sheet were made with the Audio Precision System One which greatly simplifies such repetitive measurements. The measurement technique can, however, be performed with manual distortion measurement instruments.

CAPACITIVE LOADS

The dynamic characteristics of the OPA2604 have been optimized for commonly encountered gains, loads and operating conditions. The combination of low closed-loop gain and capacitive load will decrease the phase margin and may lead to gain peaking or oscillations. Load capacitance reacts with the op amp's open-loop output resistance to form an additional pole in the feedback loop. Figure 2 shows various circuits which preserve phase margin with capacitive load. Request Application Bulletin AB-028 for details of analysis techniques and applications circuits.

For the unity-gain buffer, Figure 2a, stability is preserved by adding a phase-lead network, R_C and C_C. Voltage drop across R_C will reduce output voltage swing with heavy loads. An alternate circuit, Figure 2b, does not limit the output with low load impedance. It provides a small amount of positive feedback to reduce the net feedback factor. Input impedance of this circuit falls at high frequency as op amp gain rolloff reduces the bootstrap action on the compensation network.

Figures 2c and 2d show compensation techniques for noninverting amplifiers. Like the follower circuits, the circuit in Figure 2d eliminates voltage drop due to load current, but at the penalty of somewhat reduced input impedance at high frequency.

Figures 2e and 2f show input lead compensation networks for inverting and difference amplifier configurations.

NOISE PERFORMANCE

Op amp noise is described by two parameters—noise voltage and noise current. The voltage noise determines the noise performance with low source impedance. Low noise bipolar-input op amps such as the OPA27 and OPA37 provide very low voltage noise. But if source impedance is greater than a few thousand ohms, the current noise of bipolar-input op amps react with the source impedance and will dominate. At a few thousand ohms source impedance and above, the OPA2604 will generally provide lower noise.

SIG. GAIN	DIST. GAIN	R_1	R_2	R_3
1	101	—	5kΩ	50Ω
10	101	500Ω	5kΩ	500Ω
100	101	50Ω	5kΩ	—
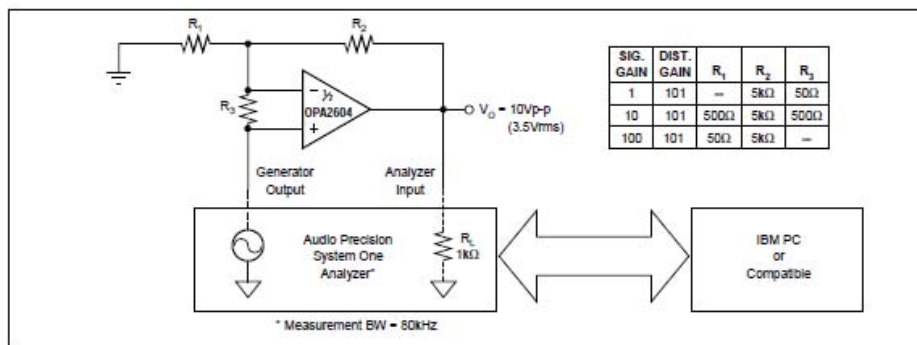
FIGURE 1. Distortion Test Circuit.
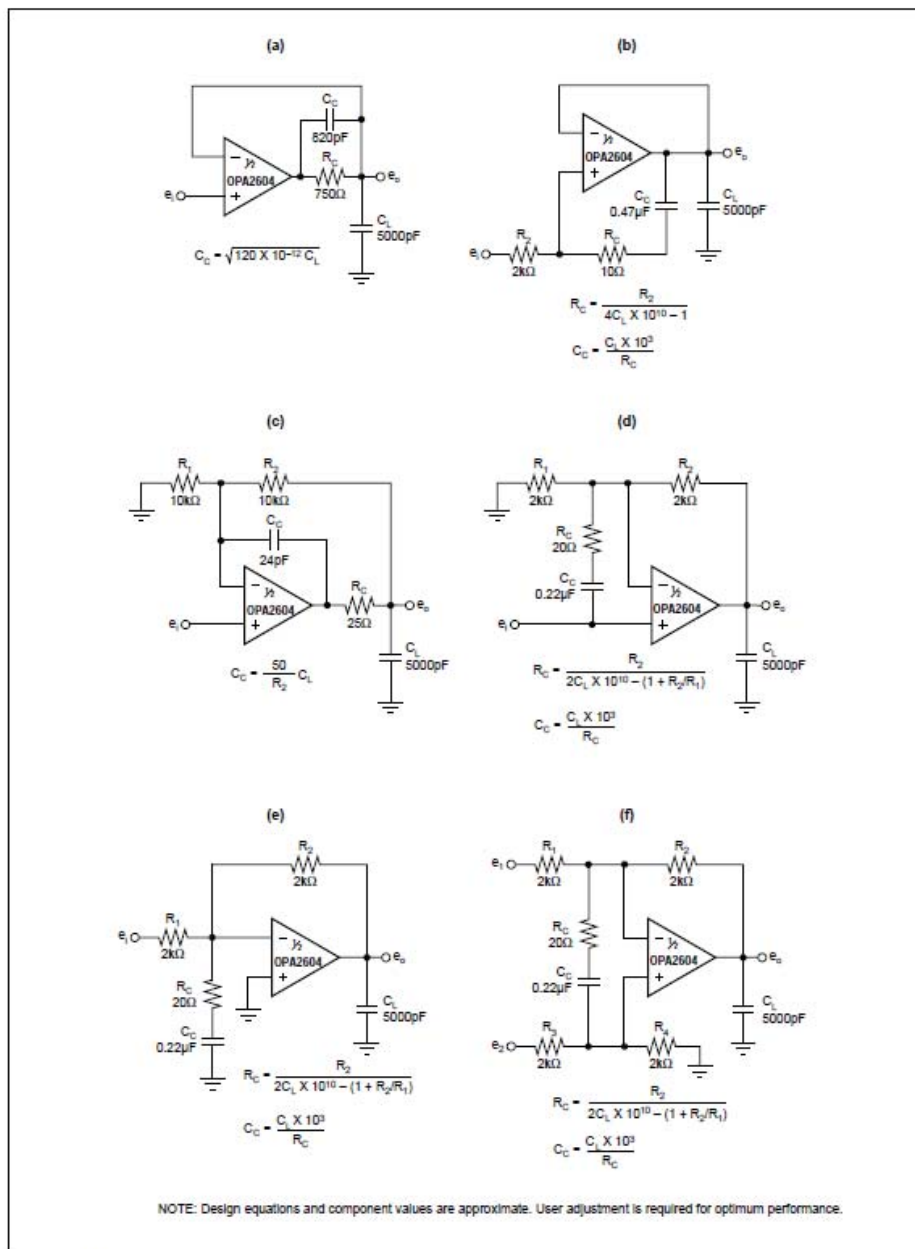
FIGURE 2. Driving Large Capacitive Loads.

OPA2604

146

POWER DISSIPATION

The OPA2604 is capable of driving 600Ω loads with power supply voltages up to $\pm24V$. Internal power dissipation is increased when operating at high power supply voltage. The typical performance curve, Power Dissipation vs Power Supply Voltage, shows quiescent dissipation (no signal or no load) as well as dissipation with a worst case continuous sine wave. Continuous high-level music signals typically produce dissipation significantly less than worst case sine waves.

Copper leadframe construction used in the OPA2604 improves heat dissipation compared to conventional plastic packages. To achieve best heat dissipation, solder the device directly to the circuit board and use wide circuit board traces.

OUTPUT CURRENT LIMIT

Output current is limited by internal circuitry to approximately $\pm40mA$ at $25°C$. The limit current decreases with increasing temperature as shown in the typical curves.
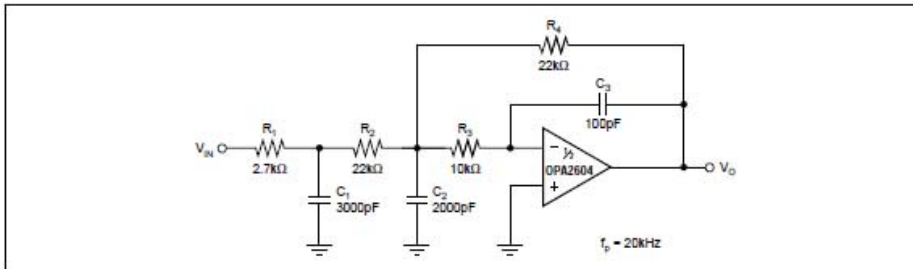
FIGURE 3. Three-Pole Low-Pass Filter.
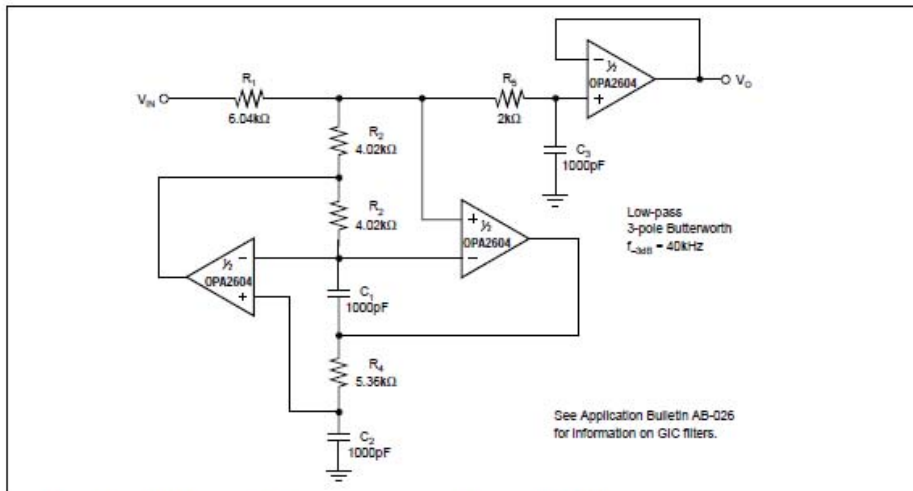
FIGURE 4. Three-Pole Generalized Immittance Converter (GIC) Low-Pass Filter.

BURR-BROWN®

OPA2604

10

FIGURE 5. DAC I/V Amplifier and Low-Pass Filter.

FIGURE 6. Differential Amplifier with Low-Pass Filter.

11

OPA2604

148

FIGURE 7. High Impedance Amplifier.

FIGURE 8. Digital Audio DAC I-V Amplifier.

FIGURE 9. Using the Dual OPA2604 Op Amp to Double the Output Current to a Load.

149

PACKAGING INFORMATION

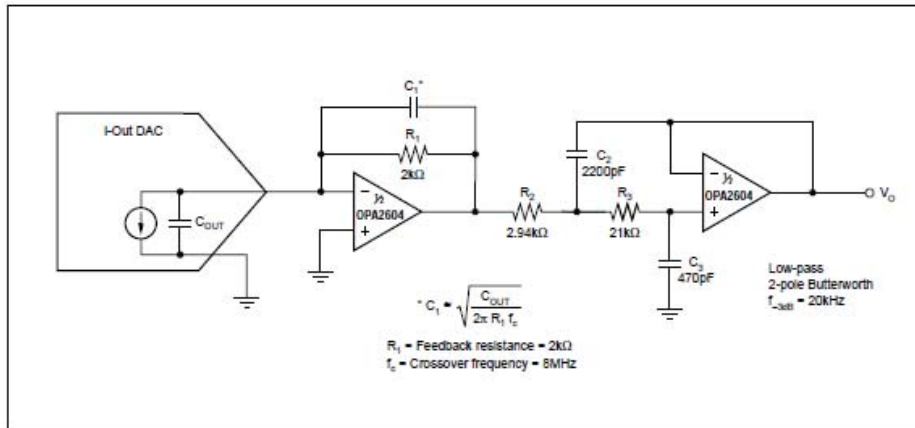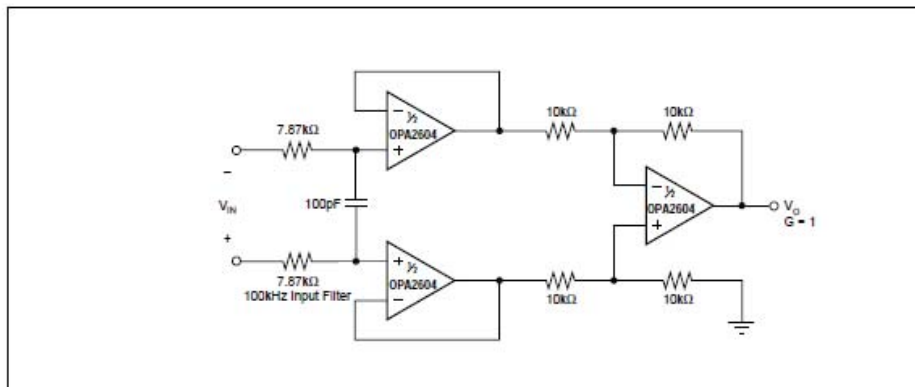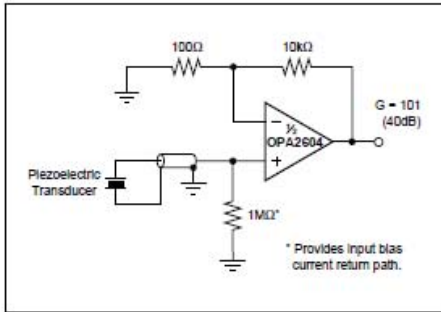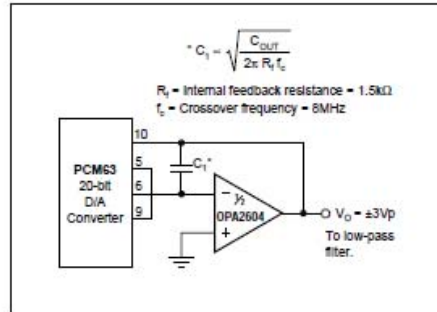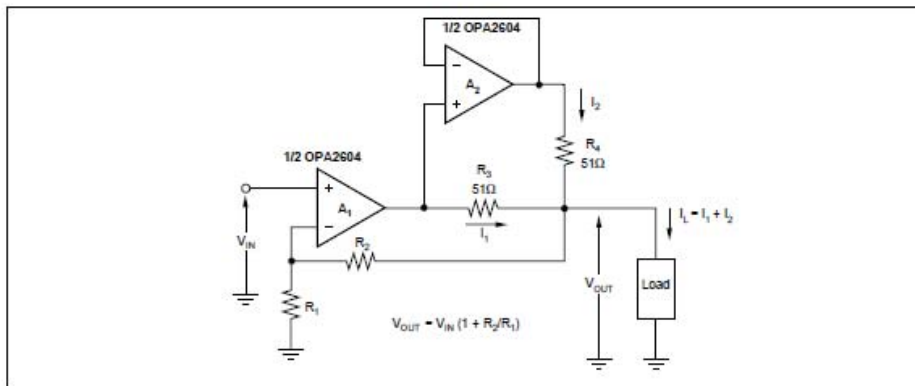| Orderable Device	Status [1]	Package Type	Package Drawing	Pins	Package Qty	Eco Plan [2]	Lead/Ball Finish	MSL Peak Temp [3]
OPA2604AP	ACTIVE	PDIP	P	8	50	Green (RoHS & no Sb/Br)	CU NIPDAU	N / A for Pkg Type
OPA2604APG4	ACTIVE	PDIP	P	8	50	Green (RoHS & no Sb/Br)	CU NIPDAU	N / A for Pkg Type
OPA2604AU	ACTIVE	SOIC	D	8	75	Green (RoHS & no Sb/Br)	CU NIPDAU	Level-3-260C-168 HR
OPA2604AU/2K5	ACTIVE	SOIC	D	8	2500	Green (RoHS & no Sb/Br)	CU NIPDAU	Level-3-260C-168 HR
OPA2604AU/2K5E4	ACTIVE	SOIC	D	8	2500	Green (RoHS & no Sb/Br)	CU NIPDAU	Level-3-260C-168 HR
OPA2604AUE4	ACTIVE	SOIC	D	8	75	Green (RoHS & no Sb/Br)	CU NIPDAU	Level-3-260C-168 HR
OPA2604AUG4	ACTIVE	SOIC	D	8	75	Green (RoHS & no Sb/Br)	CU NIPDAU	Level-3-260C-168 HR

[1] The marketing status values are defined as follows:
ACTIVE: Product device recommended for new designs.
LIFEBUY: TI has announced that the device will be discontinued, and a lifetime-buy period is in effect.
NRND: Not recommended for new designs. Device is in production to support existing customers, but TI does not recommend using this part in a new design.
PREVIEW: Device has been announced but is not in production. Samples may or may not be available.
OBSOLETE: TI has discontinued the production of the device.

[2] Eco Plan - The planned eco-friendly classification: Pb-Free (RoHS), Pb-Free (RoHS Exempt), or Green (RoHS & no Sb/Br) - please check http://www.ti.com/productcontent for the latest availability information and additional product content details.
TBD: The Pb-Free/Green conversion plan has not been defined.
Pb-Free (RoHS): TI's terms "Lead-Free" or "Pb-Free" mean semiconductor products that are compatible with the current RoHS requirements for all 6 substances, including the requirement that lead not exceed 0.1% by weight in homogeneous materials. Where designed to be soldered at high temperatures, TI Pb-Free products are suitable for use in specified lead-free processes.
Pb-Free (RoHS Exempt): This component has a RoHS exemption for either 1) lead-based flip-chip solder bumps used between the die and package, or 2) lead-based die adhesive used between the die and leadframe. The component is otherwise considered Pb-Free (RoHS compatible) as defined above.
Green (RoHS & no Sb/Br): TI defines "Green" to mean Pb-Free (RoHS compatible), and free of Bromine (Br) and Antimony (Sb) based flame retardants (Br or Sb do not exceed 0.1% by weight in homogeneous material)

[3] MSL, Peak Temp. -- The Moisture Sensitivity Level rating according to the JEDEC industry standard classifications, and peak solder temperature.

Important Information and Disclaimer: The information provided on this page represents TI's knowledge and belief as of the date that it is provided. TI bases its knowledge and belief on information provided by third parties, and makes no representation or warranty as to the accuracy of such information. Efforts are underway to better integrate information from third parties. TI has taken and continues to take reasonable steps to provide representative and accurate information but may not have conducted destructive testing or chemical analysis on incoming materials and chemicals. TI and TI suppliers consider certain information to be proprietary, and thus CAS numbers and other limited information may not be available for release.

In no event shall TI's liability arising out of such information exceed the total purchase price of the TI part(s) at issue in this document sold by TI to Customer on an annual basis.

OTHER QUALIFIED VERSIONS OF OPA2604 :
• Automotive: OPA2604-Q1

NOTE: Qualified Version Definitions:
  • Automotive - Q100 devices qualified for high-reliability automotive applications targeting zero defects

TAPE AND REEL INFORMATION

REEL DIMENSIONS

TAPE DIMENSIONS

A0	Dimension designed to accommodate the component width
B0	Dimension designed to accommodate the component length
K0	Dimension designed to accommodate the component thickness
W	Overall width of the carrier tape
P1	Pitch between successive cavity centers
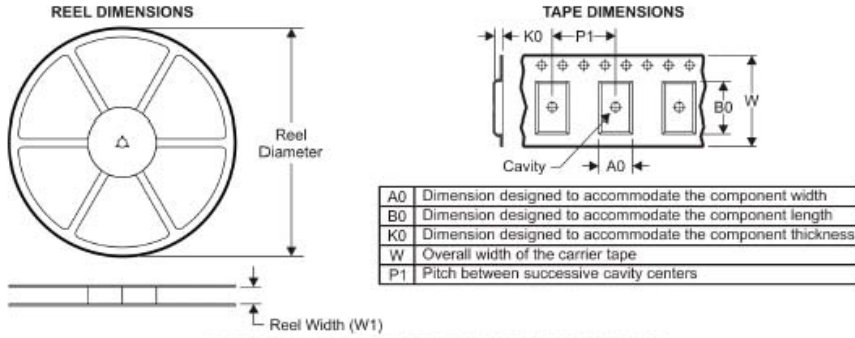
QUADRANT ASSIGNMENTS FOR PIN 1 ORIENTATION IN TAPE
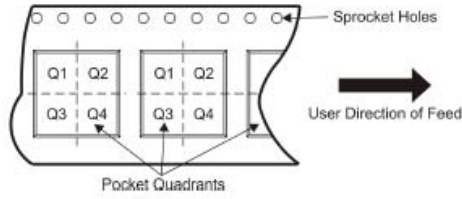
User Direction of Feed

*All dimensions are nominal

Device	Package Type	Package Drawing	Pins	SPQ	Reel Diameter (mm)	Reel Width W1 (mm)	A0 (mm)	B0 (mm)	K0 (mm)	P1 (mm)	W (mm)	Pin1 Quadrant
OPA2604AU/2K5	SOIC	D	8	2500	330.0	12.4	6.4	5.2	2.1	8.0	12.0	Q1

TAPE AND REEL BOX DIMENSIONS
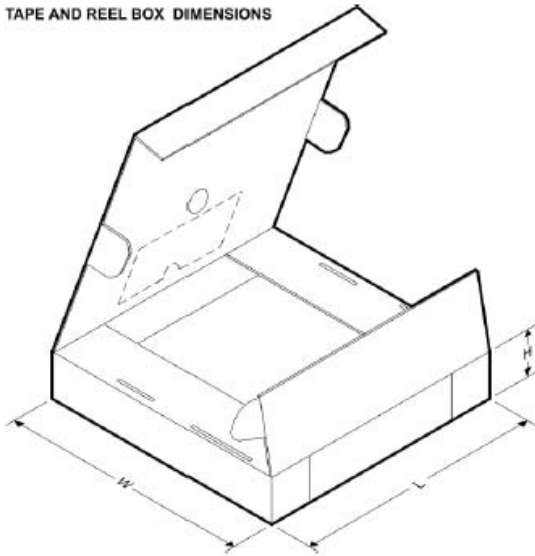
*All dimensions are nominal

Device	Package Type	Package Drawing	Pins	SPQ	Length (mm)	Width (mm)	Height (mm)
OPA2604AU/2K5	SOIC	D	8	2500	346.0	346.0	29.0

152

10.3 Appendix 3 - Arduino Code

```
1    //-------------------------------------------------//
2    //-------------Pin allocations & Initializations-------------//
3    //-------------------------------------------------//
4
5    int Motor1Driverpin = 2;
6    int Motor2Driverpin = 4;
7    int Motor3Driverpin = 7;
8    int Motor4Driverpin = 8;
9    int Motor5Driverpin = 12;
10   int Motor6Driverpin = 13;
11   int Motor1DriverPWMpin = 3;
12   int Motor2DriverPWMpin = 5;
13   int Motor3DriverPWMpin = 6;
14   int Motor4DriverPWMpin = 9;
15   int Motor5DriverPWMpin = 10;
16   int Motor6DriverPWMpin = 11;
17   int EMGin1 = A0;
18   int EMGin2 = A1;
19   int Motor1Current = A2;
20   int Motor2Current = A3;
21   int Motor3Current = A4;
22   int Motor4Current = A5;
23   int Motor5Current = A6;
24
25   //-------------------------------------------------//
26   //-----------------------Variables-----------------------//
27   //-------------------------------------------------//
28   float CurrentAnalouge1;
29   float CurrentAnalouge2;
30   float CurrentAnalouge3;
31   float CurrentAnalouge4;
32   float CurrentAnalouge5;
33   boolean Motor1Stall = false;
34   boolean Motor2Stall = false;
35   boolean Motor3Stall = false;
36   boolean Motor4Stall = false;
37   boolean Motor5Stall = false;
38   boolean Motor1ReverseStall = false;
39   boolean Motor2ReverseStall = false;
40   boolean Motor3ReverseStall = false;
41   boolean Motor4ReverseStall = false;
42   boolean Motor5ReverseStall = false;
43   boolean AllMotorsStalled = false;
44   boolean AllMotorsReverseStalled = false;
45
46   //-------------------------------------------------//
47   //-----------------------Constants-----------------------//
48   //-------------------------------------------------//
49   float EMGThreshold1 = 400;  //Threshold for reverse EMG activation - Found in Test Environment approximately 2V - N.B The hardware amplificaation can be taylored to this value
50   float EMGThreshold2 = 400;  //Threshold for reverse EMG activation - Found in Test Environment approximately 2V - N.B The hardware amplificaation can be taylored to this value
52
53
54   void setup() // Setting all of the pins to either INPUT or OPUTPUT depending on their use
55   {
56     //--------------------Static Drive Mode Pins--------------------//
57     pinMode( Motor1Driverpin, OUTPUT);
58     pinMode( Motor2Driverpin, OUTPUT);
59     pinMode( Motor3Driverpin, OUTPUT);
60     pinMode( Motor4Driverpin, OUTPUT);
61     pinMode( Motor5Driverpin, OUTPUT);
62
63     //--------------------PWM Pins--------------------//
64     pinMode( Motor1DriverPWMpin, OUTPUT);
65     pinMode( Motor2DriverPWMpin, OUTPUT);
66     pinMode( Motor3DriverPWMpin, OUTPUT);
67     pinMode( Motor4DriverPWMpin, OUTPUT);
68     pinMode( Motor5DriverPWMpin, OUTPUT);
69
70     //--------------------Analouge Pins--------------------//
71     pinMode( EMGin1, INPUT);
72     pinMode( EMGin2, INPUT);
73     pinMode( Motor1Current, INPUT);
74     pinMode( Motor2Current, INPUT);
75     pinMode( Motor3Current, INPUT);
76     pinMode( Motor4Current, INPUT);
77     pinMode( Motor5Current, INPUT);
78   }
79   //-------------------------------------------------//
80   //--------------------Main Function--------------------//
81   //-------------------------------------------------//
82
83   void loop ()
84   {
85
86     //-------------Read the Analogue Pins--------------------//
87     EMGin1 = analogRead(A0);
88     EMGin2 = analogRead(A1);
89     CurrentAnalouge1 = analogRead(A2);
90     CurrentAnalouge2 = analogRead(A3);
91     CurrentAnalouge3 = analogRead(A4);
92     CurrentAnalouge4 = analogRead(A5);
93     CurrentAnalouge5 = analogRead(A6);
94
95   //-------------Forward EMG Activation--------------------//
96
97     if( EMGin1 > EMGThreshold1 && EMGin2 < EMGThreshold2)
98     {
99       allmotorstallcheck ();
100      if (AllMotorsStalled = false)
101      {
102          if(Motor1Stall = false)
```

```
103              {
104               IndexTighten();
105               Motor1SenseCurrent();
106              }
107              if(Motor2Stall = false)
108              {
109               MiddleTighten();
110               Motor2SenseCurrent();
111              }
112              if(Motor3Stall = false)
113              {
114               RingTighten();
115               Motor3SenseCurrent();
116              }
117              if(Motor4Stall = false)
118              {
119               PinkyTighten();
120               Motor4SenseCurrent();
121              }
122              if(Motor5Stall = false)
123              {
124               ThumbTighten();
125               Motor5SenseCurrent();
126              }
127         }
128
129     }
130
131     //-------------Reverse EMG Activation-------------------//
132
133     if (EMGin2 > EMGThreshold2 && EMGin1 < EMGThreshold1)
134     {
135       allmotorstallReversecheck ();
136       if (AllMotorsReverseStalled = false)
137       {
138        if(Motor1ReverseStall = false)
139              {
140               IndexFlex();
141               Motor1ReverseSenseCurrent();
142              }
143              if(Motor2ReverseStall = false)
144              {
145               MiddleFlex();
146               Motor2ReverseSenseCurrent();
147              }
148              if(Motor3ReverseStall = false)
149              {
150               RingFlex();
151               Motor3ReverseSenseCurrent();
152              }
153              if(Motor4ReverseStall = false)
154               {
155                PinkyFlex();
156                Motor4ReverseSenseCurrent();
157               }
158              if(Motor5ReverseStall = false)
159              {
160               ThumbFlex();
161               Motor5ReverseSenseCurrent();
162              }
163        }
164     }
165
166      //-------------No EMG Input - All Stop--------------//
167
168     if( EMGin1 < EMGThreshold1 && EMGin2 < EMGThreshold2)
169     {
170          Motor1Stop();
171          Motor2Stop();
172          Motor3Stop();
173          Motor4Stop();
174          Motor5Stop();
175      }
176
177       //-------------Both EMG Input - All Stop--------------//
178
179     if( EMGin1 > EMGThreshold1 && EMGin2 > EMGThreshold2)
180     {
181          Motor1Stop();
182          Motor2Stop();
183          Motor3Stop();
184          Motor4Stop();
185          Motor5Stop();
186      }
187    }
188  //----------------------------------------------------------------//
189  //----------------------Movement Functions-----------------------//
190  //----------------------------------------------------------------//
191  void IndexTighten() //Function to bend the index finger to grip an object
192  {
193     analogWrite(Motor1DriverPWMpin, 127); // This is the 50% duty Cycle for the forward movement (Can be modified)
194     //Insert the current sense portion here to deactivate
195     digitalWrite(Motor1Driverpin, LOW); //OR digitalWrite(Motor1Driverpin, HIGH) for a fast brake
196     AllMotorsReverseStalled = false;
197  }
198
199  void IndexFlex() //Function to bend the index finger to grip an object
200  {
201     digitalWrite(Motor1DriverPWMpin, LOW); // Set the forward pin to low for allowance of moving backwards.
202     digitalWrite(Motor1Driverpin, HIGH); //Set the reverse pin to high if this was not decided on in the forward stage (Active brake)
203     //Insert the current sense portion here to deactivate
204     AllMotorsStalled = false;
```

```
205    └}
206    void MiddleTighten() //Function to bend the index finger to grip an object
207    ⊟{
208        analogWrite(Motor2DriverPWMpin, 127); // This is the 50% duty Cycle for the forward movement (Can be modified)
209        //Insert the current sense portion here to deactivate
210        digitalWrite(Motor2Driverpin, LOW); //OR digitalWrite(Motor1Driverpin, HIGH) for a fast brake
211        AllMotorsReverseStalled = false;
212    └}
213
214    void MiddleFlex() //Function to bend the index finger to grip an object
215    ⊟{
216        digitalWrite(Motor2DriverPWMpin, LOW); // Set the forward pin to low for allowance of moving backwards.
217        digitalWrite(Motor2Driverpin, HIGH); //Set the reverse pin to high if this was not decided on in the forward stage (Active brake)
218        //Insert the current sense portion here to deactivate
219        AllMotorsStalled = false;
220    └}
221
222    void RingTighten() //Function to bend the index finger to grip an object
223    ⊟{
224        analogWrite(Motor3DriverPWMpin, 127); // This is the 50% duty Cycle for the forward movement (Can be modified)
225        //Insert the current sense portion here to deactivate
226        digitalWrite(Motor3Driverpin, LOW); //OR digitalWrite(Motor1Driverpin, HIGH) for a fast brake
227        AllMotorsReverseStalled = false;
228    └}
229
230    void RingFlex() //Function to bend the index finger to grip an object
231    ⊟{
232        digitalWrite(Motor3DriverPWMpin, LOW); // Set the forward pin to low for allowance of moving backwards.
233        digitalWrite(Motor3Driverpin, HIGH); //Set the reverse pin to high if this was not decided on in the forward stage (Active brake)
234        //Insert the current sense portion here to deactivate
235        AllMotorsStalled = false;
236    └}
237
238    void PinkyTighten() //Function to bend the index finger to grip an object
239    ⊟{
240        analogWrite(Motor4DriverPWMpin, 127); // This is the 50% duty Cycle for the forward movement (Can be modified)
241        //Insert the current sense portion here to deactivate
242        digitalWrite(Motor4Driverpin, LOW); //OR digitalWrite(Motor1Driverpin, HIGH) for a fast brake
243        AllMotorsReverseStalled = false;
244    └}
245
246    void PinkyFlex() //Function to bend the index finger to grip an object
247    ⊟{
248        digitalWrite(Motor4DriverPWMpin, LOW); // Set the forward pin to low for allowance of moving backwards.
249        digitalWrite(Motor4Driverpin, HIGH); //Set the reverse pin to high if this was not decided on in the forward stage (Active brake)
250        //Insert the current sense portion here to deactivate
251        AllMotorsStalled = false;
252    └}
253
254    void ThumbTighten() //Function to bend the index finger to grip an object
255    ⊟{
256        analogWrite(Motor5DriverPWMpin, 127); // This is the 50% duty Cycle for the forward movement (Can be modified)
257        //Insert the current sense portion here to deactivate
258        digitalWrite(Motor5Driverpin, LOW); //OR digitalWrite(Motor1Driverpin, HIGH) for a fast brake
259        AllMotorsReverseStalled = false;
260    └}
261
262    void ThumbFlex() //Function to bend the index finger to grip an object
263    ⊟{
264        digitalWrite(Motor5DriverPWMpin, LOW); // Set the forward pin to low for allowance of moving backwards.
265        digitalWrite(Motor5Driverpin, HIGH); //Set the reverse pin to high if this was not decided on in the forward stage (Active brake)
266        //Insert the current sense portion here to deactivate
267        AllMotorsStalled = false;
268    └}
269
270    void Motor1Stop()
271    ⊟{
272        digitalWrite(Motor1DriverPWMpin, LOW);
273        digitalWrite(Motor1Driverpin, LOW);
274    └}
275
276    void Motor2Stop()
277    ⊟{
278        digitalWrite(Motor2DriverPWMpin, LOW);
279        digitalWrite(Motor2Driverpin, LOW);
280    └}
281
282    void Motor3Stop()
283    ⊟{
284        digitalWrite(Motor3DriverPWMpin, LOW);
285        digitalWrite(Motor3Driverpin, LOW);
286    └}
287
288    void Motor4Stop()
289    ⊟{
290        digitalWrite(Motor4DriverPWMpin, LOW);
291        digitalWrite(Motor4Driverpin, LOW);
292    └}
293
294    void Motor5Stop()
295    ⊟{
296        digitalWrite(Motor5DriverPWMpin, LOW);
297        digitalWrite(Motor5Driverpin, LOW);
298    └}
299
300
301
302    //------------------------------------------------------------------//
303    //---------------------Current Sense Functions----------------------//
304    //------------------------------------------------------------------//
305
306    //------------------------Forward Functions-------------------------//
```

156

```
307    void Motor1SenseCurrent()
308  ⊟{
309  |       CurrentAnalouge1 = Motor1Current;
310  ⊟    if ( CurrentAnalouge1 > CurrentsenseThreshold){
311  |        Motor1Stop();
312  |        Motor1Stall = true;
313  ⊢   }
314  └ }
315
316    void Motor2SenseCurrent()
317  ⊟{
318  |       CurrentAnalouge2 = Motor2Current;
319  ⊟    if ( CurrentAnalouge2 > CurrentsenseThreshold){
320  |        Motor2Stop();
321  |        Motor2Stall = true;
322  ⊢   }
323  └ }
324
325    void Motor3SenseCurrent()
326  ⊟{
327  |       CurrentAnalouge3 = Motor3Current;
328  ⊟    if ( CurrentAnalouge3 > CurrentsenseThreshold){
329  |        Motor3Stop();
330  |        Motor3Stall = true;
331  ⊢   }
332  └ }
333
334    void Motor4SenseCurrent()
335  ⊟{
336  |       CurrentAnalouge4 = Motor4Current;
337  ⊟    if ( CurrentAnalouge4 > CurrentsenseThreshold){
338  |        Motor4Stop();
339  |        Motor4Stall = true;
340  ⊢   }
341  └ }
342
343    void Motor5SenseCurrent()
344  ⊟{
345  |       CurrentAnalouge5 = Motor5Current;
346  ⊟    if ( CurrentAnalouge5 > CurrentsenseThreshold){
347  |        Motor5Stop();
348  |        Motor5Stall = true;
349  ⊢   }
350
351  └ }
352
353    //------------------------Reverse Functions--------------------------//
354
355    void Motor1ReverseSenseCurrent()
356  ⊟{
357  |       CurrentAnalouge1 = Motor1Current;
358  ⊟    if ( CurrentAnalouge1 > CurrentsenseThreshold){
359  |        Motor1Stop();
360  |        Motor1ReverseStall = true;
361  ⊢   }
362  └ }
363
364    void Motor2ReverseSenseCurrent()
365  ⊟{
366  |       CurrentAnalouge2 = Motor2Current;
367  ⊟    if ( CurrentAnalouge2 > CurrentsenseThreshold){
368  |        Motor2Stop();
369  |        Motor2ReverseStall = true;
370  ⊢   }
371  └ }
372
373    void Motor3ReverseSenseCurrent()
374  ⊟{
375  |       CurrentAnalouge3 = Motor3Current;
376  ⊟    if ( CurrentAnalouge3 > CurrentsenseThreshold){
377  |        Motor3Stop();
378  |        Motor3ReverseStall = true;
379  ⊢   }
380  └ }
381
382    void Motor4ReverseSenseCurrent()
383  ⊟{
384  |       CurrentAnalouge4 = Motor4Current;
385  ⊟    if ( CurrentAnalouge4 > CurrentsenseThreshold){
386  |        Motor4Stop();
387  |        Motor4ReverseStall = true;
388  ⊢   }
389  └ }
390
391    void Motor5ReverseSenseCurrent()
392  ⊟{
393  |       CurrentAnalouge5 = Motor5Current;
394  ⊟    if ( CurrentAnalouge5 > CurrentsenseThreshold){
395  |        Motor5Stop();
396  |        Motor5ReverseStall = true;
397  ⊢   }
398
399  └ }
400
401    //------------------------Allmotor Functions--------------------------//
402
403    void allmotorstallcheck ()
404  ⊟{
405  |    if (Motor1Stall == true)
406  ⊟    {
407  |      if (Motor2Stall == true)
408  ⊟      {
```

```
409          if (Motor3Stall == true)
410          {
411              if (Motor4Stall == true)
412              {
413                  if (Motor5Stall == true)
414                  {
415                      AllMotorsStalled = true;
416                  }
417              }
418          }
419      }
420   }
421 }
422
423
424 void allmotorstallReversecheck ()
425 {
426   if (Motor1ReverseStall == true)
427   {
428      if (Motor2ReverseStall == true)
429      {
430          if (Motor3ReverseStall == true)
431          {
432              if (Motor4ReverseStall == true)
433              {
434                  if (Motor5ReverseStall == true)
435                  {
436                      AllMotorsReverseStalled = true;
437                  }
438              }
439          }
440      }
441   }
442 }
443
```

10.4 Appendix 4 - Arduino Nano Datasheet

Arduino Nano (V2.3)

User Manual

Released under the Creative Commons Attribution Share-Alike 2.5 License

http://creativecommons.org/licenses/by-sa/2.5/

More information:

www.arduino.cc

Rev. 2.3

Arduino Nano Pin Layout
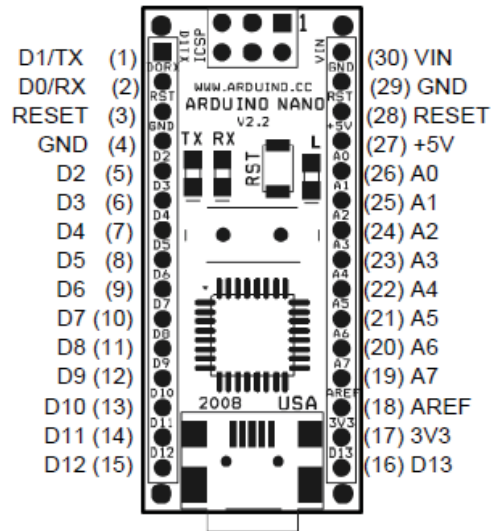
Pin No.	Name	Type	Description
1-2, 5-16	D0-D13	I/O	Digital input/output port 0 to 13
3, 28	RESET	Input	Reset (active low)
4, 29	GND	PWR	Supply ground
17	3V3	Output	+3.3V output (from FTDI)
18	AREF	Input	ADC reference
19-26	A7-A0	Input	Analog input channel 0 to 7
27	+5V	Output or Input	+5V output (from on-board regulator) or +5V (input from external power supply)
30	VIN	PWR	Supply voltage

Arduino Nano Mechanical Drawing
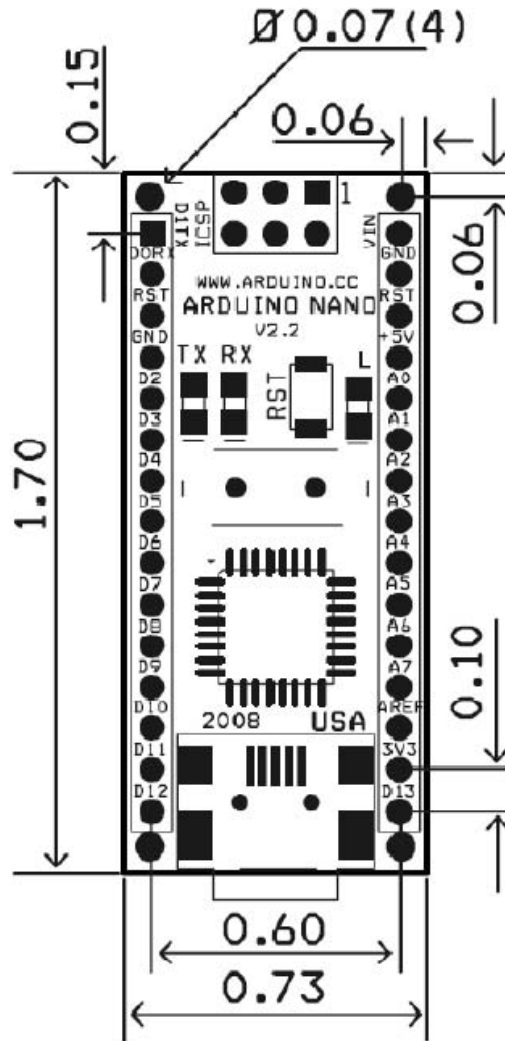
ALL DIMENTIONS ARE IN INCHES

Arduino Nano Bill of Material

Item Number	Qty.	Ref. Dest.	Description	Mfg. P/N	MFG	Vendor P/N	Vendor
1	5	C1,C3,C4,C7,C9	Capacitor, 0.1uF 50V 10% Ceramic X7R 0805	C0805C104K5RACTU	Kemet	80-C0805C104K5R	Mouser
2	3	C2,C8,C10	Capacitor, 4.7uF 10V 10% Tantalum Case A	T491A475K010AT	Kemet	80-T491A475K010	Mouser
3	2	C5,C6	Capacitor, 18pF 50V 5% Ceramic NOP/COG 0805	C0805C180J5GACTU	Kemet	80-C0805C180J5G	Mouser
4	1	D1	Diode, Schottky 0.5A 20V	MBR0520LT1G	ONSemi	863-MBR0520LT1G	Mouser
5	1	J1,J2	Headers, 36PS 1 Row	68000-136HLF	FCI	649-68000-136HLF	Mouser
6	1	J4	Connector, Mini-B Recept Rt. Angle	67503-1020	Molex	538-67503-1020	Mouser
7	1	J5	Headers, 72PS 2 Rows	67996-272HLF	FCI	649-67996-272HLF	Mouser
8	1	LD1	LED, Super Bright RED 100mcd 640nm 120degree 0805	APT2012SRCPRV	Kingbright	604-APT2012SRCPRV	Mouser
9	1	LD2	LED, Super Bright GREEN 50mcd 570nm 110degree 0805	APHCM2012CGCK-F01	Kingbright	604-APHCM2012CGCK	Mouser
10	1	LD3	LED, Super Bright ORANGE 160mcd 601nm 110degree 0805	APHCM2012SECK-F01	Kingbright	04-APHCM2012SECK	Mouser
11	1	LD4	LED, Super Bright BLUE 80mcd 470nm 110degree 0805	LTST-C170TBKT	Lite-On Inc	160-1579-1-ND	Digikey
12	1	R1	Resistor Pack, 1K +/-5% 62.5mW 4RES SMD	YC164-JR-071KL	Yageo	YC164J-1.0KCT-ND	Digikey
13	1	R2	Resistor Pack, 680 +/-5% 62.5mW 4RES SMD	YC164-JR-07680RL	Yageo	YC164J-680CT-ND	Digikey
14	1	SW1	Switch, Momentary Tact SPST 150gf 3.0x2.5mm	B3U-1000P	Omron	SW1020CT-ND	Digikey
15	1	U1	IC, Microcontroller RISC 16kB Flash, 0.5kB EEPROM, 23 I/O Pins	ATmega168-20AU	Atmel	556-ATMEGA168-20AU	Mouser
16	1	U2	IC, USB to SERIAL UART 28 Pins SSOP	FT232RL	FTDI	895-FT232RL	Mouser
17	1	U3	IC, Voltage regulator 5V, 500mA SOT-223	UA78M05CDCYRG3	TI	595-UA78M05CDCYRG3	Mouser
18	1	Y1	Cystal, 16MHz +/-20ppm HC-49/US Low Profile	ABL-16.000MHZ-B2	Abracon	815-ABL-16-B2	Mouser

Arduino Nano Schematic

Copyright 2008 under the Creative Commons Attribution Share-Alike 2.5 License
http://creativecommons.org/license/by-sa/2.5/

10.5 Appendix 5 - TiDA Quote

SALES QUOTE

RECIPIENT:	
Company Name:	Massey University
	Christopher Scott
Client Address:	

TiDA
Titanium Industry
Development Association Inc

Quote Prepared by: Warwick   Date: 15 January 2014   Sales Quote Number:
Material Required: Titanium   Lead time from Date of Order:

Item:	Quantity:	Price:
Index J1 bottom	1	$81.05
Index J1 top	1	$62.85
Palm middle	1	$428.92
Palm	1	$800.94
Part 7	1	$529.25
Total:		$1903.01

NOTES:
Files in
Clients/Quotes/Massey-C Scott

Sales quotes are valid for 30 days, and are estimates only, and subject to change. All quotes are subject to TiDA and/or RAM Terms and Conditions. Individual project amendments, changes and custom requests will amend the Sales Quote provided. Prices exclude GST and are in NZ Dollars.
Any queries, please do not hesitate to contact us.
Angela Werder, Titanium Industry Development Association, *ph.* (07) 557 0344, *email.* info@tida.co.nz

For Office Use only		
Job Confirmation Date:	Customer Purchase Order #:
Tida Job Number:	Estimated Dispatch Date:
Actual Dispatch Date:	Signoff:

10.6 Appendix 6 – Ethical Approval

MASSEY UNIVERSITY
TE KUNENGA KI PŪREHUROA

8 July 2013

Christopher Scott
131A Church Street
West End
PALMERSTON NORTH 4412

Dear Christopher

Re: Intelligent Bio-Robotic System Using Biometric Signals

Thank you for your Low Risk Notification which was received on 19 June 2013.

Your project has been recorded on the Low Risk Database which is reported in the Annual Report of the Massey University Human Ethics Committees.

The low risk notification for this project is valid for a maximum of three years.

Please notify me if situations subsequently occur which cause you to reconsider your initial ethical analysis that it is safe to proceed without approval by one of the University's Human Ethics Committees.

Please note that travel undertaken by students must be approved by the supervisor and the relevant Pro Vice-Chancellor and be in accordance with the Policy and Procedures for Course-Related Student Travel Overseas. In addition, the supervisor must advise the University's Insurance Officer

A reminder to include the following statement on all public documents:

"This project has been evaluated by peer review and judged to be low risk. Consequently, it has not been reviewed by one of the University's Human Ethics Committees. The researcher(s) named above are responsible for the ethical conduct of this research.

If you have any concerns about the conduct of this research that you wish to raise with someone other than the researcher(s), please contact Professor John O'Neill, Director (Research Ethics), telephone 06 350 5249, e-mail humanethics@massey.ac.nz".

Please note that if a sponsoring organisation, funding authority or a journal in which you wish to publish requires evidence of committee approval (with an approval number), you will have to provide a full application to one of the University's Human Ethics Committees. You should also note that such an approval can only be provided prior to the commencement of the research.

Yours sincerely

John G O'Neill (Professor)
Chair, Human Ethics Chairs' Committee and Director (Research Ethics)

cc   Dr Liqiong Tang
       School of Engineering and Advanced
           Technology
       PN456

Prof Don Cleland, HoS
School of Engineering and Advanced
    Technology
PN456

Massey University Human Ethics Committee
Accredited by the Health Research Council